

HIPPOCAMPAL AND NEOCORTICAL DYNAMICS DURING LONG-TERM MEMORY IN
MACAQUES

AHMED T. HUSSIN

A DISSERTATION SUBMITTED TO THE FACULTY OF GRADUATE STUDIES IN
PARTIAL FULFILLMENT OF THE REQUIREMENTS FOR THE DEGREE OF DOCTOR
OF PHILOSOPHY

GRADUATE PROGRAM IN BIOLOGY

YORK UNIVERSITY

TORONTO, ONTARIO

AUGUST 2020

© AHMED HUSSIN, 2020

ABSTRACT

Memory is one of the most important faculties of the mind. Memory keeps a record of our experiences which enriches our sense of self, enables us to make adaptive decisions in the present and informed plans for the future. Historically, memory research has focused on the hippocampal formation in the medial temporal lobes which is critical in the initial stages of memory formation. More recently, memory research expanded to include neocortical areas especially with regards to remote memory. An open question in neuroscience is what happens to memory representations in the brain with time. It remains unclear whether the contribution of the hippocampus to memory decreases with time in favour of the neocortex, or if both their contributions stay the same. In this dissertation, I use the non-human primate model to examine the neural mechanism underlying memory formation in the hippocampus, as well as the contribution of neocortical areas during remote memory. In the first study, I present findings that the neural mechanism underlying memory is heterogenous; varying by waking state and underlying spiking of different neuronal types. In the second study, I focus on two neocortical areas alongside the hippocampus and present findings that support a greater role for neocortical areas during remote memory. These findings support the idea that memory dependence shifts to areas outside the hippocampus with time.

Thesis Supervisor: Kari Hoffman

سَأُرِيهِمْ آيَاتِنَا فِي الْأَفَاقِ وَفِي أَنْفُسِهِمْ حَتَّىٰ يَتَبَيَّنَ لَهُمْ أَنَّهُ الْحَقُّ

We will show them our signs in the horizons and in themselves until it becomes clear to them that it is the Truth

Acknowledgements

I wish to sincerely thank Professor Kari Hoffman for her mentorship and supervision. Her enthusiasm for science has been truly inspiring and it has been a privilege to learn from her how to think like a scientist. Thank you to Professors Thilo Womelsdorf and Dale Stevens whose constructive feedback has been integral to my scientific training and the development of this dissertation. Thank you to Samia Ali and Tarek Hussin, my parents, for their unconditional love, support and faith in me, without which I would not have made it this far. Last but not least, thank you to Emily Tallon, my partner and best friend, for accompanying me on this journey, and supporting me with her love, kindness and patience.

TABLE OF CONTENTS

Abstract.....	ii
Quote.....	iii
Acknowledgements.....	iv
Table of Contents.....	v
List of Figures.....	vii
Chapter 1: Background.....	1
Introduction: brain area for experiential memory.....	2
Memory of experiences or what-happened-where-and-when.....	3
The brain’s sea monster.....	6
Synaptic plasticity and memory hypothesis.....	9
The sharp-wave ripple: The brain’s plasticity inducer.....	11
Replay of neuronal activity patterns during sleep and waking.....	13
Standard model of Systems Consolidation.....	17
Incongruent findings lead to an alternative interpretation.....	21
Retrosplenial Cortex and Memory.....	24
Anterior Cingulate Cortex and Memory.....	28
Current Dissertation.....	29
Chapter 2: Sharp-wave ripples vary with state and memory.....	32
Introduction.....	34
Materials and Methods.....	37
Results.....	41
Discussion.....	47
Chapter 3: Dissociations in neocortical and hippocampal synchrony for remotely learned episodic memory.....	59
Introduction.....	61
Materials and Methods.....	64

Results.....	70
Discussion.....	74
Chapter 4: Conclusions.....	91
Bibliography.....	103
Appendices	115
Appendix I: Hussin et al. 2018.....	115
Appendix II: Hussin et al. 2020.....	126

LIST OF FIGURES

Chapter 1

Figure 1.....	14
---------------	----

Chapter 2

Figure 1.....	51
Figure 2.....	52
Figure 3.....	53
Figure 4.....	54
Figure 5.....	55
Supplementary Figure 1.....	56
Supplementary Figure 2.....	57
Supplementary Figure 3.....	58

Chapter 3

Figure 1.....	77
Figure 2.....	79
Figure 3.....	81
Figure 4.....	82
Supplemental Figure 1.....	83
Supplemental Figure 2.....	84
Supplemental Figure 3.....	85
Supplemental Figure 4.....	86
Supplemental Figure 5.....	88
Supplemental Figure 6.....	89
Supplemental Figure 7.....	90

Chapter 4

Figure 1.....	96
---------------	----

Chapter 1: Background

Our daily personal experiences induce long-lasting changes in the brain that form the physiological representation of our memory for these experiences. Where in the brain do these changes occur? what is their nature? and what happens to the physiological representation of a memory as time goes on? Memory of our personal events would not be possible without the hippocampal formation in the medial temporal lobes. Daily experiences induce changes in the brain area that come in various forms and timescales – such as receptor trafficking, changes in the efficacy of synaptic transmission, replay of experiential activity and systems-level morphological changes - all working in tandem to lay down the foundation for the physical machinery of memory. These myriad and flexible changes are the tools the brain uses to create memories of our valuable experiences. This chapter reviews our understanding of event memory, the role of the hippocampal formation in retaining memory for events, synaptic plasticity mechanisms, the role of sharp-wave ripples and systems consolidation.

Introduction: brain area key for experiential memory

One of our most cherished abilities is our capacity for mental time travel. It allows us to keep records of our past, defines who we are in the present, and enables us to plan for the future. Daily life experiences leave lasting physical changes in the brain which are thought to underlie our memory of them. Studying these changes enables us to understand how our remembered experiences are represented in the brain, and how in some disease states these representations gradually fade away. But how could a lump of tissue consisting of billions of cells represent memory of an everyday life event?

One of the most important milestones in answering this challenging question was the discovery that the medial temporal lobes are particularly important for the long-term preservation of memory for experiences. This discovery has its origins with observations that individuals with perturbations in this brain area are unable to form long-term memories of everyday life events. The most studied and documented case of this kind is that of Henry Molaison, better known as H.M who struggled with debilitating seizures, and as treatment had sizable portions of his medial temporal lobes excised (including the hippocampal formation and most of the amygdala (Corkin et al. 1997)). Although his seizures were successfully controlled by this procedure, H.M suffered a peculiar side-effect; he was unable to remember new people, names, places and events a few minutes after encountering them (*anterograde amnesia*), and had lost memories of events that happened close in time to surgery (*graded retrograde amnesia*; (Scoville and Milner 1957; Corkin 2002). H. M's state was akin to being permanently stuck in the present moment, or in his own words "*like waking from a dream...every day is alone in itself*" (Milner et al. 1968). He had largely lost the ability to update his personal life narrative through cumulative life experiences, the process through which we maintain and develop our sense of self in the world.

Closer examination of H. M's memory revealed that this inability to make new memories was limited to memory for facts and events encountered in everyday life, but that other kinds of memory were intact. For example, he had a reasonably functional short-term memory – meaning he could remember a limited amount of information for a few seconds to minutes. He could solve motor tasks that have an extensive learning component despite denying ever seeing the task or having learned it (Corkin 2002). He could also learn simple associations, such as blinking in response to a tone that predicts an air puff to the eye (Woodruff-Pak 1993). Empirical evidence from H.M and other amnesic individuals with perturbations in the same area due to surgery or damage (Baddeley and Warrington 1970; Brooks and Baddeley 1976; Cohen and Squire 1980) confirmed that structures in the medial temporal lobe (hippocampal formation and nearby sites) are critical for creating long-lasting conscious recollections of everyday experiences. Based on these findings, the hippocampal formation in the medial temporal lobe emerged as a brain area through which neuroscientists can begin to understand how this most-cherished kind of memory is represented in the brain.

Memory of experiences or what-happened-where-and-when

Accumulating evidence about the medial temporal lobe's role in conscious recollection helped to solidify the previously intuited distinctions between different memory types. Tulving (1972) and Squire (1988) distinguished between forms of memory that are expressed through performance (called nondeclarative or implicit memory) and those expressed through recollection (also called declarative or explicit memory). Nondeclarative memory is procedural in nature and allows us to remember motor skills such as how to play a musical instrument or ride a bicycle. It does not require conscious recollection or awareness of the memory content and

includes priming (learning based on exposure and lack of conscious guidance or attention) and other stimulus-response habits. Nondeclarative memories rely on brain sites such as the striatum, cerebellum and sensory cortical areas. In contrast, declarative memory is memory that can be consciously recollected, and is often classified into memory of episodes or events of everyday life (also called autobiographical or episodic memory) and memory of semantic items such as facts (Tulving 1987; Squire and Zola-Morgan 1988). The findings from amnesic individuals with medial temporal lobe damage suggested that the hippocampal formation is critical for the retention of the conscious recollection kind of memory.

In humans, declarative memory is relatively simple to study and often relies on subjective verbal recall of experiences. However, a sizable portion of research on the biology of memory is conducted on nonhuman animals which do not speak, expressing their memory solely through performance therefore hindering the possibility of evaluating their conscious or declarative memory. To circumvent this fact, researchers have carefully designed proxy tasks that tap into elements of declarative memory in order to gain indirect knowledge about how the hippocampal formation contributes to conscious memory (Murray and Wise 2010). One such proxy task which is used extensively is the object-in-place scene task developed for use in monkeys by David Gaffan. This task requires monkeys to find one of two objects in a composite scene of geometric forms of different size, shape and colour for food reward. Memory for the correct object-scene combination is impaired following damage to the hippocampal system (Gaffan 1994b). The idea behind object-in-scene memory is that episodic memory is often defined by the spatial, temporal and other sensory contexts in which it occurred. An episodic memory contains information about an item, object or event (the “*what*”) that occurred at a specific time (“*when*”) in a particular place (“*where*”) (Clayton and Dickinson 1998; Clayton et al. 2001). Capitalizing on these

features, researchers developed behavioural tests in animals to examine 1) content: that an animal remembers an event (“*what*”) and its associated context (“*where*” or “*when*” it occurred), 2) structure: that event and context information make up a single representation, and 3) flexibility: that the memory can be used to produce an adaptive behavioural response in a different but similar event. Because memory on these tasks is evaluated through performance and not through assessing conscious recollection, it is customary to describe these tasks in animals as *episodic-like* memory tasks (Allen and Fortin 2013).

The *what-where-when* characterization of episodic memory has guided the development of memory tasks to study of episodic memory in humans (Holland and Smulders 2011), nonhuman primates (Hoffman et al. 2009; Martin-Ordas et al. 2010) and rodents (Babb and Crystal 2006; Ergorul and Eichenbaum 2004; Eacott et al. 2005; Kart-Teke et al. 2006; Dere et al. 2006). A common variant of these tasks involves isolating two of the three components to study the underlying neural mechanisms. For example, *what-where* tasks require subjects to remember where specific events occurred or *what-where* associations, also commonly called *object-place* (Allen and Fortin 2013). The “*what*” component is usually an object, an odor or a particular food and the “*where*” component is typically a place in the environment in rodent studies, or a location on a screen or a visual scene in primate studies. Behavioural tasks involving *what-where* associations have been extensively conducted in humans, non-human primates (Gaffan 1994a) and rodents (Gilbert and Kesner 2003a; Gilbert and Kesner 2003b; Day et al. 2003).

The current working framework for the neural process underlying episodic-like memory suggests that during an experience, information flows from primary sensory areas into two partially overlapping streams representing the “*what*” and “*where*” components which become

bound into a conjunctive “*what happened where*” representation in the hippocampus. Information about the “*what*” component (items/objects/events which represent the *content* of an experience) is channeled through the perirhinal and lateral entorhinal areas, while information about “*where*” (which represent the spatial *context* of an experience) is channeled through the parahippocampal and medial entorhinal areas (Burwell 2000; Lavenex and Amaral 2000; Eichenbaum et al. 2007; Knierim et al. 2014). These streams integrate in the hippocampus which serves to bring the “*what-where*” components of episodic memory into a single representation (Gaffan 1994a; Gilbert and Kesner 2003a; Gilbert and Kesner 2003b; Day et al. 2003; Rajji et al. 2006). Consistent with this framework, damage to the hippocampus does not impair item or object (“*what*”) memory, but rather impairs the specific “*what-where*” representations. Similar findings are observed in “*what-when*” tasks although the processing of the temporal component of episodic memory is much less understood (Buhusi and Meck 2005; Lehn et al. 2009; Eichenbaum 2018). In the next section, I describe the anatomical features of the hippocampal formation and the neural properties that allow it to retain information long after an experience has passed.

The brain’s sea monster

Contained within the medial portion of the temporal lobe is the hippocampal formation, which consists of the entorhinal cortex, parasubiculum, presubiculum, dentate gyrus (DG), and the hippocampus proper with its three subdivisions; cornu ammonis 1, 2 and 3 (or CA1, CA2 and CA3). Unlike the common organizational feature of connections in neocortical regions that connect reciprocally (region A connects to B and B connects back to A), the circuit in the hippocampal formation is unidirectional with signal flowing in one direction. Superficial layers

of the entorhinal cortex receive most of the neocortical input to the hippocampal formation. From there, axons project on the perforant path to the dentate gyrus (among other sites). Granule cells in the dentate then give rise to axons called the mossy fibers that synapse on pyramidal cells of the CA3, which in turn project axon fibers (Schaffer collaterals) to the CA1. CA1 cells then project to the subiculum and then back to the deeper layers of the entorhinal cortex (Andersen et al. 2006).

The advent of macro- and micro-electrodes placed carefully within the hippocampal formation to study the electrical activity of its neurons greatly improved our understanding of hippocampal function. Such recordings made *in vitro* using brain slices and *in vivo* in awake animals led to the exciting discovery that the strength of synaptic transmission between hippocampal neurons can change in an experience-dependent manner. By inducing high-frequency stimulation to the perforant path of the hippocampus for a few seconds, Tim Bliss and Terje Lømo discovered that synaptic efficacy in downstream neurons can be enhanced for several minutes and hours afterwards (Bliss and Lomo 1973). The discovery of what has become known as *long-term potentiation* (LTP) demonstrated that activity between neurons - in a brain area believed to be involved in the retention of everyday experiences - can change in a long-lasting manner. LTP represented the first mechanistic explanation for how the hippocampus can possibly retain information from an experience long after it has passed.

A substantial body of work on LTP has demonstrated that the potentiation duration varies with the intensity and duration of stimulation which can last more than a year (Abraham et al. 2002). The molecular mechanisms underlying this long-lasting change in efficacy were identified and found to depend on the NMDA receptor of the excitatory neurotransmitter glutamate. When activated, NMDA receptors produce a strong influx of post-synaptic Ca^{+2} which triggers a

secondary messenger cascade recruiting kinases such as CAMKII, PKA and MAPK (Kandel et al. 2014). The kind of kinases recruited, and the downstream results vary depending on how long the change in efficacy will last. Short-term or *early-LTP* results from increased trafficking of AMPA receptors to the post-synaptic terminal increasing the response to synaptic transmission. Long-term or *late-LTP* results from kinases inducing gene expression changes that modify the structure of the synaptic terminals such as the enlargement or addition of new dendritic spines enhancing synaptic efficacy in a prolonged manner (Bosch and Hayashi 2012). Long-term changes in efficacy are bi-directional; just as synaptic strength can increase, it can also decrease (called long-term depression, LTD) using similar but opposing molecular mechanisms to LTP. This up- and down- regulation of synaptic strength as a result of use came to be known as *synaptic plasticity*, and provided a physiological substrate for memory formation theorised by Jerzy Konorski and Donald Hebb over twenty years earlier (Hebb 1949).

Since the discovery of LTP in the hippocampus, synaptic plasticity was observed in the cerebellum (McCormick et al. 1982), subcortical areas such as the amygdala (Bauer et al. 2001), nucleus accumbens and ventral tegmental area (Citri and Malenka 2008), and neocortical areas such as visual cortical area V1 (Schuett et al. 2001), motor cortical area M1 (Rioult-Pedotti et al. 1998; Teskey et al. 2002), prefrontal cortex (Lüscher and Malenka 2011), and auditory cortex (Ahissar et al. 1992). This ubiquity strongly suggested that synaptic plasticity is a fundamental property of the brain and a candidate mechanism through which the brain learns and remembers. In the following section, I describe evidence that links synaptic plasticity mechanisms to the formation of memory representations in the brain.

Synaptic plasticity and memory hypothesis

In order to test the hypothesis that synaptic plasticity underlies learning and memory, (Martin and Morris 2002) proposed four assessment criteria; **1) detectability**; that it should be possible to detect changes in synaptic efficacy following learning, **2) anterograde alteration**; that if some manipulation that blocks, enhances or alters synaptic plasticity were to be given prior to learning, memory should be affected accordingly, **3) retrograde alteration**; if learning were to occur, and then a treatment is given that affects the expression of synaptic plasticity, what has been learned should also be affected, and lastly **4) mimicry**; if memory resides in a specific distributed pattern of altered synaptic weights in specific neurons, the artificial creation of such a pattern or trace should create a ‘false memory’ for an experience or event that did not occur.

To date, all four criteria have been met in studies using rodent subjects. Detectability was demonstrated in studies where learning is immediately followed by an examination of hippocampal electrophysiology. Similar to early-LTP, learning was found to induce persistent increases in synaptic transmission (Rogan et al. 1997; Whitlock et al. 2006) through AMPA receptor trafficking (Rumpel et al. 2005; Matsuo et al. 2008; Mitsushima et al. 2011). Similar to late-LTP, learning was also shown to induce changes in DNA structure through methylation and histone modification (Day and Sweatt 2011) that regulate the transcriptional machinery of a host of genes involved in altering synaptic transmission. Additionally, learning was shown to increase dendritic spine size and number (Moser et al. 1994), and induce post-transcriptional changes in kinases such as *CaMKII* necessary for the induction of LTP through AMPA receptor trafficking (Lisman et al. 2002).

Retro- and antero-grade alterations were tested through interventions to the molecular cascade of LTP either before or after a learning experience and testing the effects on memory.

For example, inhibiting NMDA receptors (whose activation is necessary for LTP induction) either pharmacologically using the antagonist *APV* (Morris et al. 1986) or through genetic knockouts of NMDA subunits (Tsien et al. 1996) prior to learning impaired subsequent memory. In a similar manner, applying ζ -*pseudo-substrate inhibitory peptide* (*ZIP*) after learning was observed to disrupt memory of the learned task (Pastalkova et al. 2006). *ZIP* is an inhibitor of *protein kinase Mzeta* (*PKM- ζ*) which is necessary and sufficient for LTP maintenance (Sajikumar et al. 2005; Yao et al. 2008).

Testing the last of the assessment criteria – i.e. mimicry - involved recreating a distributed pattern of altered synaptic weights – or re-activating cells that were active during an experience – to test whether it would illicit recall. To identify cells active during a brief learning experience researchers typically couple the expression of an IEG - such as *c-fos* which is promptly up-regulated due to neuronal activity – to a permanent label such as a fluorescent protein for later visualization or light-sensitive ion channels such as *channelrhodopsin-2* (ChR2) for subsequent artificial activation with laser light. This allows only cells active during a brief learning experience to be “*tagged*” for later observation or manipulation. For example, Liu and colleagues tagged hippocampal DG neurons that were active during contextual fear conditioning in a group of mice with ChR2. Days later, the mice were placed in a different context and the tagged cells were activated using a focused light probe (Liu et al. 2012). This artificial activation of the cells active during the brief conditioning experience elicited retrieval of the conditioned fear memory (freezing behaviour). Alternatively, inhibiting those cells in the DG, CA3 or CA1 regions of the hippocampus - using another opsin called *halorhodopsin* permeable only to Cl⁻ ions – active during fear conditioning inhibits freezing (Denny et al. 2014; Tanaka et al. 2014). In another study, DG neurons active when mice explored a particular chamber (context A) were

tagged with ChR2 and later activated in a different context (context B) as the mice received foot-shocks. When placed back in context A, where the mice never received any shocks, the mice displayed freezing behaviour suggesting that simply activating neurons representing context A during foot shocks in a different context is sufficient to create a memory between context A and foot-shocks (Ramirez et al. 2013).

Tag-and-manipulate studies provided strong evidence for the idea that neurons active during an experience are the same neurons active when that experience is recalled. This idea was first tested by fluorescently tagging neurons active during learning and retrieval and quantifying the overlap of active cells (Reijmers et al. 2007). Consistent with the synaptic plasticity and memory hypothesis, cells active during an experience are observed to undergo strengthening of synaptic transmission measured by an increase in AMPA/NMDA postsynaptic current ratio indicating upregulation of AMPA receptors and spine density (Ryan et al. 2015). Despite the reliance on an impoverished form of memory ironically expressed through behaviour cessation-freezing in response to a context— these *tag-and-manipulate* studies demonstrated proof-of-principle for the idea that neurons active during an experience are also active during recall, that their re-activation can elicit recall and that they undergo long-lasting synaptic plasticity changes. In the next section, I describe a candidate mechanism through which neurons active during an experience can induce long-term plasticity changes resulting in stable memory representations.

The sharp-wave ripple: the brain's plasticity inducer

A large body of evidence supported the synaptic plasticity and memory hypothesis – that biochemical and morphological changes on the level of circuits and systems underlie learning

and memory formation. And while we understood how to trigger such mechanisms experimentally through electrical stimulation, it was unclear for some time how synaptic plasticity is triggered endogenously. Does the brain engage in an endogenous, activity-dependent, high-frequency electrical activity similar to experimentally induced protocols that could induce long-lasting changes in synaptic efficacy? The answer is yes.

If we place an electrode in the hippocampus and observe the electrical activity as a subject goes about its day, a world of electrical activity patterns is uncovered that vary in their oscillation frequency, duration and incidence. These patterns of electrical activity reflect the summed activity of large numbers of neurons working in tandem around the electrode tip leading to synchronous neuronal activity or rhythmical electroencephalographic (EEG) activity (Buzsáki et al. 2012; Einevoll et al. 2013). One of the most important of these electrical patterns in the hippocampus is the *sharp-wave ripple* (SWR), which is a brief (50-200 ms) neural population event resulting from the synchronised spiking of CA field neurons. When recorded extracellularly, it consists of a large amplitude negative polarity deflection called a *sharp-wave*, and a fast-oscillatory pattern called a *ripple*. The frequency of the fast oscillation varies between 80 to 140 Hz in non-human primates and humans (Bragin et al. 1999; Le Van Quyen et al. 2008; Staresina et al. 2015; Logothetis et al. 2012; Leonard et al. 2015) and 140 to 200 Hz in rodents (Ylinen et al. 1995; Sullivan et al. 2011; Hulse et al. 2016; Buzsáki et al. 2003). The participation and temporal dynamics of different cell types and CA regions during the sharp-wave ripple remain under investigation and much is yet to be uncovered. Broadly speaking however, there is consensus that the sharp-wave component results from the inward currents brought about by the synchronous discharge of CA3 pyramidal cells onto the mid-apical dendrites of the CA1 field, whereas the ripple component results from the high-frequency synchronous discharge of

pyramidal cells and interneurons of CA1 cell layer (Buzsáki et al. 1983; Sullivan et al. 2011). Recently, CA2 neurons have been shown to synchronously activate before CA3 and CA1 neurons suggesting it might be involved in the initiation of the ripple (Oliva et al. 2016). Additionally, CA regions are not believed to act in a functionally uniform manner during ripples but that their involvement depends on laminar location of their neurons (deep vs superficial). For example, the strength of PV-mediated inhibition of pyramidal neurons during ripples was found to be increase along a gradient from superficial to deep layers which determines CA1 pyramidal cell participation (Valero et al. 2015).

Replay of neuronal activity patterns during sleep and waking

The most remarkable feature of the sharp-wave ripple is its representational content. A closer look at the pyramidal cells participating in the high-frequency ripple component reveals that their spiking activity reflects a temporally compressed version of earlier sequential spiking patterns. In the rodent, these spiking sequences of hippocampal pyramidal neurons represent earlier navigation-related experiences (Wilson and McNaughton 1994; Skaggs and McNaughton 1996; Nádasdy et al. 1999; Lee and Wilson 2002). In other words, during ripples neurons replay their earlier spiking patterns during navigation experiences in a time-compressed manner as shown in Figure 1.

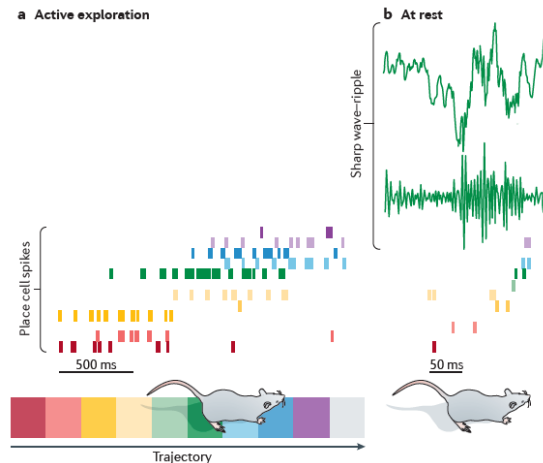


Figure 1. Replay of navigation spiking sequences during sharp wave ripples. a. Spikes from activate place cells are ordered by their activation sequence (top) as a rodent passes through the cells' place fields on a linear track (bottom). b. An example sharp-wave ripple (top = broadband, bottom = bandpass filter 150-300 Hz) is shown on top and its decoded spike content is shown below. Note how spike content replays a time compressed version of the spiking sequence from the earlier navigation trajectory on the left. Adapted from (Colgin 2016).

In primates, this replay phenomenon is similarly observed during ripples, although the type of content that the spiking represents remains unknown (Vaz et al. 2020). Replay during rodent ripples starts in the hippocampus (Nádasy et al. 1999; Lee and Wilson 2002; Foster and Wilson 2006; Csicsvari et al. 2007; Diba and Buzsáki 2007; Ji and Wilson 2007) and initiates replay of spiking sequences in various cortical (Qin et al. 1997; Ji and Wilson 2007; Peyrache et al. 2009) and subcortical areas (Pennartz et al. 2004; Gomperts et al. 2015). This distributed and widespread repetition of earlier neuronal activity patterns during ripples is well-suited to promote the consolidation of earlier experiences into stable, long-term memory representations (Carr et al. 2011; Girardeau and Zugaro 2011; Sadowski et al. 2011; Roumis and Frank 2015; Buzsáki 2015). An experience is therefore thought to be initially encoded in ensembles of hippocampal neurons, which are then repeatedly reactivated leading to strengthening of the neural representation of the experience throughout the brain.

Thus, the ripple provides 1) an endogenous, synchronous and spontaneous population event that occurs in the brain area necessary for episodic memory formation, 2) where neural activity underlying experience is *replayed* several times in a time-compressed manner, 3) co-activating large numbers of neurons and organizing their firing in a fast event similar to the tetanic train used to induce LTP. These factors have led to the hypothesis that ripples are the mechanism by which the brain induces synaptic plasticity changes that underlie memory formation (Buzsáki et al. 1987; Bliss and Collingridge 1993). If that indeed is the mechanism by which memory representations are formed, then we could predict that disrupting ripples would impair learning and memory formation. The current evidence supports this prediction and shows that memory is impaired when ripples occurring after learning are interrupted using brief closed-loop electrical pulses (Girardeau et al. 2009; Ego-Stengel and Wilson 2010; Nokia et al. 2012). Adding further support to this hypothesis, ripple-associated replay of firing patterns has been observed to induce LTP at CA1 synapses *in vitro* (Sadowski et al. 2016), while optogenetic silencing of CA1 pyramidal neurons during ripples has been observed to reduce the stability of place cells that replay their activity during disrupted ripples (Roux et al. 2017).

In humans and non-human primates, ripples were initially observed during *offline* states when the brain is not actively engaging with sensory information. These offline states include sleep (Axmacher et al. 2008; Staresina et al. 2015), anaesthesia (Logothetis et al. 2012; Ramirez-Villegas et al. 2015) and quiet wakefulness which refer to awake but non-active states such as eyes closed in a hospital bed (Le Van Quyen et al. 2008) or in a darkened booth (Skaggs et al. 2007). In 2015, ripples were observed during online states as well when the brain is actively engaged in a cognitively demanding task. While recording from rhesus macaques, Leonard et al. observed ripples occurring as the monkeys were actively searching for targets in visual scenes

(Leonard et al. 2015). This suggested that ripples may play a broader role than simply serve to facilitate consolidation of memory in subsequent offline states. A new working hypothesis developed and suggested that reactivation of previously learned information during waking ripples may be a mechanism to guide ongoing behaviour (Roumis and Frank 2015; Carr et al. 2011; Joo and Frank 2018). This hypothesis is based on the understanding that episodic memory retrieval depends on the recovery of neural activity present when the memory was first experience, which often occurs during ripples in the form of replay. In 2017, Leonard & Hoffman found that ripple incidence increases when monkeys are viewing familiar scenes, and that ripples occur more frequently when the animals' gaze is close to the remembered target in a visual scene (Leonard and Hoffman 2017). This suggested that the increased incidence near remembered targets may be facilitating the retrieval of the remembered target location and therefore guiding gaze towards it consistent with a role in memory retrieval. A similar finding was reported in humans where ripple rate increased 1-2 prior to successful retrieval in a free recall task (Norman et al. 2019) and a paired associate verbal memory task (Vaz et al. 2019). Successful retrieval was also associated with greater synchrony between the hippocampus and the medial temporal gyrus emphasising the importance of hippocampal-neocortical coupling for recall. More recently, successful retrieval in the paired-associate verbal task was shown to be associated with trial-specific ripple-locked replay of neuronal spikes that occurred during learning in the medial temporal gyrus (Vaz et al. 2020). These findings complement observations in rodent studies where waking ripples have been shown to; be important for memory-guided decision making (Jadhav et al. 2012), represent potential future trajectories (Pfeiffer and Foster 2013; Wu et al. 2017), and increase in incidence with learning (Papale et al. 2016). In this section I reviewed a promising mechanism by which memory representations are created and

recalled through replaying of experience-associated neural activity. In the following section I discuss what happens with these representations with time, as memories age.

Standard Model of Systems Consolidation

The plasticity mechanisms underlying memory revealed that memory formation is a time-dependent process. For an experience to be represented in long-term memory, relatively slow genetically induced mechanisms are employed to create new dendritic spines, synaptic connections and to reorganize synaptic weights across neuronal circuits to represent new information (Kandel et al. 2014). Long before we understood these time-dependent physiological changes, empirical psychologists Müller and Pilzecker had found that immediately following learning memory is easily disrupted through learning newer information, but that with time this vulnerability to disruption decreases. They concluded that immediately following learning, some physiological process works to strengthen the memory of the newly learned information, and that the intensity of this process decreases with time, explaining why interfering with this process was disruptive to the memory early after learning but not after some time has passed (McGaugh 1999). They called this process by which memory is solidified with time *consolidation*.

Consolidation theory appeared to explain the puzzling condition of *temporally graded amnesia* observed in individuals after traumatic brain injury where memory-loss is stronger for recent memories and gradually weaker for older or more remote memories (Russell and Nathan 1946; Squire et al. 1975). It suggested that brain injury is more likely to affect recent memory because it hasn't yet been consolidated, while sparing already-consolidated older memory. This early work by empirical psychologists coupled with later findings about the medial temporal lobe

and temporally graded retrograde amnesia led to the development of the *systems consolidation* framework. In this framework, memory is initially dependent on the hippocampus, and is liable to being disrupted (with disruption to the hippocampus), but that with time the memory gradually becomes less dependent on the hippocampus as a more permanent memory develops in distributed regions of the neocortex (Squire et al. 2015). Memory representations are thought to develop upon learning in the neocortex but require time to undergo changes in structure, distribution and connectivity among distant brain regions that ensure a memory becomes stable and long-lasting. During this gradual development, some interaction is held to occur between the hippocampus and neocortex during which initially vulnerable representations in the neocortex are strengthened. Based on this understanding, the neocortex is often described as a “slow learner”, requiring the hippocampus to gradually guide the development of connections across multiple cortical regions that are active at the time of learning and that represent the memory. The rate at which the neocortex can develop stable representations is thought to depend on prior knowledge with faster learning occurring when new information is consistent with previously learned information (McClelland 2013).

Evidence for this framework of how memory representations change over time comes from studies on memory-impaired individuals, brain imaging of blood flow during normal memory and animal studies. Studies on memory-impaired individuals typically involve memory assessments of patients with bilateral damage to the hippocampus (and nearby areas because pure bilateral hippocampal damage is rare). Patients are quizzed on their memory of recent and remote events (of autobiographical or news events for example) and are often found to have memory loss for recent but not remote memories (Kapur and Brooks 1999; Bayley et al. 2003; Kirwan et al. 2008; Manns et al. 2003; Buchanan et al. 2005; Kopelman and Bright 2012).

Studies on healthy volunteers using neuroimaging tools typically examine blood flow to different structures – as a proxy for neural activity – when recall of recent or remote memories. The better-designed of these studies use a prospective approach where participants learn similar information at two different time points before being scanned (for example, 1-week before and 15-minutes before scanning to represent remote and recent memory). A number of findings from such studies is consistent with systems consolidation showing that the hippocampus is more active during recall of recent memory compared to remote, and that the neocortex shows the opposite pattern being more active during remote compared to recent recall (Takashima et al. 2009; Yamashita et al. 2009; Furman et al. 2012).

Another approach to verifying systems consolidation is to use animals and a prospective approach to control when material is learned along with the enhanced ability to selectively target specific brain areas. For example, Zola-Morgan and Squire trained monkeys on a series of object discrimination problems encountered at varying timepoints (2-16 weeks prior to lesions to the hippocampus and parahippocampal cortex). Two weeks later, memory assessment revealed that whereas problems learned shortly before surgery were impaired, ones learned 12-16 weeks earlier were spared (Zola-Morgan and Squire 1990). Rodent studies using memory tests such as social transmission of food preference and fear conditioning have also found a temporal gradient of memory impairment when the hippocampus is damaged (Kim and Fanselow 1992; Anagnostaras et al. 1999; Winocur et al. 2001).

The development of tools for more precise spatial and temporal monitoring and control of neural activity allowed for more refined methods to probe the same question, and determine which areas are engaged during recent versus remote memory. Compared to lesion studies, these tools allow for a more elegant approach that does not require irreversibly damaging an area to

examine its engagement and instead allowing for a better assessment of their contribution. Some of the tools used to monitor cell activity include tools for selectively ‘*tagging*’ only cells that were active during a recall experience either through radioactive labeling (Bontempi et al. 1999), or quantifying cell activity through immediate early gene (IEG) expression (Maviel et al. 2004; Tayler et al. 2013) or dendritic spine growth (Restivo et al. 2009). Other tools allow for selective activation or inhibition of cell populations in different areas during recall using optogenetics (Goshen et al. 2011; Bero et al. 2014; Cowansage et al. 2014; Kitamura et al. 2017) or DREADDs (Varela et al. 2016). Others use pharmacological interventions to inhibit synaptic plasticity mechanisms such as DNA methylation (Miller et al. 2010), AMPA transmission (Einarsson et al. 2015) or NMDA transmission (Corcoran et al. 2011).

Several studies using the high-resolution approaches described above have found evidence supporting a temporal gradient whereby a memory’s dependence on the hippocampus is initially high when the memory is recent, and then gradually decreases with time and increases towards neocortical areas as the memory becomes older. For example, Bontempi et al. 1999 trained mice on a radial arm maze. Following training, mice were tested for recall either 5 days (recent memory) or 25 days later (remote memory) and their brains were analyzed for differential uptake of a radioactively labeled version of glucose immediately following recall. While the hippocampus and neocortical areas were active during recent recall, neocortical areas were more active during remote recall and hippocampal activity as well as correlation with performance was diminished. Studies using a variety of approaches described earlier have found similar evidence of a dependence shift towards several neocortical hot spots that include the anterior cingulate cortex (Maviel et al. 2004; Frankland et al. 2004; Restivo et al. 2009; Miller et al. 2010; Goshen et al. 2011; Vetere et al. 2011; Bero et al. 2014; Einarsson et al. 2015; Kitamura et al. 2017),

retrosplenial cortex (Maviel et al. 2004; Corcoran et al. 2011; Tayler et al. 2013), parietal (Frankland et al. 2004; Tayler et al. 2013), posterior cingulate, infralimbic, prelimbic, temporal cortices (Frankland et al. 2004).

Incongruent findings lead to an alternative interpretation: Multiple Memory Traces

Despite numerous studies confirming the temporally graded nature of memory loss when the hippocampus is damaged, other studies found equal amounts of loss for both remote and recent memory. For example, testing of patients with medial temporal lobe damage that carefully distinguished between semantic (knowledge of events and facts) and episodic (autobiographical) memory showed a *flat gradient*; that remote episodic memory is equally impaired at recent and remote time points (Rosenbaum et al. 2005; Steinvorth et al. 2005). This suggested that hippocampal damage also impairs recall of remote memory. This finding is supported by studies on healthy volunteers showing equal hippocampal engagement during remote memory recall (Fink et al. 1996; Ryan et al. 2001; Maguire and Frith 2003; Addis et al. 2004; Viard et al. 2007), yet many of these findings are confounded by having interviewed the participants about their memory during pre-screening which would engage the hippocampus (Buckner et al. 2001). A later study correcting for this confound found hippocampal activity correlated not with memory age but with vividness of remote memory (Gilboa et al. 2004). More recent studies have shown that the hippocampus continues to be activated reliably during retrieval of remote episodic memory (Bonnici et al. 2012; Sekeres, Winocur, Moscovitch, et al. 2018). Moreover, some rodent studies that lesioned the hippocampus and probed remote spatial and fear-conditioning also found a flat gradient after hippocampal lesions (Sutherland et al. 2001; Clark et al. 2005; Lehmann et al. 2007; Sutherland et al. 2008; Sparks et al. 2011; Broadbent and Clark 2013;

Ocampo et al. 2017; Sekeres, Winocur, Moscovitch, et al. 2018). Perhaps, the strongest such evidence comes from optogenetic studies that tag encoding hippocampal neurons (in DG, CA3 and CA1) during contextual fear conditioning. When cells encoding the remote memory are silenced during retrieval, memory is impaired (Goshen et al. 2011).

The incongruity of findings regarding whether the hippocampus remains actively involved in remote memory led to the suggestion that the hippocampus may be required for retrieval of episodic memory regardless of age (Nadel and Moscovitch 1997). This interpretation of the findings is referred to as *multiple trace theory*, MTT (or *transformation theory*) and suggests that despite early neocortical engagement, the hippocampus is always required for retrieval of episodic memory despite age. This argument is based on the architecture of the hippocampus and its importance for spatial navigation making it necessary for representing spatial contexts that are an inherent requisite of episodic memory (Tulving 2002). Damage to the hippocampus is argued to result in a flat temporal gradient of retrograde amnesia whereby even remote memory would not be recalled in its entirety. According to this explanation, each time a memory is retrieved, the hippocampal-neocortical trace supporting it is expanded and/or updated and hence strengthened. Subsequently, the neocortex is then able to support a decontextualized version of repeatedly remembered remote memories in the absence of the hippocampus.

The most supported prediction put forward by MTT is the prediction that extensive hippocampal damage causes comparable retrograde amnesia for recent and remote episodic. Other predictions of MTT such as a temporally-limited amnesia after hippocampus damage in semantic memory, temporally-limited amnesia for episodic memory after partial hippocampal damage or the existence of multiple hippocampal traces with repeated activations have yet to find experimental support (Sutherland et al. 2019). Overall, MTT has had a profound

contribution to refining what we mean by episodic memory and in developing memory assessments in humans and animals that better tap into episodic memory by emphasizing spatiotemporal elements of an experience to distinguish it from more gist-like semantic memory. This has been challenging given the frequent overlap between episodic and semantic memory where episodic memories will gain a semantic component with time, and where semantic memory can often have an episodic component.

The debate regarding hippocampal involvement in remote memory is yet to be resolved. The difficulty in reconciling the evidence and reaching consensus comes in part from the large variance across experiments. In human studies, damage locus and extent vary considerably across patients and so do the memory assessments used. Imaging studies on normal memory fail to account for the possibility that over time, memory representations may change in a way that the blood flow signal is affected without altering the functional role of a particular region (Andersen et al. 2006). More direct physiological measurements from the medial temporal lobes and neocortical areas are therefore needed to inform about if and how these areas are engaged during memory. A similarly large variance exists in rodent studies with lesion methods and locations and well as memory assessments that can be based on spatial navigation, conditioning or recognition.

Despite the inconclusion regarding which proposed framework more closely describes how memory representations actually change with time, there is growing consensus that 1) episodic memory initially engages the hippocampus which stores an index of neocortical areas representing the content of memory, 2) neocortical memory representations begin at the time of learning and stabilise with time guided by hippocampal interactions (Restivo et al. 2009; Kitamura et al. 2017; Xia et al. 2017; Abate et al. 2018; Matos et al. 2019), and that 3)

neocortical memory representations are stable over time. The second notion comes from evidence showing that hippocampal-neocortical interaction is necessary for the remote memory dependence on neocortical sites and begins during learning. For example, Restivo et al. 2009 found that lesioning the hippocampus only in a short window immediately after learning impairs remote memory recall and prevents learning-associated spine growth in the anterior cingulate cortex. Others have shown that frontal cortex encoding cells active during learning require hippocampal input to functionally mature with time (Lesburguères et al. 2011; Bero et al. 2014; Kitamura et al. 2017). In the following sections I take a closer look at two neocortical areas highly implicated in the support of remote memory.

Retrosplenial Cortex and Memory

The retrosplenial cortex (RSC) is an important node of the episodic memory network whose engagement appears to increase with familiarity and age. This cortical area is located behind the splenium of the corpus callosum and has major connections to the prefrontal and parahippocampal cortices, hippocampal formation through the entorhinal cortex, and the anterior and lateral dorsal nuclei of the thalamus (Kobayashi and Amaral 2000; Aggleton et al. 2012). In humans, damage to the RSC causes retrograde amnesia for episodic memory, and topographic amnesia; the inability to use known landmarks to navigate (Valenstein et al. 1987; Aguirre and D'Esposito 1999; Maguire 2001; Ino et al. 2007). Individuals are typically described as being able to recognize familiar landmarks and describe specific places in detail but are unable to find their way using those landmarks as well as unable to learn new routes (Maguire 2001). Imaging studies of healthy individuals show that the RSC is active in tasks of spatial navigation (Maguire 2001; Epstein 2008), processing of objects in scenes (Bar and Aminoff 2003; Bar 2004) and

landmarks (Auger and Maguire 2013; Auger et al. 2012; Mullally et al. 2012; Spiers and Maguire 2006), and recall of episodic memory (Svoboda et al. 2006; Spreng et al. 2009). Studies examining older memories in healthy subjects show that the RSC is particularly engaged during recall of remote episodic memory (Svoboda et al. 2006; Oddo et al. 2010; Benuzzi et al. 2018), although one study shows greater activation during recall of recent memory (Gilboa et al. 2004). More recent studies show that the RSC is particularly involved during navigation of familiar environments (Sulpizio et al. 2013; Sherrill et al. 2013; Shine et al. 2016; Patai et al. 2019) and that activation strength increases with learning (Wolbers and Büchel 2005).

Findings from rodent studies mirror our understanding of the RSC function gleaned from humans. Lesions to the RSC impair spatial memory on tasks that require using allocentric spatial cues to navigate such as the Morris water maze or the radial arm maze (Sutherland et al. 1988; Whishaw et al. 2001; Vann and Aggleton 2004; Vann and Aggleton 2002; Harker and Whishaw 2004; Pothuizen et al. 2008; St-Laurent et al. 2009). Path integration without the use of any spatial cues in the dark is also impaired by RSC lesions (Cooper and Mizumori 1999; Cooper et al. 2001). Additionally, lesions impair contextual fear conditioning (Keene and Bucci 2008b), active avoidance (Lukoyanov and Lukoyanova 2006), and object-recognition (Hindley et al. 2014).

Findings from animal studies are also consistent with a role for the RSC in remote episodic memory. In macaques, RSC lesions impair remote memory of object-in-scene memory (Buckley and Mitchell 2016). Monitoring of RSC activity using IEG fluorescence labeling methods in rodents shows that it is one of the few neocortical areas active during recall of remote memory (Bontempi et al. 1999; Maviel et al. 2004; Tayler et al. 2013). Some studies have also

found that lesions to the RSC impair non-spatial remote memory in the form of cue-shock associations where cue is auditory (Todd et al. 2016) or visual (Jiang et al. 2018). In a more causal examples; blocking of RSC NMDARs impairs recall of remote contextual fear memory (Corcoran et al. 2011), and inhibiting RSC protein synthesis (Katche, Dorman, Gonzalez, et al. 2013) or *c-fos* expression (Katche and Medina 2017) shortly after learning impairs remote but not recent recall. Real-time PCR to quantify IEG expression shows increases in *arc* and *c-fos* in the RSC during fear-conditioning, suggesting that the RSC engagement begins during learning (Robinson et al. 2012).

More recent studies have used the tag-and-manipulate approach described earlier and have helped have shed greater light on RSC function. By coupling the expression of green fluorescent protein (GFP) to the promotor for the IEG *c-fos*, Czajkowski et al. monitored the activity of neurons in the RSC during a spatial memory task. They found that learning in the Morris water maze activated the same subset of cells over seven days of training, and when these cells were disrupted using CNQX (AMPA blocker), performance on the task was impaired (Czajkowski et al. 2014). In another study, Cowansage et al. tagged active RSC cells during contextual fear conditioning with channelrhodopsin and found that artificial stimulation of those cells on a later probe was sufficient to re-instate the conditioned response of freezing suggesting that these RSC cells are part of the memory trace (Cowansage et al. 2014). More recently, Milczarek et al. used *in vivo* 2-photon imaging to monitor the activity of *c-fos* expressing neurons in the RSC during a spatial memory task (Milczarek et al. 2018). Over the course of a three-week learning period, there was a gradual emergence of context-specific neural activity whose stability correlated with memory retention. These studies demonstrated that RSC neurons form representations during episodic learning that support recall several days and weeks later.

This support for remotely learned events seems to depend on plasticity mechanisms. This was demonstrated recently by de Sousa et al. who selectively tagged RSC neurons active during contextual fear conditioning with channelrhodopsin. During the subsequent rest period, they applied high-frequency stimulation to the tagged cells to mimic the kind of stimulation that induces LTP. One day later, when neural activity in the hippocampus was blocked with a mixture of TTX (Na channel blocker) and CNQX, retrieval of fear memory was successful only in mice that received stimulation to tagged RSc cells (de Sousa et al. 2019). This suggested that the high-frequency stimulation speeded the process by which the memory became RSC-dependent and hippocampus-independent.

What do RSC neurons code for? While the answer to this question is still the subject of ongoing research, it appears that RSC neurons – at least in part – code for spatial trajectories associated with rewards. Electrophysiological recordings from the RSc in rodents reveal that the RSC has place cells similar to the hippocampus. Except these place fields are almost three times larger than those in the hippocampus (Cho and Sharp 2001; Smith et al. 2012; Mao et al. 2017). About 10% of RSC neurons are also head direction cells (Chen et al. 1994). Recordings in the RSC during the acquisition phase of reward-related memory tasks show that RSC neurons preferentially encode contexts associated with rewards and cues to reward locations (Smith et al. 2012; Vedder et al. 2017). In a follow up study by the same group, RSC neurons that encoded reward locations were found to fire as the rats approached the choice point suggesting the RSC may be engaged in memory-guided behaviour (Miller et al. 2019). These findings have motivated the hypothesis that the RSC may be a site for the integration of contextual information with reinforcing outcomes, especially at remote timepoints (Todd et al. 2019). In a more comprehensive study by of RSC cell coding during maze running (Alexander and Nitz 2015),

RSC cells were found to map position in internal and external frames of reference. Rate coding was found in a subset of cells associated with heading direction (left versus right turns in an egocentric frame of reference), while other cells were turn-insensitive and instead showed firing rate related to specific routes in the maze (allocentric reference). This coding versatility suggests that the RSC may exercise a broad role in supporting long-term memory for reward-associated spatial navigation which would explain several of the damage-related impairments observed in humans. Currently, electrophysiological evidence of RSC function is lacking in primates.

Anterior Cingulate Cortex and Memory

The anterior cingulate cortex (ACC) is perhaps the neocortical area most implicated in remote episodic memory. This large cortical area is further subdivided into regions based on their location with respect to the genu of the corpus callosum into midcingulate, pregenual and sub-genua regions (Stevens et al. 2011). In this dissertation, I will refer to the ACC as the region encompassing midcingulate and pre-genua regions (Brodmann areas 24 and 32) which correspond to the rodent's ACC and part of the prelimbic cortex (Laubach et al. 2018). The main role of the ACC is thought to be reinforcement-guided decision making or action-outcome learning (Camille et al. 2011; Rudebeck et al. 2008). It is thought to receive input about actions from the posterior cingulate cortex with which the ACC has strong bilateral connections and receive input about the outcome of actions (whether reward or punishment) from the orbitofrontal cortex. The ACC then serves as an integration site for actions and outcomes and remembers actions to perform to obtain reward or avoid punishment (Rolls 2019; Rolls and Wirth 2018).

The ACC has been shown to be an important node in the remote memory network. Animal studies have shown that as time passes, the role of the ACC in retrieving contextual-based memory increases (Frankland et al. 2004; Teixeira et al. 2006; Takehara-Nishiuchi and McNaughton 2008). Successful retrieval of remote memory is dependent on an intact ACC and is associated with increased activity (Bontempi et al. 1999; Maviel et al. 2004; Takehara-Nishiuchi and McNaughton 2008; Ding et al. 2008; Restivo et al. 2009; Vetere et al. 2011; Zhang et al. 2011; Weible et al. 2012; Einarsson and Nader 2012; Kitamura et al. 2017). Similar to the RSC, the electrophysiology behind the ACC support of remote memory in primates remains unexplored.

Current Dissertation

In the preceding sections I (briefly) reviewed the literature on the role of the hippocampal formation in episodic memory, associated neural mechanisms and current models about what happens to memory with age and the areas outside the medial temporal lobes that are thought to be involved during recall of remote memory. In this dissertation I focus the spotlight on two separate areas; 1) neuronal mechanisms underlying waking and quiescence ripples, and 2) neocortical physiological contributions towards recall of remote episodic memory.

Increasing evidence continues to link hippocampal ripples with memory consolidation and retrieval. Evidence reviewed earlier shows that ripples occur robustly during offline states where their associated replay of spiking sequences serves to facilitate memory consolidation. Also reviewed was evidence that ripples occur during online states – albeit with a lower incidence rate – where they serve to retrieve relevant memory to guide ongoing behaviour.

Despite a broader understanding of the function that ripples play, it remains unclear whether quiescent and waking ripples are physiologically distinct. In Chapter 2 of this dissertation, I compared ripples that occurred during inactive quiescent periods with those that occurred when non-human primates completed a memory-based visual search task. This chapter was motivated by the increasingly evident functional distinction between quiescence and waking ripples. To date, studies have focused on ripple incidence rate and the representational content of spiking sequences. Yet, whether ripples in different states have unique characteristics in terms of amplitude, duration or post-ripple wave remained unclear. Additionally, it remains unknown how different hippocampal neurons contribute to these spatiotemporal features. Knowledge about differences in features and underlying neuronal contributions is important for understanding the underlying computations involved and for development of real-time detection strategies.

In Chapter 3, I conducted an experiment to compare the neural activity of the hippocampus, RSC and ACC during recall of remote and recent episodic-like memory. Earlier in this chapter, I reviewed evidence linking the RSC and ACC to remote memory representations. The evidence in primate to date has mostly relied on imaging and lesion approaches while physiological reports of neural activity have been lacking. To our knowledge, this experiment is the first to simultaneously record the physiological activity of the primate hippocampus, RSC and ACC during recall of stimuli learned over one year earlier. We chronically implanted multichannel electrode arrays targeting the hippocampus, RSc and ACC of the left hemisphere of two female macaques. Both monkeys completed a memory-guided visual search task with stimuli they learned 12-18 months prior (comprising *remote* memory) and novel stimuli (comprising *recent* memory). Initially, we planned to study hippocampal-neocortical synchrony during ripples and observe how this synchrony varies between recent and remote episodic-like

memory. Given that ripples mediate consolidation and retrieval, we hypothesized that synchrony during ripples would inform us on the contributions of the hippocampus, RSC and ACC during retrieval of remote memory. For example, if remote memory was more dependent on neocortical areas than the hippocampus as the standard systems consolidation model predicts, we would predict greater synchrony during ripples when remote memory was successfully recalled compared to recent memory. If recall of episodic-like memory was dependent on the hippocampus despite memory age, we would see no difference in synchrony. However, while we successfully targeted the desired areas, we failed to observe ripples in both animals after surgery. We hence modified the original plan of examining synchrony during ripples to instead compare the spectral responses of the different areas and the synchrony between them across several frequency bands during recall of remote and recent memory. We looked at how the different areas respond to the presentation of recent versus remote scenes in terms of changes in oscillation frequency or power at different frequencies. We examined locking of oscillation phase with the onset of visual fixations to determine influences of areas on guiding gaze across a scene while searching for targets. And lastly, we examined phase-phase synchrony during successful recall in the different areas to determine the degree of inter-regional communication during remote memory recall.

Chapter 2: Sharp-wave ripples vary with state and memory

Recognizing that ripples occur in different states (quiescence/sleep and waking) and that they can mediate either consolidation or retrieval, we asked whether ripples differ by state in their electrophysiological signature. In this chapter, using the macaque ripple dataset acquired by Leonard et al. - which recorded hippocampal LFP and single unit activity during periods of quiescence and as macaques performed a memory-guided visual search task - I examined differences in mesoscopic ripple features - duration and amplitudes of the ripple as it appears in the LFP - across quiescence and visual exploration. Additionally, I examined the spiking contribution of different hippocampal cell types to the ripple amplitude and the amplitude of the post-ripple wave – a large positive deflection occurring immediately after the high frequency ripple oscillation. We observed that 1) quiescence ripples have greater amplitude and post-ripple waves compared to visual exploration ripples, 2) ripples that occur on *remembered* trials have larger amplitude compared to ripple on *forgotten* trials, with no change in duration or post-ripple wave. Our examination of underlying spiking activity across all ripples revealed that 3) ripple amplitude is associated with putative pyramidal and basket interneuron (IN) spiking, even when the spikes occur outside the high-frequency ripple oscillation. 4) Spiking activity by low firing rate neurons was associated with an attenuation of the post-ripple wave, while spiking by high firing rate neurons was associated with an enhancement. On examining spiking differences across search and quiescence ripples, we found fewer spikes from regular spiking (non-bursting low firing) pyramidal neurons during search which was associated with greater post-ripple waves. The selective changes in ripple features as a function of waking state, memory, spiking

time and cell type suggest that this mesoscopic field event can offer additional information on the underlying network computations than incidence rates alone.

Introduction

The *sharp-wave ripple (SWR)* is a spontaneous, synchronized neural population event that occurs in the hippocampus and is associated with widespread activation of the neocortex (Chrobak and Buzsáki 1994; Siapas and Wilson 1998; Sirota et al. 2003; Battaglia et al. 2004; Isomura et al. 2006; Mölle et al. 2006; Logothetis et al. 2012). Ripples occur most frequently during non-REM sleep, where they are important for memory consolidation (Girardeau et al. 2009; Ego-Stengel and Wilson 2010; Nokia et al. 2012), and less frequently during waking, where they appear to be important for memory-based decision-making (Jadhav et al. 2012; Leonard and Hoffman 2017; Wu et al. 2017) as learning progresses (Papale et al. 2016). During ripples, firing sequences observed during earlier waking periods are replayed among local populations within the hippocampus (Nádasy et al. 1999; Lee and Wilson 2002; Foster and Wilson 2006; Csicsvari et al. 2007; Diba and Buzsáki 2007; Ji and Wilson 2007), and at distant neocortical (Qin et al. 1997; Ji and Wilson 2007; Peyrache et al. 2009) and subcortical (Pennartz et al. 2004; Gomperts et al. 2015) sites. This “replay” phenomenon is thought to involve the synaptic modifications of relevant neural ensembles, supporting theories about the role of ripples in memory consolidation (Carr et al. 2011; Girardeau and Zugaro 2011; Sadowski et al. 2011; Roumis and Frank 2015; Buzsáki 2015). When ripples are disrupted, memory is impaired, suggesting a causal role for the neural activity occurring during ripples in memory formation (Girardeau et al. 2009; Ego-Stengel and Wilson 2010; Nokia et al. 2012).

Because the ripple mean field potential (or ripple-LFP) arises from the synchronous activity of neuronal ensembles thought to be critical for memory formation, it is important to understand how the activity of local cell populations shapes the ripple-LFP. Following a ripple, a brief period of hyperpolarization ensues where spikes are suppressed (English et al. 2014; Hulse

et al. 2016). This period, which is observed in the ripple-LFP as a positive polarity deflection (or postripple wave, PRW), may be additionally valuable in decoding local circuit activity immediately prior to and during the ripple. In general, neuronal firing rate and/or phase-locked firing are associated with high frequency (>50 Hz) LFP (Anastassiou et al. 2015; Belluscio et al. 2012; Montefusco-Siegmund et al. 2017; Ray et al. 2008; Scheffer-Teixeira et al. 2013). More specifically, the spatiotemporal features of the ripple-LFP can vary according to the specific neural ensembles active during the ripple. This relationship has been used to decode replay spiking content based on the similarity of ripple features alone (Taxidis et al. 2015).

The relationship between spiking activity and ripple features becomes more complicated when considering different vigilance states and corresponding changes in neuromodulatory tone (Atherton et al. 2015). Despite numerous reports measuring ripple occurrence, few studies have investigated how ripple-LFP features vary with learning. In one study, ripple amplitude was observed to be greater during sleep when followed by learning (Eschenko et al. 2008). Sharp-wave amplitude during sleep has also been shown to be greater than in waking (O'Neill et al. 2006; Buzsáki 2015). Other investigations into the variance in ripple amplitude found a positive correlation with spiking activity of a cell class in the cingulate cortex, suggesting that ripple-LFP features can be used to predict spiking activity not only locally in the hippocampus but even in distal neocortical areas (Wang and Ikemoto 2016).

Characterization of cell-type specific firing during ripples and their relation to SWR features is especially lacking in behaving primates where ripple physiology seems to be generally complementary to that observed in rats and mice (Bragin et al. 1999; Skaggs et al. 2007; Le Van Quyen et al. 2008; Logothetis et al. 2012; Leonard and Hoffman 2017). Despite the many similarities, a key difference is that ripples occur not only during awake immobility in

primates but also during active visual exploration (Leonard et al. 2015; Leonard and Hoffman 2017). To date, the only feature measured during exploratory SWRs were their rate of occurrence and peak frequency, which did not differ by state.

In this study, we examined how three ripple-LFP features vary across waking states and as a function of learning, in addition to their modulation by spiking activity (single-unit activity, SUA). We found that ripple and post-ripple wave amplitude in macaques are greater during quiescence than waking, and that on remembered trials in a visual-search memory task, ripple amplitude is increased, with no change to duration or post-ripple waves. We also describe the SWR modulation by cell types, classified by burstiness and firing rate, and found that low-firing rate cells (putative principal cells) are associated with enhanced ripple amplitude and attenuated post-ripple amplitude, whereas high-firing bursting and non-bursting cell types (putative basket interneurons) are associated with enhanced ripple and post-ripple wave amplitudes.

Materials and Methods

Subjects and experimental design

Two adult female macaques (*Macaca mulatta*, named LU and LE) completed a visual target-detection task that requires hippocampal function in primates (Chau et al. 2011), during daily recording sessions (this dataset was used in Leonard et al 2015; Leonard and Hoffman, 2017). The flicker change-detection task (previously described in Leonard et al., 2015, Leonard and Hoffman, 2017) required the animals to find and select a target object from non-targets in unique visual scenes for fluid reward (Figure 1A). Selection of a scene-unique target object was accomplished by holding gaze in the target region for a prolonged (≥ 800 ms) duration. The target object was defined as a changing item in a natural-scene image, where the original and changed images were presented in alternation, each lasting 500 ms, with a brief grey-screen (50 ms) shown between image presentations. Displayed this way, detection of the changing part of the scene requires effortful search in humans and macaques (Chau et al., 2011). An inter-trial interval (ITI) of 2-20 s followed each trial. The daily sessions began and ended with a period of at least 10 min when no stimulus was presented within the darkened booth and animals were allowed to sleep or sit quietly (quiescent period). Eye movements were recorded using video-based eye tracking (iViewX Hi-Speed Primate remote infrared eye tracker). All experimental protocols were conducted with approval from the local ethics and animal care authorities (Animal Care Committee, Canadian Council on Animal Care).

Electrophysiological recordings

Both animals were chronically implanted with independently moveable platinum/tungsten multicore tetrodes (96 μm outer diameter; Thomas Recordings) lowered into

the anterior hippocampal CA3/DG regions corresponding to the rodent ventral hippocampus. Animal LE had a 9-tetrode bundle centered at AP +11 mm verified post-implant with MRI. For this study we analyzed activity from the 4/9 tetrodes placed to optimize ripple and unit responses; these tetrodes were separated by $<600\ \mu\text{m}$ in the bundle. Animal LU had 8 tetrodes divided into two bundles: one at AP +11 mm and the other at AP +8 mm verified with post-operative CT co-registration to MRI. Based on ripple and unit activity we analyzed 3 tetrodes from each bundle, with separation $<500\ \mu\text{m}$ in the bundles). Local field potentials (LFPs) were digitally sampled at 32 kHz using a Digital Lynx acquisition system (Neuralynx) and filtered between 0.5 Hz and 2 kHz. Single-unit activity was sampled at 32 kHz and filtered between 600 Hz and 6 kHz, recording the waveform for 1 ms around a threshold triggered spike events. Single units were isolated using MClust based on wave-shape principle components, energy and peak/valley across channels. Only well-isolated cells were included, based on $<1\%$ interspike intervals (ISIs) within 2 ms and cross-correlograms between bursting cell pairs that had to be free of burst-latency peaks (asymmetric, $<10\ \text{ms}$ peak that could indicate the erroneous splitting of one CS unit into two; Harris et al., 2000). Units were classified as putative principal units (PR) if they had a burst firing mode (ISI mode peak, $<10\ \text{ms}$, comprising $\geq 10\%$ of ISIs) and under $<1\ \text{Hz}$ overall firing rate. Units were classified as putative interneurons (IN) if they had no burst firing mode ($>10\ \text{ms}$ ISI) and a firing rate $>1\ \text{Hz}$. The remaining two possible categories were the burst firing mode with $>1\ \text{Hz}$ firing rate (BHF), and nonburst firing mode, with $<1\ \text{Hz}$ spiking rate (NBLF). Waveshape parameters such as spike width and peak-trough asymmetry can vary as a function of recording location relative to the cell body and not only by cell type (Henze et al. 2000), therefore these waveshape measures were not used for cell type classification in this study (Fig 8).

SWR detection and feature estimation

SWR events were detected using the tetrode channel with the most visibly apparent ripple activity. The LFP signal was bandpass filtered (100-250 Hz), transformed into z-scores, rectified and then lowpass filtered (1-40 Hz). Ripple events were defined as threshold crossings 3 SDs above the mean, with a minimum duration of 50 ms beginning and ending at 1 SD. This time period also defined the ripple duration. SWR amplitude was defined as the maximum peak of the ripple envelope (z-score). The amplitude of the post-ripple wave (PRW) was defined as the maximum peak (z-score) of a narrower lowpass filter (1-5 Hz, Figure 1B). SWR amplitude, duration and PRW amplitude values were then normalized per tetrode for each animal to account for any across-tetrode differences in overall SWR magnitude. These features of the SWR (ripple duration, amplitude and PRW amplitude) were then compared across different states and task epochs (see supplementary Fig 1. for distributions of features).

SWR features across behavioral epochs

SWRs were clustered depending on time of occurrence into three behavioural epochs; quiescence (10 min dark-booth time period at the beginning and end of every session, qSWR), ITI (2-22 s interval between scene presentations representing quiet waking “inactive” states, iSWR) and exploratory search (during “active” visual search, eSWR). We excluded search ripples that occurred while the monkey fixated off-screen, and during search trials where the monkey spent >40% of trial time fixating off-screen. Task SWRs were further clustered by stimulus repetition into novel (scene repetition number = 0) and repeated trials (scene repetition number >0), and repeated trial ripples were further clustered into ripples occurring during trials where the target was successfully found (HIT), and when target was not (MISS).

Statistical analysis

Ripple features across waking state and task epochs were compared using the Wilcoxon Rank-sum test and the Kolmogorov-Smirnov (K-S) test. For the single-unit and ripple-LFP waveform analysis, a Kruskal-Wallis test was conducted with a Bonferroni correction for multiple-comparisons.

Results

Based on SWR clustering described above, we detected 2526 qSWRs (LU = 1866, LE = 660), 536 iSWRs (LU = 340, LE = 196) and, 664 eSWRs (LU = 462, LE = 202) from a total of 77 recording sessions (LU = 45, LE = 32). Based on unit clustering described earlier, we recorded from a total of 509 units; 242 PR (LU = 88, LE = 154), 133 NBLF (LU = 39, LE = 94), 48 BHF (LU = 0, LE = 48) and 86 IN (LU = 45, LE = 41) units.

SWR features across states

We first examined SWR duration, amplitude and PRW amplitude across the different states (qSWR, iSWR and eSWR; Figure 2). SWR duration was not different across states (rank sum $p > 0.5$; Figure 2A), whereas ripple amplitude was greater during qSWRs compared to eSWRs (rank sum $z = 2.48$, $p = 1.31 \times 10^{-2}$; K-S $d = 8.0 \times 10^{-2}$, $p = 8.4 \times 10^{-3}$, Figure 2B), and PRW amplitude was greater in qSWRs compared to iSWRs (rank sum: $z = 2.79$, $p = 5.30 \times 10^{-3}$, K-S $d = 7.0 \times 10^{-2}$, $p = 2.3 \times 10^{-2}$) and eSWRs (rank-sum: $z = 3.33$, $p = 8.63 \times 10^{-4}$, K-S $d = 9.1 \times 10^{-2}$, $p = 2.0 \times 10^{-3}$, Figure 2C).

SWR features during recognition memory task

Previously, we found that ripples occur more frequently and closer to a visual target with learning (Leonard and Hoffman, 2017). We therefore asked whether ripples that occur on repeated trials are different in duration or amplitude. First, we examined whether features vary by scene repetition by splitting ripples into novel (repetitions = 0) and repeated (repetitions > 0), but found no differences in ripple duration, amplitude or PRW amplitude between novel and repeated trials (rank sum $p > 0.05$). Next, we split repeated trials into trials where the target was successfully found (indicating memory for the target location), and not found (indicating

forgetting). Ripple duration (Figure 3A) and PRW amplitude (Figure 3C) were not different between remembered and forgotten trials (rank sum $p > 0.5$). During remembered trials ($n = 112$) ripple amplitude was larger than forgotten trials ($n = 220$) (rank sum $z = 2.11$, $p = 3.5 \times 10^{-2}$, K-S test $d = 0.16$, $p = 3.6 \times 10^{-2}$, Figure 3B). Because we had observed a greater ripple amplitude during quiescence compared to search, we compared ripple amplitude on remembered trials and quiescence but found no difference (rank sum: $z = 0.59$, $p = 0.55$, K-S $d = 8.5 \times 10^{-2}$, $p = 0.41$).

SUA analysis

Next, we examined local cell-type specific firing underlying ripples. Spikes occurring in a 400 ms time window centered around the peak of the ripple envelope were clustered based on spike-timing relative to the ripple event. Spikes were clustered into: Pre-Ripple, if they occurred before the ripple, Ripple; if they occurred during the ripple or Post-Ripple; if they occurred after the ripple (during the post-ripple wave). For each functional-unit type, the average ripple-LFP waveform was calculated based on the window of spike-time occurrence and aligned to ripple peak (Figure 4). Also calculated for each unit is the average ripple waveform where no spikes were observed (Null), and below each waveform plot is the normalized spike count distribution for each unit class in the ripple window clustered by spike-timing (pre-ripple, ripple and post-ripple).

SUA effects on ripple trough

We observed different effects on the magnitude of the ripple trough (defined as nearest trough to ripple peak) based on spike-time occurrence for PR (Figure 4A, $H(3) = 78.65$, $p = 5.99 \times 10^{-17}$), NBLF (Figure 4B, $H(3) = 141.10$, $p = 2.2 \times 10^{-30}$), IN (Figure 4D, $H(3) = 360.89$, $p = 6.53 \times 10^{-78}$), but not BHF cells (Figure 4C, $H(3) = 5.19$, $p = 0.16$). In PR cells, spiking in any

of the time windows (pre-ripple, ripple or post-ripple) was associated with a larger trough compared to no spikes ($p < 0.05$, Bonferroni post-hoc test; mean LE-PR-ripple = $-1.79z$, LE-PR-null = $-1.59z$, LU-PR-ripple = $-2.74z$, LU-PR-null = $-1.58z$). In NBLF cells, spiking in the ripple window was associated with a greater trough compared to spiking in pre- and post-ripple windows, as well as no spiking ($p < 0.05$, Bonferroni post-hoc; mean LE-NBLF-ripple = $-1.92z$, LE-NBLF-null = $-1.61z$; LU-NBLF-ripple = $-2.75z$, LU-NBLF-null = $-1.54z$). In IN cells, a similar pattern followed whereby ripple spikes were associated with a larger trough compared to pre-ripple and no spikes ($p < 0.05$, Bonferroni post-hoc; LE-INT-ripple = $-1.73z$, LE-INT-null = $-1.59z$; LU-INT-ripple = $-2.3z$, LU-INT-null = $-1.04z$). Interestingly, for non-bursting low firing rate cells that fired during the ripple, the LFP showed slow negative deflections in the ~ 200 ms leading up to the ripple event.

SUA effects on the post-ripple wave

The peak magnitude of the post-ripple wave (PRW) in the broadband signal varied according to spike-time occurrence and as a function of cell type, among PR ($H(3) = 693.67$, $p = 4.94 \times 10^{-150}$), NBLF ($H(3) = 150.59$, $p = 1.96 \times 10^{-32}$), IN ($H(3) = 25.10$, $p = 1.47 \times 10^{-5}$), and BHF cells ($H(3) = 11.90$, $p = 7.7 \times 10^{-3}$). The spiking of low firing-rate cells (PR and NBLF cells, Figure 4A and 4B) during the ripple window was associated with smaller peaks compared to null spiking ($p < 0.05$, Bonferroni post-hoc), whereas the opposite effect was seen with high firing-rate cells (BHF and IN cells, Figure 4C and 4D) where spiking was associated with a larger PRW ($p < 0.05$, Bonferroni post-hoc). For low firing-rate cells (Figure 4A and 4B), spiking during the post-ripple window resulted in the smallest peak ($p < 0.05$, Bonferroni post-hoc). For high firing-rate cells (Figure 4C and 4D), spiking during the ripple was associated with the largest peaks ($p < 0.05$, Bonferroni post-hoc). The heightened modulation for both peaks and

troughs found for the IN group suggests a stronger overall ripple amplitude, measured explicitly below.

SUA effects on the amplitude of the ripple envelope

In the earlier analysis of SWR feature changes with behavioral state, the ripple amplitude envelope was greater during quiescence than search (Figure 2B), and larger during remembered compared to forgotten trials (Figure 3B). We therefore sought to examine how spiking in different time windows (pre-ripple, ripple and post-ripple) by different cells types affects ripple amplitude (Figure 5). We found that spiking by PR ($H(3) = 934.73$, $p = 2.60 \times 10^{-202}$), NBLF ($H(3) = 659.32$, $p = 1.39 \times 10^{-142}$), and IN cells ($H(3) = 613.21$, $p = 1.38 \times 10^{-132}$) during any period in the 400 ms ripple window was associated with an increase in ripple amplitude (Figure 5A, 5B and 5D), whereas spikes from BHF cells had no effect on amplitude (Figure 5C, $H(3) = 9.83$, $p = 0.20$; LE-BHF-ripple = 0.35z, LE-BHF-null = 0.35z, LU had no BHF cells). The contribution of PR and NBLF spiking to ripple amplitude based on spike-timing followed a similar trend where spiking during the ripple window yielded a larger ripple amplitude compared to the post-ripple window and null spiking (Figure 5A & 5B, $p < 0.05$, Bonferroni post-hoc; LE-PR-ripple = 0.38z, LE-PR-null = 0.25z; LU-PR-ripple = 0.41z, LU-PR-null = 0.25z; LE-NBLF-ripple = 0.37z, LE-NBLF-null = 0.33). With NBLF cells there was also a difference in ripple-window amplitude compared to pre-ripple spikes ($p < 0.05$, Bonferroni post-hoc). Ripple-aligned spikes from NBLF cells resulted in the largest ripple amplitude across all cell classes and spike-times ($p < 0.05$, Bonferroni post-hoc). With IN cells, spikes during the three time-windows yielded a larger amplitude compared to that seen without IN spiking (Figure 5D, $p > 0.05$, Bonferroni post-hoc).

SUA effects on the amplitude of the post-ripple wave (PRW) envelope

All four cell classes showed differences in PRW amplitude based on spike-timing; PR ($H(3) = 600.57$, $p = 7.59 \times 10^{-130}$), NBLF ($H(3) = 111.86$, $p = 4.37 \times 10^{-24}$), BHF ($H(3) = 13.20$, $p = 4.20 \times 10^{-3}$) and IN cells ($H(3) = 17.98$, $p = 4.0 \times 10^{-4}$). Not surprisingly, the effects on PRW amplitude were similar to those reported earlier on the broadband signal. Spiking by low-spiking cells (PR and NBLF cells) was associated with smaller PRW amplitudes compared to no spikes (mean LE-PR-ripple = 0.96z, LE-PR-null = 1.39z, LU-PR-ripple = 0.77z, LU-PR-null = 1.21z, LE-NBLF-ripple = 1.11z, LE-NBLF-null = 1.37z, LU-NBLF-ripple = 0.94z, LU-NBLF-null = 1.17z), whereas spiking by high firing-rate cells (BHF and IN cells) was associated with larger PRW amplitudes (mean LE-BHF-ripple = 1.12z, LE-BHF-null = 0.47z; LU had no BHF units; LE-IN-ripple = 1.51z, LE-IN-null = 0.92z, LU-IN-ripple = 1.46z, LU-IN-null = 1.12z). In PR cells, null spiking was associated with the largest PRW amplitude, whereas spiking during the ripple resulted in a larger amplitude compared to pre- and post-ripple spikes (Figure 5A, $p < 0.05$, Bonferroni post-hoc). For NBLF cells, although the pattern was similar to PR cells, the decrease in amplitude due to spiking in the window was not as profound (Figure 5B). Null spiking was associated with a larger PRW amplitude compared to spikes during the ripple, pre-ripple and post-ripple, and ripple spikes yielded a larger amplitude than post-ripple spikes ($p < 0.05$, Bonferroni post-hoc). High firing rate cells had a similar trend to PRW amplitude by spike-time but with different direction of magnitude. Spikes during the ripple by BHF cells resulted in larger PRW amplitude compared to no spikes (Figure 5C, $p < 0.05$, Bonferroni post-hoc). But of all cell types, the IN group showed the most striking effects, with spiking during the ripple producing a larger PRW amplitude compared to pre-ripple and no spikes (Figure 5D,

$p < 0.05$, Bonferroni post-hoc), as well the largest PRW amplitude compared to all other cell classes and spike times ($p < 0.05$, Bonferroni post-hoc).

SUA underlying quiescence and waking ripples

We found that activity of regular spiking putative pyramidal neurons was associated with greater PRW during search (supplemental fig. 2) compared to quiescence ripples (supplemental fig. 3). Spiking activity of the three other classes of neurons was similar across quiescence and search ripples.

Dependency of spiking across ripple time windows

The apparent relationship between spiking in one epoch and LFP/ripple feature in another epoch could in principle be due to joint spiking across epochs, and not to a true time-lagged modulation. For each unit of each cell type, we calculated the conditional probability of spiking in one time window given a spike from that cell during another window of a ripple event (pre, during, post). Across units from all cell types across all pairs of epochs, a spike in one window typically predicted the absence of spikes in the other ripple window. Median probabilities per cell type and window pair ranged from 0 to 0.33. Thus, LFP fluctuations that occur with a lag from the time of spikes do not appear to be an artifact of latent concurrent spiking.

Discussion

In this study, we showed for the first time in primates that ripple features vary with waking state and memory. By comparing ripple events during quiescent and active periods, we observed that; 1) quiescent ripples have larger amplitudes and larger post-ripple waves. Further examination of awake ripples during the memory task revealed that 2) ripples during remembered trials have greater amplitudes compared to forgotten trials. By analyzing ripple-associated single-unit activity, we found that 3) ripple amplitude is associated with the activity of low-firing cells and putative INs, whereas the peak and elaboration of the post-ripple wave is enhanced by even coarsely timed activity from putative INs.

Ripple amplitude is a measure of the magnitude of the high-frequency ripple oscillation that is thought to reflect both post-synaptic currents and spiking activity by cells within a radius of ~100-200 μ m around a recording electrode (Schomburg et al. 2012). The amplitude is dictated by the size and number of active neuronal ensembles that are made up of principal cells and interneurons (Csicsvari et al. 2000), and can be used to predict if similar ensembles are active across ripples (Taxidis et al. 2015).

We classified cells physiologically into four types using burst firing mode and firing rate, although additional functional cell type divisions are possible. All four cell types showed positive modulation of firing rate during ripples, yet only the activity of low-firing cells and the non-busting high-firing cells was associated with increasing ripple amplitude. Low-firing cells were associated with a decrease in PRW amplitude whereas high-firing cells showed the opposite effect. Critically, we found that spiking effects on ripple and PRW amplitude were strongest when spikes occurred within the ripple window, yet effects were also observable when spiking occurred within the pre- and post-ripple periods. This suggests that the effects of spiking

on the ripple-LFP can be extended in time, consistent with previous reports showing similar delayed spike-LFP relationships (Esghaei et al. 2017). This time-offset cannot be explained by an increase in the conditional probability of spikes in the pre- or post- window and spiking within the ripple as we observe that the probability stays the same. The low-firing cells are likely pyramidal cells, which in the rodent hippocampus are known to display bursting modes (Hemond et al. 2008), with a variable composition across and within subfields (Schwartzkroin 1975; Masukawa et al. 1982). Whereas bursting pyramidal cells have been singled out as necessary for the fast oscillation of ripples (Dzhala and Staley 2004) and for affecting LFP amplitude (Constantinou et al. 2016), our results suggest that non-bursting principal cells are also strongly associated with the amplitude of the fast ripple oscillation. This positive ripple-associated modulation of principal cell activity is consistent with previous findings (Pennartz et al. 2004; Csicsvari et al. 1999; Csicsvari et al. 2000; Klausberger et al. 2003; Klausberger et al. 2004; Le Van Quyen et al. 2008; Hájos et al. 2013). Most of our spikes and ripples (~92%) were detected on the same electrodes and so we were unable to systematically examine the dependence of the relationship spikes have on the ripple field potential as function of distance. Although the bundled tetrode arrays used in this study are not ideal for spatial sampling along the septotemporal and transverse hippocampal axes, this is an interesting area for future investigation given the spatiotemporal spread of ripples along the septotemporal axis (Patel et al. 2013).

The non-bursting high-firing cell type in our study is likely to contain parvalbumin-positive interneurons. Parvalbumin-positive (PV+) and bistratified cells show the greatest ripple-associated increase in spiking rate (Klausberger et al. 2003; Klausberger and Somogyi 2008), with PV+ cells having the greatest excitatory conductance after the ripple peak (Hájos et al.

2013). Axo-axonic and O-LM cells typically display negative modulation where they cease to spike during ripples, whereas CCK⁺ interneurons appear to be unmodulated by ripples (Klausberger et al. 2003; Klausberger and Somogyi 2008). Of the high-firing cells in our data, we only observed a ripple-associated positive modulation in spiking (likely due to limited sampling). Perisomatic-targeting PV⁺ interneurons have been shown to be critical for the initiation of the ripple fast-oscillation through their recurrent connectivity leading to highly organized inhibition which creates opportunity for synchronous pyramidal cell ensemble activity in CA1/CA3 (Ellender et al. 2010; Schlingloff et al. 2014; Stark et al. 2014; Valero et al. 2015). Pharmacologically blocking perisomatic inhibition on pyramidal cells impairs spontaneous ripple activity and decreases sharp-wave ripple amplitude (Stark et al. 2014; Schlingloff et al. 2014; Gan et al. 2017), moreover, inhibitory conductance in pyramidal neurons during ripples is more dominant than excitatory conductance, correlates with ripple amplitude, and depends on PV⁺ interneurons (Gan et al. 2017). The effects of inhibitory neurons also trails the SWR event, where inhibitory synaptic input leads to the collective afterhyperpolarization of local principal cells following ripples, visible as a post-ripple deflection in the LFP (English et al. 2014; Hulse et al. 2016). These results are consistent with our finding that spiking of putative PV⁺ interneurons is associated with both larger amplitude ripples and the post-ripple ‘inhibitory’ wave. The observed increase in ripple amplitude and PRW amplitude during quiescence could therefore be a result of greater PV interneuronal activation in that state compared to during the task. The increased pyramidal-cell synchrony and larger ensemble activity associated with PV IN ripple activity could form a spatiotemporal ‘burst’ to better propagate efferent signals during sleep, consistent with BOLD responses seen in macaques under anesthesia (Logothetis et al.

2012). Other mechanisms are likely to underlie the differences we observed in waking, e.g. during memory-guided search.

Waking ripples are increasingly implicated in memory-guided decision-making (Jadhav et al. 2012; Papale et al. 2016; Wu et al. 2017). In rodents, waking ripples contain a higher proportion of co-activated cell pairs during correct memory recall in a spatial alternation task, suggesting a higher level of coordinated neural activity on remembered trials (Singer et al. 2013). In primates, waking ripples in a visual-search task occur more frequently and closer to the target during remembered trials suggesting a possible role in memory retrieval (Leonard and Hoffman 2017). Since the amplitude indexes the size of ripple-associated ensembles (Csicsvari et al. 2000; Taxidis et al. 2015), it is possible that on average, larger and/or more synchronized ensembles are activated during ripples on remembered trials, though we note that the magnitude of the effects in this study was modest. It's possible that familiar scene stimuli and/or prediction of reward support stronger, more coherent excitatory drive to activate relevant ensembles during the SWR, though determining how such drive modifies ripple magnitude and not other features warrants further study.

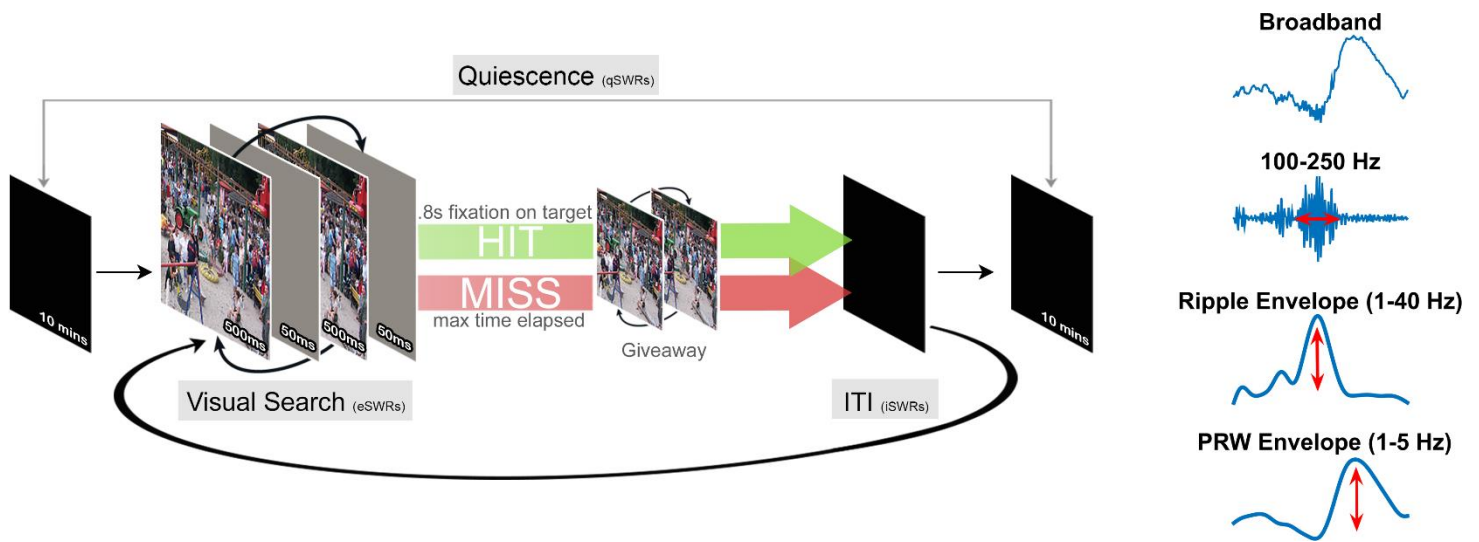


Figure 1. Experimental design of memory-guided visual search task and signal processing.

(A) An original and modified scene are presented in alternation, interleaved with a brief grey mask, requiring effortful search to detect the changing target. A trial ends with a 0.8s fixation on the target for which a fluid reward is delivered (‘HIT’), or when maximum trial time is reached (‘MISS’). A “giveaway” then follows in which the two scenes are displayed without a mask, revealing the target location. A trial ends with a black screen inter-trial-interval (ITI) of 4s before the next trial is presented. During daily recording sessions scenes are presented in blocks of 30 and the task is bookended with two rest periods (quiescence; ≥ 10 mins) where a black screen is presented and animals sleep. See Materials and Methods for more details. (B) The broadband LFP signal is band pass filtered in the ripple band (100-250 Hz), transformed into z-scores, rectified and then low pass filtered (1-40 Hz) to create the ripple envelope whose maximum value represents the ripple amplitude. The PRW envelope is a low pass filter (1-5 Hz) of the broadband signal and its peak represents the PRW amplitude.

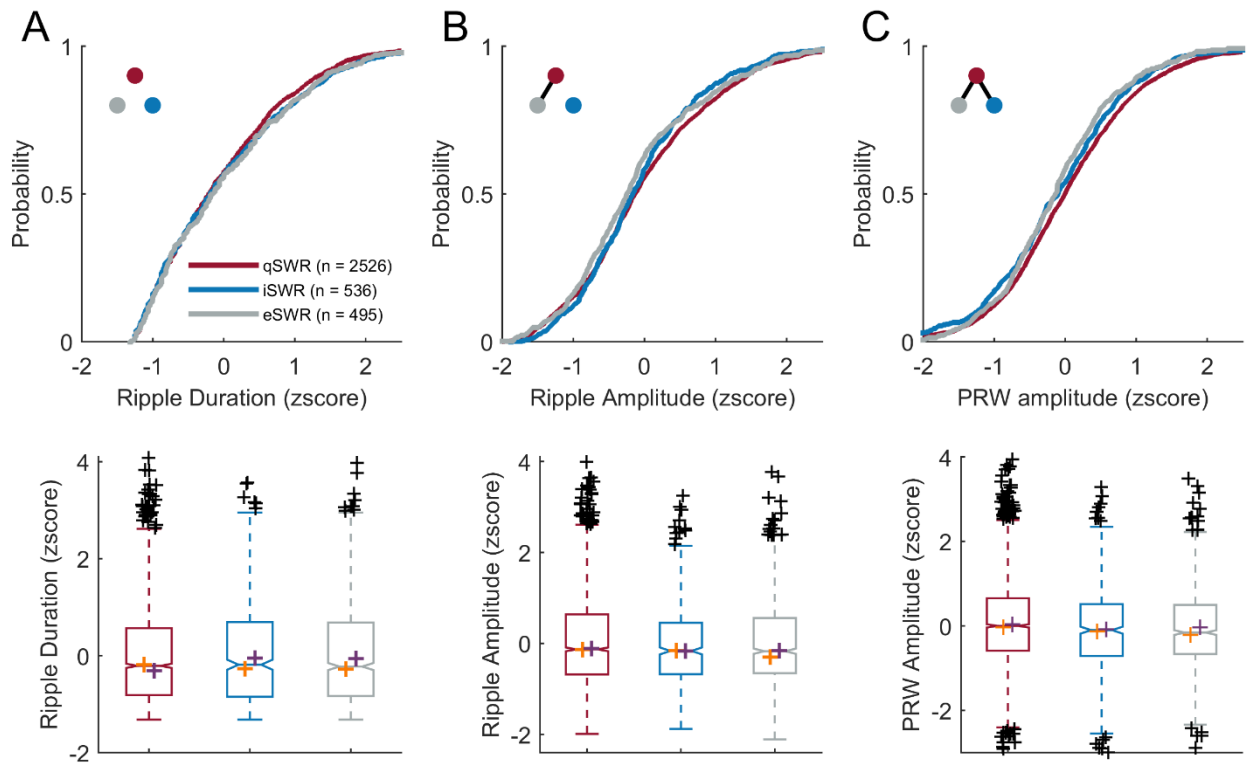


Figure 2. Ripple and PRW amplitudes are greater during qSWRs than iSWRs and eSWRs.

Top; cumulative probability distribution. Black line connecting dots in the top left inset of top panels indicates $p < 0.05$ between groups, as represented by dot color. Bottom; boxplots of corresponding distributions above with median values for each animal plotted in orange (for LU) and purple (for LE) crosses, for SWR duration (A), amplitude (B) and PRW amplitude (C) across qSWRs ($n=2526$), iSWRs ($n=536$) and eSWRs ($n=495$).

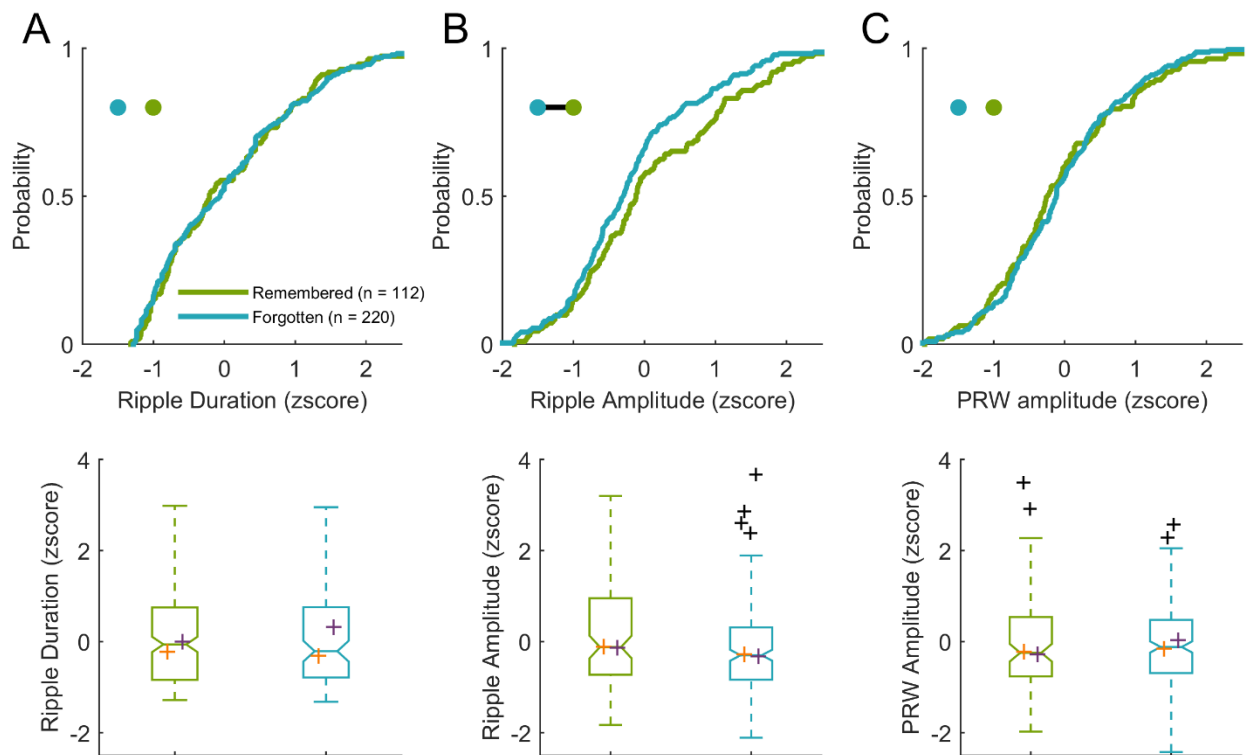


Figure 3. SWR amplitude, but not duration or PRW amplitude, is greater during remembered trials during goal-directed visual search. Top; cumulative probability distribution. Black line connecting dots in the top left inset of top panels indicates $p < 0.05$ between groups, as represented by dot color. Bottom; boxplots of corresponding distributions above. Median values for each animal are plotted in orange (LU) and purple (LE) crosses for SWR duration (A), amplitude (B) and PRW amplitude (C) during remembered ($n=220$) and forgotten ($n=112$) trials.

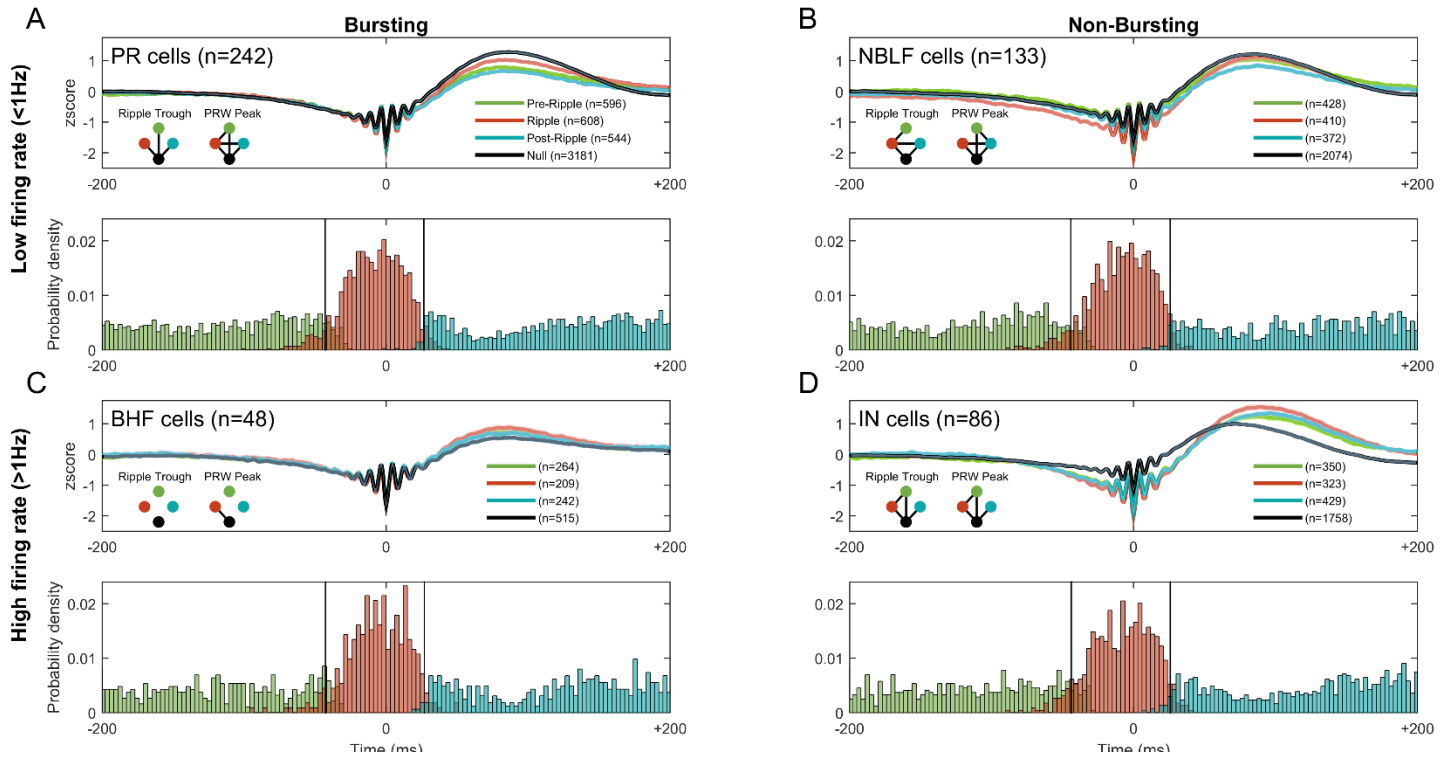


Figure 4. Ripple waveform varies by cell-type activity and spike timing relative to the SWR event. A. Top, mean $\pm 95\%$ confidence intervals of broadband SWRs grouped by putative principal cells' spike-timing into: pre-ripple, ripple, post-ripple wave, and null. Black line connecting dots in the lower left inset of top panel indicates $p < 0.05$ between groups, as represented by dot color, for respective ripple feature. Bottom: probability density histogram of spike counts in a ± 200 ms window centered around the maximum ripple amplitude for putative principal units. (B) as in (A) but for non-bursting low-firing rate units; (C) for bursting high-firing rate, and (D) for putative interneuron units.

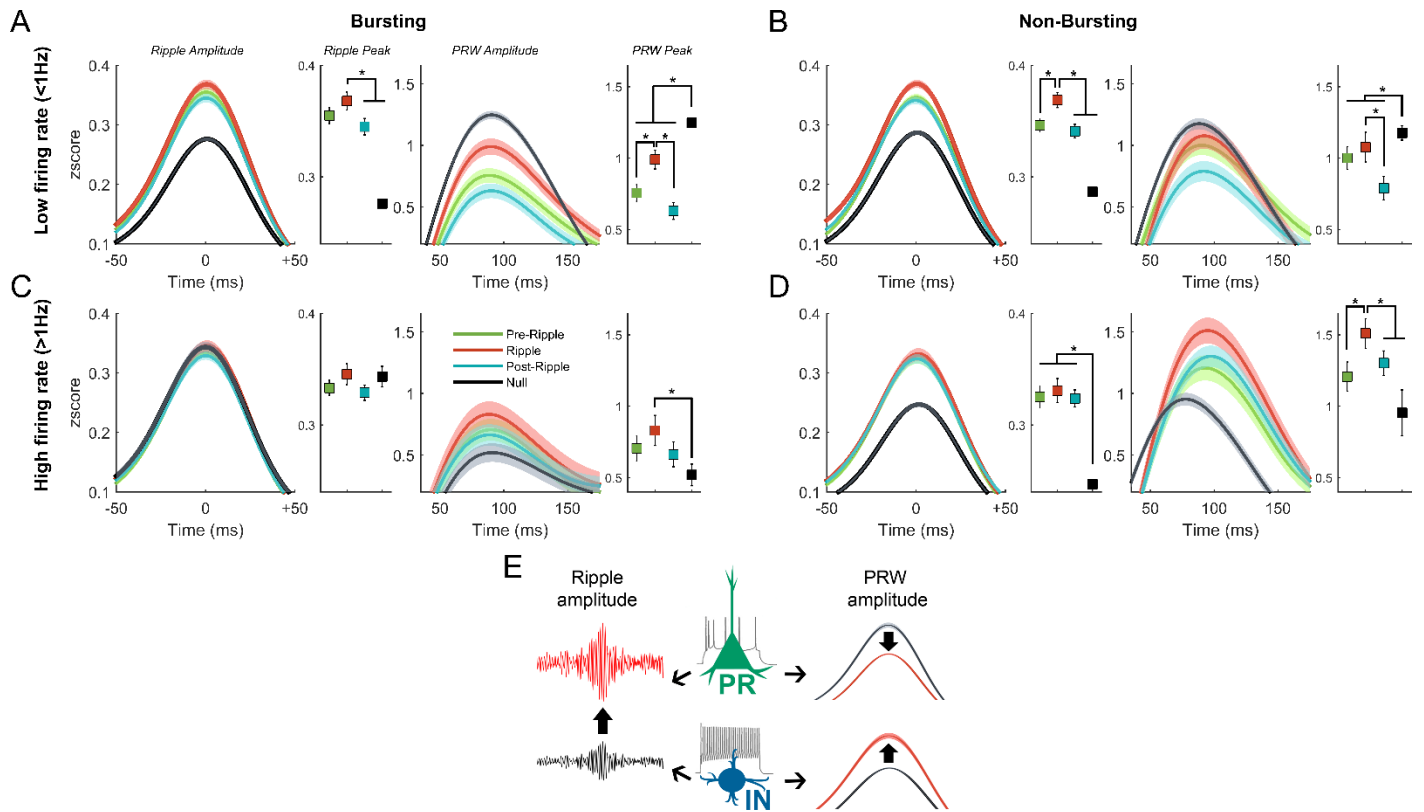
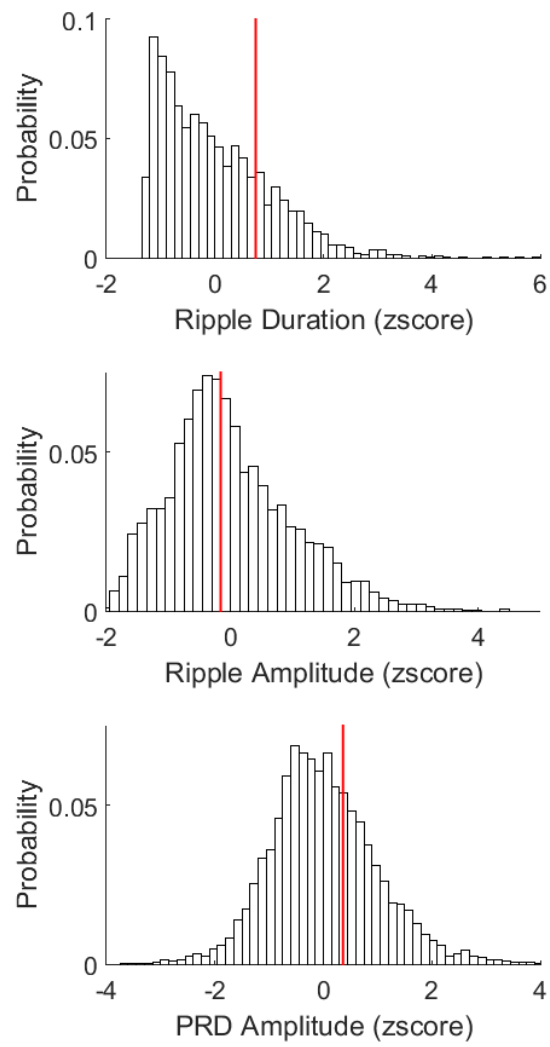
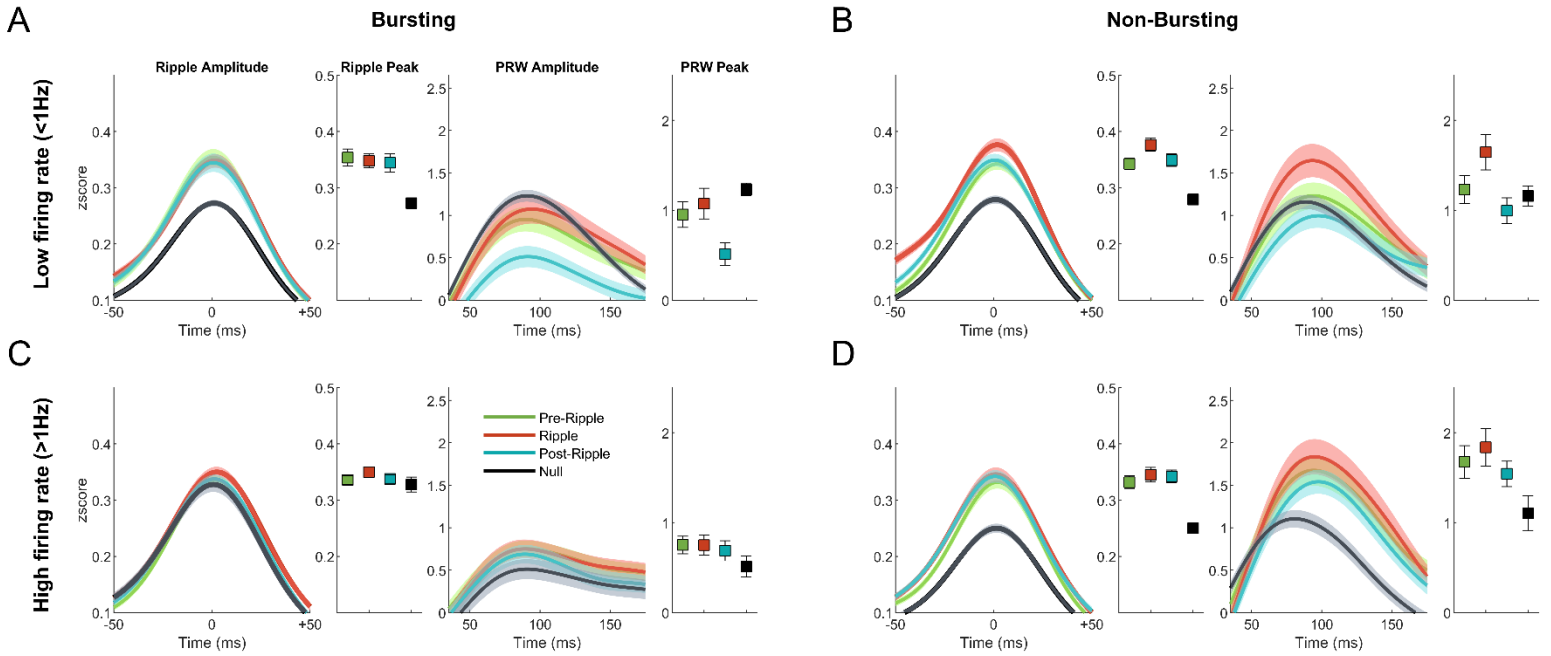


Figure 5. Ripple and PRW amplitudes vary by cell-type activity and spike-timing. Mean $\pm 95\%$ confidence intervals of ripple (left) and PRW (right) envelope amplitudes along with peak values with error bars indicating 95% confidence intervals for principal units (A), non-bursting low-spiking units (B), bursting high-spiking (C) and putative interneurons (D). Schematic of main effects; spikes from principal cells (PR) and interneurons (IN) are associated with greater ripple amplitude, PR spikes are associated with attenuated PRW while IN spikes are associated with enhanced PRW (E). * = $p < 0.05$ between groups.



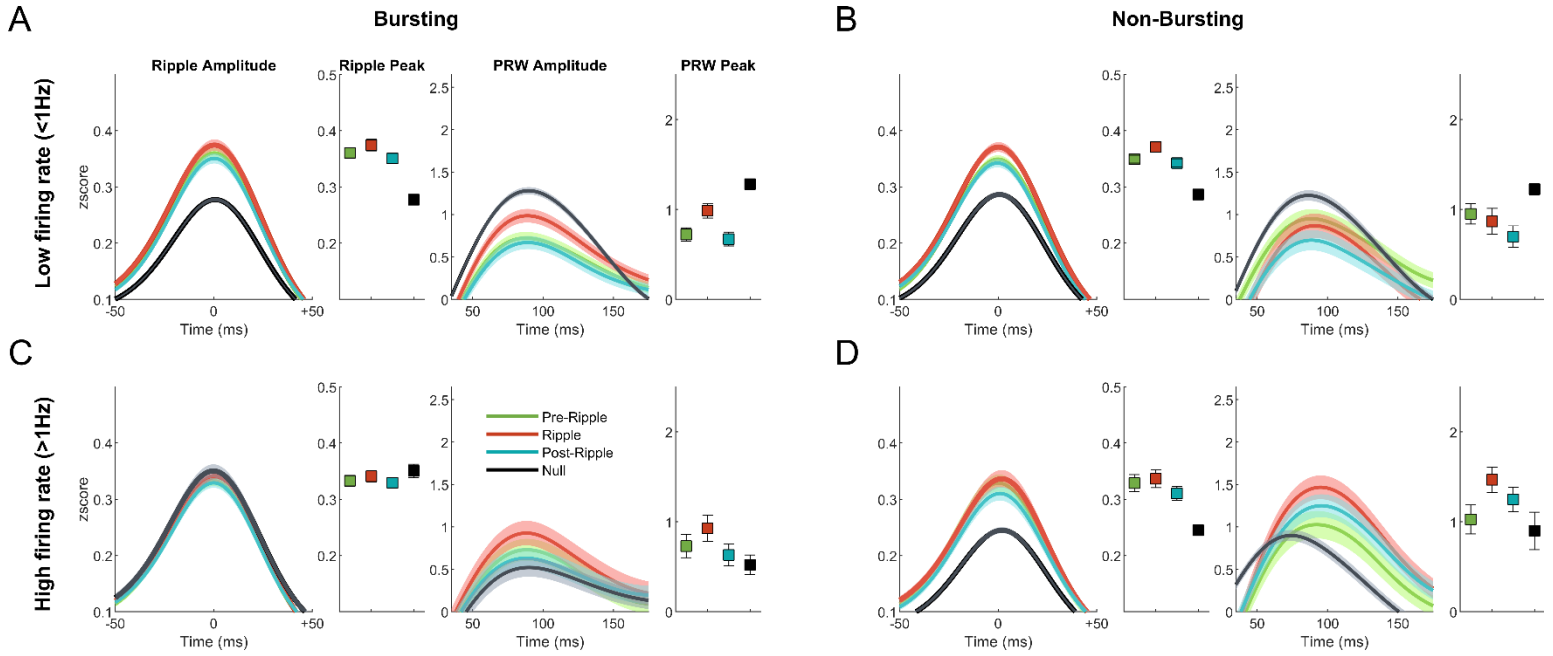
Supplemental Fig 1. Distribution of normalised ripple duration (top), ripple amplitude (middle) and PRW amplitude (bottom). Red line indicates median value for each plot.

Search



Supplemental Fig 2. Variance of ripple amplitude and PRW amplitude by cell-type and spike-timing for search ripples. Mean \pm 95% confidence intervals of ripple (left) and PRW (right) envelope amplitudes along with peak values with error bars indicating 95% confidence intervals for principal units (A), non-bursting low-spiking units (B), bursting high-spiking (C) and putative interneurons (D).

Quiescence



Supplemental Fig 3. Variance of ripple amplitude and PRW amplitude by cell-type and spike-timing for quiescence ripples. Mean $\pm 95\%$ confidence intervals of ripple (left) and PRW (right) envelope amplitudes along with peak values with error bars indicating 95% confidence intervals for principal units (A), non-bursting low-spiking units (B), bursting high-spiking (C) and putative interneurons (D).

Chapter 3: Dissociations in neocortical and hippocampal synchrony for remotely learned episodic memory

A key question in the neuroscience is how the contribution of different brain areas towards memory change with time, as the memory becomes older. In Chapter 1, I reviewed evidence suggesting that episodic memory is initially dependent on the hippocampus but over time this dependence shifts to neocortical areas such as the ACC and RSC (standard model of systems consolidation). I also reviewed evidence showing that dependence on the hippocampus does not change with time, and that the hippocampus is always required to retrieve the contextually rich details of an episodic memory (multiple trace). The large body of literature testing the hypotheses of both models have largely lacked electrophysiological measures of neural activity which represent the main currency of neuronal communication. In this Chapter, we investigated the electrophysiological activity of neural populations in the hippocampus, ACC and RSC simultaneously, as animals completed a memory task using remotely- and recently-acquired memories. Two female macaques learned a set of object-scene associations and were trained to search, find and hold gaze on the correct target for each scene. Twelve to eighteen months later, both animals were chronically implanted with multi-channel recording probes in the hippocampus, ACC and RSC of their left hemispheres. The animals then completed recording sessions where they were shown the remotely learned object-scene sets (constituting a probe for remote memory) along with a novel set (recent memory). We found that remote scenes were associated with oscillation bouts in the ACC (~24 Hz) and RSC (~12 Hz) that were greater in power than during recent scenes. These band limited ranges in each area were the dominant frequencies throughout the task, and their greater power during remote scenes suggests greater

engagement during remote scene processing. The hippocampus had a dominant frequency around ~12 Hz similar to the RSC but we observed no power difference in this range between remote and recent stimuli. We examined how oscillations in the different brain areas are coordinated with eye movements during search and found greater phase locking during remembered remote scenes in the neocortical sites. This suggests a causal relationship with the RSC and ACC oscillations that may be guiding the animals' gaze towards remembered targets. We examined phase synchrony between the hippocampus and the neocortical sites during oscillatory bouts in their dominant frequency bands and found greater synchrony during remembered but not forgotten recent scenes. This demonstrated enhanced communication between the hippocampus and the neocortical areas during recall of recently acquired memories that is not observed for remote memories. For recent memory this synchronisation may serve to facilitate the strengthening of the neocortical memory representations or to facilitate retrieval. For remote memory, it is possible that the ACC and RSC are more engaged given that their memory representations are already strengthened, and that recall may not require the hippocampus. We recognize that our data is correlational and not causal, and that dependence in the typical sense was not explicitly tested in our experiments. Understanding how the different areas are involved in processing remote and recent memory represents the first step upon which future studies can test the causal relationships more directly. Existing tools such as optogenetic inhibition or closed-loop interruption are capable of interrupting neocortical sites and testing whether they impair the recall of remote memory for example. Similarly, interrupting hippocampal-neocortical synchrony may enable testing whether such synchrony is required for recall of recent memory. The implications of our findings and future directions are discussed in greater detail in Chapter 4.

Introduction

A long-standing question in neuroscience is how neural population activity supports memory and how this support changes with time. Current evidence suggests that memory representations form simultaneously within the hippocampal formation and the neocortex during encoding (Tse et al. 2011; Lesburguères et al. 2011; Cowansage et al. 2014; Bero et al. 2014; Kitamura et al. 2017; Abate et al. 2018; Matos et al. 2019). The hippocampal representation is thought to serve as an index of the neocortical memory representation, or the activity pattern activated by an experience. Reactivation of this hippocampal index serves to also reactivate the associated neocortical representation bringing about memory recall (Teyler and DiScenna 1986).

What happens with time as memories get older remains unclear. A sizable cross-species body of literature supports a model where memories are initially dependent on the hippocampus when they are relatively new (or recent) and that as they get older (or remote) they are recalled independently of the hippocampus, relying instead on their neocortical representations (Bontempi et al. 1999; Frankland et al. 2004; Maviel et al. 2004; Teixeira et al. 2006; Restivo et al. 2009; Smith and Squire 2009; Yamashita et al. 2009; Miller et al. 2010; Corcoran et al. 2011; Goshen et al. 2011; Vetere et al. 2011; Tayler et al. 2013; Bero et al. 2014; Cowansage et al. 2014; Einarsson et al. 2015; Kitamura et al. 2017). However, comparably strong evidence also exists suggesting that the hippocampus is required for recall of memories regardless of their age, particularly where the memory is context rich, as in episodic memories (Rosenbaum et al. 2001; Steinvorth et al. 2005; Lehmann et al. 2007; Corkin 2002; Maguire and Frith 2003; Addis et al. 2004; Gilboa et al. 2004; Rosenbaum et al. 2005; Viard et al. 2007; Winocur et al. 2007; Goshen et al. 2011; Sutherland et al. 2008; Sparks et al. 2011; Bonnici et al. 2012; Broadbent and Clark

2013; Denny et al. 2014; Ocampo et al. 2017; Sekeres et al. 2017; Sekeres, Winocur, Moscovitch, et al. 2018).

The retrosplenial cortex (RSC) is one of the neocortical areas that has emerged as an important node in the memory network, particularly in episodic memory in humans (Valenstein et al. 1987; Maguire 2001; McDonald et al. 2001; Osawa et al. 2006; Maddock 1999; Svoboda et al. 2006; Spreng et al. 2009) and nonhuman primates (Buckley and Mitchell 2016), as well as spatial memory in rodents (Sutherland et al. 1988; Whishaw et al. 2001; Vann and Aggleton 2002; Vann and Aggleton 2004; Hindley et al. 2014; Harker and Whishaw 2004; Keene and Bucci 2008a; Keene and Bucci 2008b; Lukoyanov and Lukoyanova 2006; Pothuizen et al. 2008; St-Laurent et al. 2009; Czajkowski et al. 2014; Cowansage et al. 2014; Milczarek et al. 2018; de Sousa et al. 2019). In humans, the RSC is involved in spatial navigation (Maguire 2001; Epstein 2008), processing of objects-in-scenes (Bar and Aminoff 2003; Bar 2004), landmarks (Auger et al. 2012; Auger and Maguire 2013; Mullally et al. 2012; Spiers and Maguire 2006), and especially familiar landmarks (Sulpizio et al. 2013; Sherrill et al. 2013; Shine et al. 2016; Patai et al. 2019). While numerous studies have implicated the RSC as a site of remote memory representation (Anagnostaras et al. 1999; Bontempi et al. 1999; Miller et al. 2014; Frankland et al. 2004; Haijima and Ichitani 2008; Corcoran et al. 2011; Tayler et al. 2013; Katche, Dorman, Gonzalez, et al. 2013; Katche and Medina 2017; Buckley and Mitchell 2016; Todd et al. 2016; Jiang et al. 2018), few imaging studies have found the opposite, with more RSC activity during recent memory (Gilboa et al. 2004; Woodard et al. 2007; Oddo et al. 2010).

Another neocortical region implicated in remote episodic memory – alongside other cognitive functions such as emotion- and reward-related processing - is the anterior region of the cingulate cortex (ACC, Brodmann areas 24 and 32). Animal studies have shown that as time

passes, the role of the ACC in retrieving contextual-based memory increases (Frankland et al. 2004; Teixeira et al. 2006; Takehara-Nishiuchi and McNaughton 2008) and that successful retrieval of remote memory is dependent on an intact ACC (Bontempi et al. 1999; Maviel et al. 2004; Takehara-Nishiuchi and McNaughton 2008; Ding et al. 2008; Restivo et al. 2009; Vetere et al. 2011; Zhang et al. 2011; Weible et al. 2012; Einarsson and Nader 2012; Kitamura et al. 2017). Although the precise contribution of the ACC to remote memory is not completely clear, it is thought that the ACC is the integration site for remembering what actions are associated with what outcomes in order to obtain reward or avoid punishment (Rolls and Wirth 2018; Rolls 2019).

Evidence for the current views on remote memory and its dependence on the hippocampus, RSC and ACC have largely come from human damage and imaging studies or rodent lesion, imaging and optogenetic studies. While these approaches have been useful in determining necessity and sufficiency of brain areas to memory retrieval, they have not contributed to an understanding of the physiology underlying how these areas contribute to the retrieval process. An examination of the electrophysiological responses of the hippocampus, RSC and ACC during recall of remote memory is therefore key to ascertain their involvements and contributions. To address this need, we conducted simultaneous recordings of the neural population activity in the HPC, RSC and ACC using chronically implanted multi-channel electrode arrays in non-human primates, as they completed an episodic-like memory visual search task using remote and recently learned stimuli.

Materials and Methods

Surgical procedures

Two adult female macaques (*Macaca mulatta*, “LE” and “RI”, 12.4 and 9.7Kg respectively) were implanted with indwelling flexible, polyamide-based intracortical multichannel electrode arrays (‘Microflex’, Blackrock electrodes are the currently available models), targeting the hippocampus, cingulate and retrosplenial cortices of the left hemisphere, as described earlier (Talakoub et al. 2019). We successfully acquired neural signal from all areas in both animals except for the cingulate cortex where we managed to acquire signal for only one animal (RI). All surgical and experimental protocols were conducted with approval from the local ethics and animal care authorities (Animal Care Committee, Canadian Council on Animal Care). Surgery was performed and data were collected at York University, Toronto, Canada.

Task design

Both monkeys completed a memory-guided visual search task 12-18 months prior to the present recordings. During this task, a target object was embedded in a naturalistic scene, and presented alongside other objects-in-scenes, comprising the ‘remote’ stimuli used in this study (stimuli N= 276 for LE and 104 for RI). During the present experiments, the animals performed two task versions within each daily session: ACQUISITION and RECALL trials. During an acquisition trial, the scene is displayed for 2s and the animal is allowed to view the scene freely, followed by presentation of a target unique to the scene that is cued by alternating between original (500ms) and complementary colours (60ms), making the target salient and appearing to “pop out” to the observer. Target cueing began at 2s and continued until the target was selected

(designated as a HIT) or until the end of the 7s trial (designated as a MISS). Selection of the target was accomplished by holding gaze in the target region for a prolonged duration (≥ 800 ms). During a recall trial, the scene is presented without the cue and the animal had 7s to find and select the (un-cued) target for juice reward (HIT or remembered) or the trial ends without reward (MISS or forgotten). All trials ended with a giveaway, where the original and colour-modified scene alternate (100ms each x 5) revealing the target to the animal. An inter-trial interval of 4s of black screen followed each trial (Figure 1A).

Scenes were grouped into sets of 12 (monkey RI) or 16 (monkey LE) scenes. Number of scenes in a set was estimated to account for individual performance differences. Each set had three types of scenes; *recent*, *remote* and *highly familiar*. Recent scenes were novel to the animal during the first set (i.e. acquisition). Remote scenes were scenes used during initial task training 12-18 months prior. Highly familiar scenes were a preselected subset of six remote scenes that were repeated regularly throughout the experiment, and therefore have a high HIT rate. Two of these were included in each set. A set was initially presented in acquisition, followed immediately by a recall and a third presentation as either a second acquisition (monkey RI) or a second recall (monkey LE). Whether the third presentation was an acquisition or recall varied across monkeys in a way that yielded optimal performance. The following day's session began with a recall of sets from the previous day. Two new sets were presented each day. Daily sessions started and ended with a 5-minute rest period where a black screen was presented. Eye movements were recorded at 1250 Hz using video-based eye tracking (iViewX Hi-Speed Primate Remote Infrared Eye Tracker). For the analysis we excluded trials where the animals spent $>20\%$ of trial duration looking off-screen (monkey LE: 238/2755 or 8%, monkey RI: 50/1310 or 4%), to ensure only trials where the animals were attending to the task were included.

Neural recordings

Local-field potentials (LFP) were recorded simultaneously from the hippocampus, anterior cingulate and retrosplenial cortices, digitally sampled at 32 kHz using a Digital Lynx acquisition system (Neuralynx, Inc.) and filtered between 0.5 Hz and 2 kHz. The neural signal was downsampled to 1 kHz, and a notch filter (59.9 to 60.1 Hz) was used to remove 60 Hz noise. All offline behavioral and neural analysis was conducted in MATLAB using custom-written scripts and FieldTrip (Oostenveld et al. 2011).

Generalized eigendecomposition (GED)

For analyses of power, phase concentration and coherence, we designed linear spatial filters to isolate the independent, reliable sources that form the dynamics of the neural signal (based on methodology described in (Cohen 2018)). These filters provide a weighted combination of electrode activity guided by the goal of isolating sources of independent variance in multichannel data. Spatial filters were defined by the generalized eigendecomposition (GED) of channels covariance matrices. In GED, two separate covariance matrices are created based on pre-defined criteria resulting in eigenvectors that maximally differentiate the two matrices. If the signal features to be accentuated and those to be attenuated are designated by S and R respectively, the eigendecomposition problem can be written as $SW = WR\Lambda$. The solution of this problem yields W which is a matrix of eigenvectors and Λ that is a diagonal matrix of eigenvalues. The resultant filters, defined by eigenvectors, are then applied to multichannel electrode time series to obtain a set of component time series. If GED was unable to differentiate between various sources of variance, shrinkage regularization was employed 1 percent.

For power and phase concentration analyses, the S matrix was created from 1 second of signal after scene onset (start of trial) and R matrix from 1 second of baseline activity prior to the scene onset. In this design, we sought to attenuate continuous noise in the signal and accentuate the dynamics that are relevant to the task. For coherence analysis, we created the S matrix from the band-pass filtered electrode time series in 10-20Hz. R matrix was then formed from the broadband electrode time series. In this case, the column in W with the highest corresponding eigenvalue then corresponds to the eigenvector that maximally enhances the 10-20Hz frequency activity. The inputs to the GED were signal from multiple channels and trials from a given probe and the output was a single weighted time-series component per trial per probe. The analyses that follow use the resultant GED components that represent the weighted combination of activity from multiple channels in each probe.

Spectral analysis

Grand power was computed using a Fourier transform and a Hanning multi-taper frequency transformation, averaging over the whole duration of search trials including both acquisition and recall trials (N trials for LE = 1152, RI = 422). Mean power spectral density was examined in 500ms windows with a 1ms sliding window conducted on individual trials then averaged across trials. For mean time-frequency spectra, we implemented a Morlet wavelets multi-taper transformation with a width of five cycles and a frequency step-size of 1 Hz.

Phase concentration

To examine phase alignment with eye movement we inspected the LFP signal in 600ms windows centered around fixation onsets (peri-fixation signal). We examined all recall trial fixations split by remembered and forgotten trials. Mean phase concentration spectrograms were computed on the peri-fixation signal (± 1000 ms around fixations) using a sliding window of 200ms in 1ms steps to identify frequency bands for subsequent analysis. Based on these spectrograms which showed phase-concentration between 4-9 Hz, we bandpass filtered the peri-fixation neural signal between 4-9 Hz, then the phase angles of the Hilbert transform were used to compute the mean resultant vector length (or phase concentration). Circular statistical analyses were performed using the Circular Statistics Toolbox for MATLAB (Berens 2009).

Bout detection

For detection of oscillatory bouts of activity in dominant frequency bands, the signal from all trials was bandpass filtered between 10-15 Hz for RSC and 21-26 Hz for ACC, then the envelope of the analytic signal was used to detect oscillatory events crossing a threshold of 2 SDs above the mean, with a minimum duration of 100ms beginning and ending at 1 SD. This time period defined the bout duration and the amplitude was defined as the maximum peak of the envelope. Control bouts were chosen as threshold-crossings in the opposite direction to identify windows of time of weakest bandlimited power (Supp. Fig 1).

Phase synchrony

Phase locking during oscillation bouts was calculated from the cross-spectral density of the bout signal and the corresponding HPC signal using the debiased weighted phase lag index (wPLI). The debiased wPLI measure of phase-synchronization minimizes the influence of volume-conduction, noise and the sample-size bias (Vinck et al. 2011).

Statistical analysis

Proportions of hit rate and bout occurrence across scene types were compared using a two-tailed Chi-square test for comparing proportions. Search times were compared using a two-tailed rank-sum Wilcoxon test. Time-frequency spectra were compared using nonparametric permutation tests using the Monte Carlo sampling method and a cluster-based correction for multiple-comparisons. To test for statistical significance of differences between phase concentration and synchrony (wPLI values) during the recent and remote conditions, we performed a nonparametric permutation test with the difference in phase concentration or coherence between conditions as our test statistic. The test statistic was calculated for each frequency bin, then bins whose statistic value was <2.5th or >97.5th percentiles were selected, and cluster-level statistics were calculated by summing the test statistic within a cluster. This testing method corresponds to a two-tailed test with false-positive rate of 5% corrected for multiple comparisons across frequencies (Nichols and Holmes 2002; Maris and Oostenveld 2007; Jutras et al. 2009).

Results

Overall, we recorded 62 sessions (LE = 37, RI = 25), including 926 acquisition (LE = 686, RI = 240) and 1870 recall trials (LE = 1386, RI = 485). Both animals had a >90% hit rate (i.e. target found %) on acquisition trials, and during recall, a higher hit rate on highly familiar scenes compared to recent (LE: $X^2(1, 300) = 268, p < 0.05$, RI: $X^2(1, 395) = 44, p < 0.01$) and remote scenes (LE: $X^2(1, 312) = 138, p < 0.05$; RI: $X^2(1, 448) = 23.0, p < 0.001$). Remote scenes had a higher hit rate compared to recent scenes (LE: $X^2(1, 395) = 35, p < 0.01$; RI: $X^2(1, 395) = 44, p < 0.01$). Correspondingly, recall during highly familiar trials had shorter search times than recent (LE: $z = 2.40, p < 0.05$, RI: $z = 6.45, p < 0.001$) and remote trials (LE: $z = 4.52, p < 0.001$, RI: $z = 2.63, p < 0.01$). Remote scenes were found faster than recent scenes in one animal (RI: $z = 4.55, p < 0.001$), while for the second animal there was no difference in search time for remote and recent scenes (LE: $z = -1.58, p = 0.11$; Figure 1B).

Remote memory is associated with greater beta and gamma power in the RSC and ACC

We first examined the grand spectral power during search and found a prominent peak between 10-20 Hz in the RSc and HPC of both animals (Figure 1D). We then examined whether spectral power in this range varied by memory age in two main epochs; *scene-onset* consisting of the first 2s of acquisition and recall trials when the scene is first presented, and *remembered target* consisting of the last 1.5s before a trial-ending fixation on remembered recall trials (Figure 2). A nonparametric permutation test revealed greater 10-15 Hz mean power spectral density in the RSC between 0.5-2s after scene-onset (Figure 2B) and 1.25-0.25s before trial-end on remembered trials (Figure 2F). In the time-frequency representation, a non-parametric cluster-

based permutation test showed remote trials to have greater power ($p < 0.05$) in a cluster beginning as early as 1s after scene-onset (Figure 2C) and 1.25s before trial end (Figure 2G). We found no differences in HPC power between remote and recent trials (Figure 2D and 2H).

An examination of the highly familiar scenes revealed a similar trend as remote scenes with greater band limited power in the RSC compared to recent scenes (Supp. Fig. 2). We then isolated a group of recent scenes and presented them to the monkeys in recall mode for a total of ~10-20 times over daily recording sessions for two weeks to observe if the spectral response would change. The response to the repeated scenes resembled that of remote scenes with greater power occurring earlier during the onset epoch (Supp. Fig 3). The grand spectral power in the ACC during search revealed a prominent peak at ~22-28Hz (Supp. Fig 4A). Power in this band was greater during the onset epoch of remote trials in a cluster between 1.75-2s after onset (Supp. Fig. 4E).

General linear regression model

We observed that the bandlimited 10-15 Hz RSC oscillation occurs in brief bursts or bouts throughout search trials. We then used an envelope thresholding approach to identify suprathreshold RSC bouts of activity between 10-15 Hz (described in Methods, Supp.Fig.1). This was followed by a linear regression model to examine how task variables contribute to the magnitude of these bouts. We detected 4564 bouts across all trials (LE: 3278, RI: 1286), with 1290 bouts during acquisition (LE = 894, RI = 396) and 3274 during recall trials (LE = 2384, RI = 890). Bouts occurred more frequently during recent compared to remote trials during both acquisition (LE; $X^2(1, N=894) = 6.18, p < 0.05$, RI; $X^2(1, N = 396) = 28.2, p = 1.1 \times 10^{-7}$) and

recall (LE; $X^2(1, N=2384) = 42.3, p = 7.6 \times 10^{-11}$, RI; $X^2(1, N=890) = 336.4, p < 0.01$). Remote recall trials therefore had fewer, but greater bouts compared to recent trials.

A regression analysis was used to test whether the following task variables on recall trials predicted bout magnitude; scene age (remote or recent), search time, time from bout peak to trial end, the screen quadrant containing the target (to test for visual-field effects given our unilateral recordings), time to fixate on target and animal ID (to test for differences in bout amplitude by animal). The model accounted for 32% of the variance in bout amplitude ($F(6,3090) = 173, p < 8.3 \times 10^{-242}, R^2 = .32$), and showed that scene age ($t = -3.9, p < 0.001$), search time ($t = 4.2, p = 2.0 \times 10^{-5}$), bout peak to end ($t = 5.87, p = 4.64 \times 10^{-9}$) and animal id ($t = 2.8, p < 0.01$) predicted bout amplitude.

Phase synchrony between eye movements and neural oscillations

We then examined the degree by which the eye movements during search are temporally coordinated with oscillations in the different brain areas. We measured the phase concentration in a +/-300ms window around fixation onsets throughout trials and found that phase alignment was concentrated between 4-9 Hz. Phase concentration was greater in the RSC (Figure 3A and 3B) on remote scenes beginning shortly before fixations (RI: -175 ms, LE: -75 ms) and lasting until 125-200 ms post-fixation compared to recent scenes. This larger phase concentration on remote trials was present only on remembered but not forgotten trials (Supp Fig. 1). Although this phase alignment increased in the HPC as well during both remembered and forgotten trials, we found no difference between recent and remote scenes (Figure 3C and 3D). Collapsing trials by scene age, we compared phase concentration between remembered and forgotten trial

fixations in the HPC based on recent reports showing greater phase concentration during remembered trials (Kragel et al. 2020) but found no differences ($p>0.1$). In the ACC, there was a similarly greater phase alignment to fixations during remembered remote trials that began at the fixation points extending until ~200ms post-fixation (Supp. Fig 7).

Interareal phase synchrony

Having identified bouts of band-limited activity in the RSC that occur with greater power during remote scenes, we examined RSC-HPC synchrony during these bouts using the debiased weighted phase lag index (wPLI). First, we examined RSC-HPC bout synchrony during search, ITI and rest periods of the recordings and found synchrony to be most prominent during search. We then examined synchrony during search by scene type and compared synchrony across remembered and forgotten trials. We found that during remembered, but not forgotten or control trials (periods of low bout magnitude), RSC-HPC synchrony was greater for recent compared to remote scenes in the ~25-40 Hz range (Figure 4). This difference in synchrony was present only during recall trials and not during acquisition trials. We found similar synchrony between ACC-HPC in the low (20-40) and high gamma (100-120) Hz range similarly only during remembered recent scenes (Supp. Fig 5).

Discussion

In this study, we measured the neural population activity in the hippocampus, RSC and ACC simultaneously as macaques completed an episodic-like memory task. Our findings are 1) onset of remotely learned stimuli is associated with greater beta power in the RSC and greater gamma power in the ACC, 2) neural oscillations in the RSC and ACC phase-lock with eye movements during successful recall of remote memory, and 3) greater hippocampal - neocortical phase synchrony during recent memory recall.

We observed greater beta in the RSC during recall of remote memory. Our group has previously shown this to be a prominent band in this region of the primate brain during normal waking behaviours (such as walking and grooming) (Talakoub et al. 2019). Consistently, it was also the most prominent band during visual search in the present study (Figure 1E). The power increase in this band during remote memory suggests that the retrosplenial cortex may be more greatly involved in processing remote compared to recent visual spatial memory. In line with this interpretation, we found stronger phase-locking between retrosplenial cortex oscillations and eye movements made during successful recall of remote memory that began shortly before fixations. This temporal coordination observed during remembered but not forgotten trials, suggests a role for the RSC in guiding gaze towards the correct target on this task. Similar phase-locking of RSC with fixations to predict remembered trials has been reported using MEG in humans during the encoding of visual stimuli that would later be remembered (Staudigl et al. 2017). Although we observed phase-locking of fixations to hippocampal activity, as has previously been shown (Hoffman et al. 2013; Andrillon et al. 2015; Katz et al. 2018), we found no difference between remote and recent memory, suggesting a unique role for the RSC in the recall of remote memory. Results from the ACC were similar, showing greater power in its dominant gamma band during

remote trials and greater phase locking to eye movements during successful recall of remote scenes. These findings suggest a unique role for the ACC and RSC in processing remotely learned episodic-like memory. Such a role has been observed using ensemble tagging (Tayler et al. 2013; de Sousa et al. 2019), immediate early gene (Bontempi et al. 1999; Maviel et al. 2004; Frankland et al. 2004; Katche, Dorman, Gonzalez, et al. 2013; Katche and Medina 2017), lesion (Haijima and Ichitani 2008; Todd et al. 2016; Jiang et al. 2018) and pharmacological studies (Corcoran et al. 2011), macaque lesion studies (Buckley and Mitchell 2016), as well as human case (Maguire 2001) and imaging studies (Benuzzi et al. 2018; Patai et al. 2019).

We found greater coupling between RSC/ACC and HPC during recent memory recall in the gamma band. Strikingly, we observed this coupling only during remembered trials, and not during forgotten trials. This coupling based on the phases of the oscillations in the two brain areas suggests greater communication (Fries 2015), although the directionality and functional cause of this coupling remains to be understood. While this coupling could underlie consolidation of newly acquired target-scene associations, it could also indicate retrieval of recently acquired memory. That we only observed this coupling during recall and not acquisition suggests that this may be a retrieval mechanism. The RSC and HPC have strong bilateral connections (Kobayashi and Amaral 2007) and form part of an extended network of areas involved in episodic memory and spatial navigation (Ranganath and Ritchey 2012). This coupling was not observed during remote memory recall suggesting that hippocampal neocortical interaction is not needed to support recall of remote episodic-like memory. Although our findings are correlational, they point to a greater role for neocortical areas in processing remote memory and greater hippocampal-neocortical interactions during recent memory. These findings support standard consolidation theory which suggests a greater role for neocortical areas

in supporting remote memory and a decreased role for the hippocampus. Similar observations have been reported in rats using inhibitory avoidance learning where memory initially requires both HPC and RSC (Katche, Dorman, Gonzalez, et al. 2013), but after two weeks no longer requires the HPC (Izquierdo et al. 1997) and remains dependent on RSC (Katche, Dorman, Slipczuk, et al. 2013).

In summary, our findings represent the first electrophysiological evidence of RSC involvement in the processing of remote memory in primates. We found greater RSC involvement in remote memory recall and preferential RSC-HPC synchrony during recent memory suggesting functional reorganization of memory representation with age.

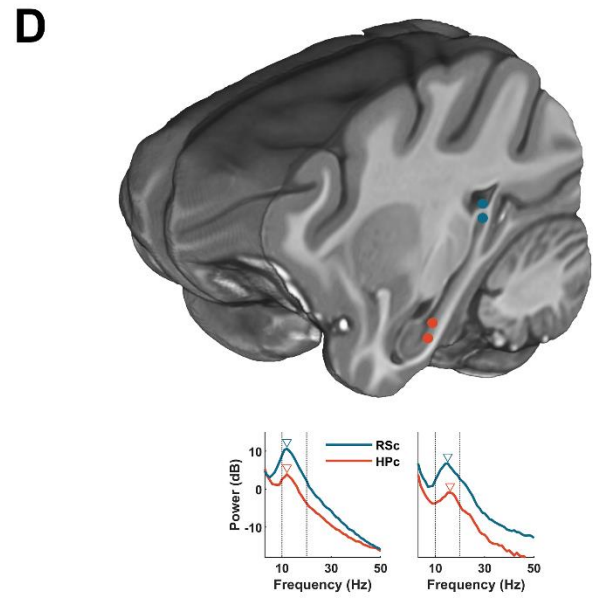
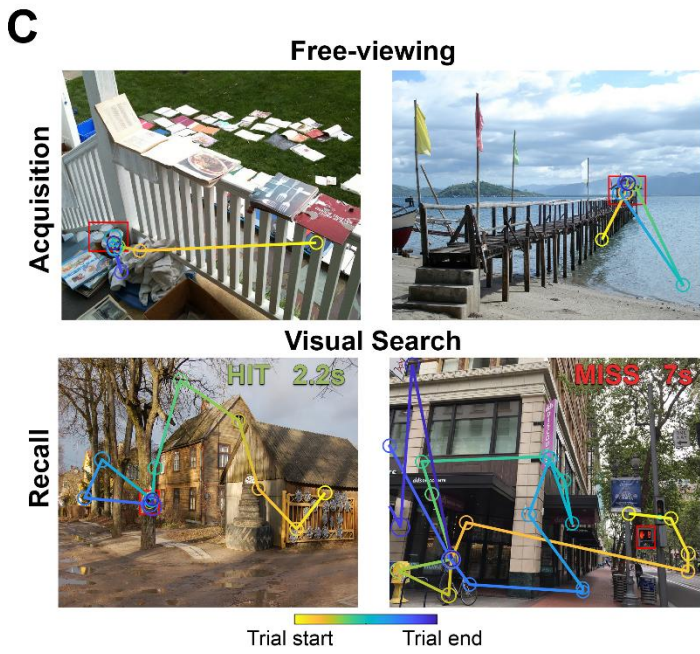
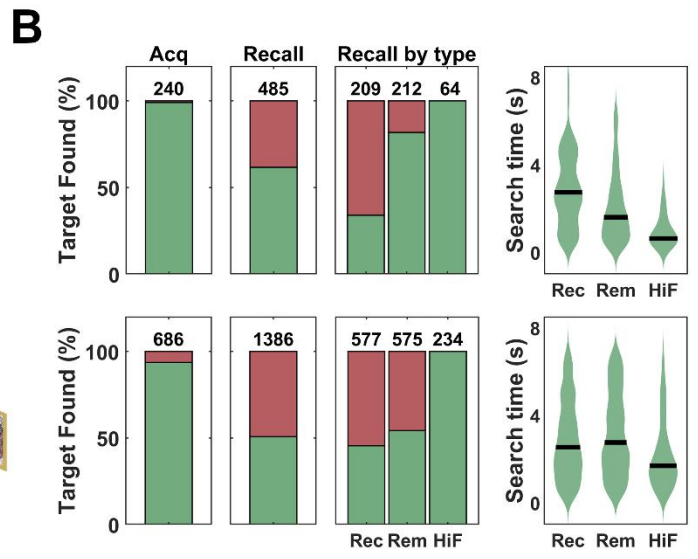
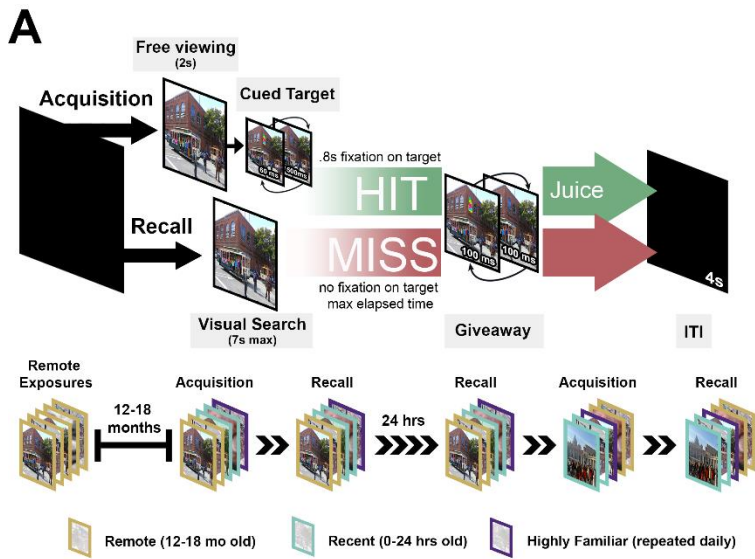


Figure 1. Experimental design, task performance and recording locations. **A)** *Top*; during acquisition, a trial begins with 2s of free-viewing followed by target cueing through quick alternations between a colour-modified version and the original. During recall, the scene is presented without the cue. A trial ends with a 0.8s fixation on target for which a fluid reward is delivered (HIT), or when the maximum trial time is reached (MISS). A *giveaway* presents the cued-target for a longer duration (100ms) at the end of a trial followed by the ITI (4s). *Bottom*; scenes were grouped in sets of 12-16 scenes and were of three types: ‘remote’ scenes which were presented 12-18 months prior, ‘recent’ which were novel scenes and ‘highly familiar’ scenes which were six remote scenes with a high HIT rate. In the present recordings, sessions began with a set shown in acquisition followed immediately by recall. Twenty-four hours later, the set is shown in recall before another set is presented in acquisition followed by recall. **B)** *Top*; from left, target found % for acquisition trials, recall trials (both immediate and next day recall), recall trials by scene age and search time during recall per scene age for monkey RI. Black bands in violin plots indicate mean value. *Bottom*; same as top but for monkey LE. Values above bars indicate number of Target Found trials in respective condition. **C)** *Top row*: example scan paths during 2s of free-viewing 2s on acquisition trials of remote scenes. Outlined in red is the target. Note that gaze goes towards the target even before the cue, suggesting preserved memory of the target. *Bottom row*: example scan paths for a HIT (or remembered trial) and a MISS (forgotten trial) during recall trials. Inset in top right of each scene indicates search time in seconds. **D)** Electrode localizations, RSC in blue and HPC in red. Insets: mean power during search for RSC and HPC. Vertical lines indicate where 10 and 20 Hz lie.

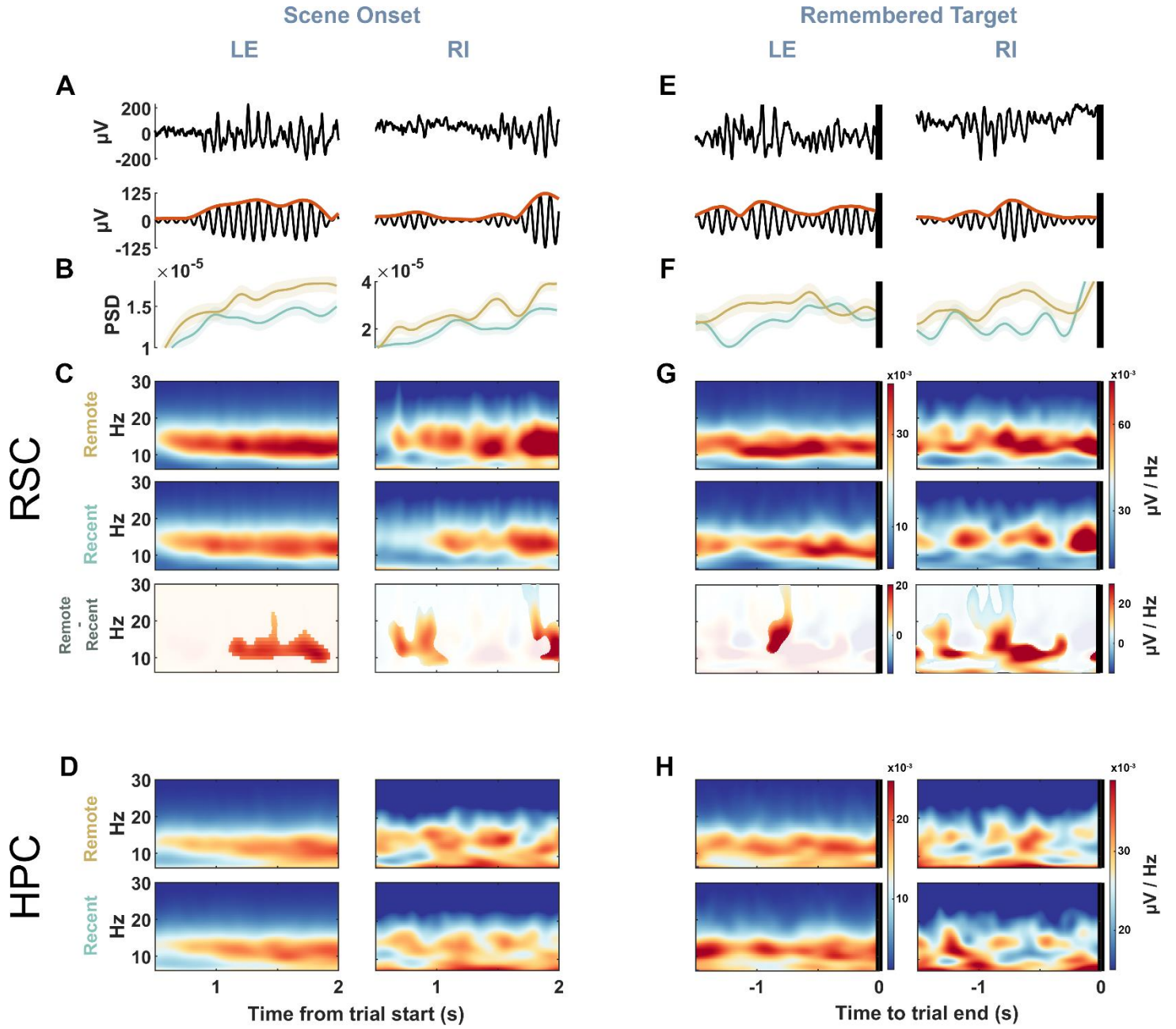


Figure 2. Retrosplenial cortex (RSC) exhibits greater 10-15 Hz power during remote scenes. A) Top; Example broadband signal during first 2s after trial onset when a scene is presented. Bottom; 10-15 Hz filter of signal above. LE indicates data for animal 1, and RI on right indicates data for animal 2. B) mean power spectral density of 10-15 Hz band using 500ms windows in 1ms steps. Shading indicated 95% bootstrap confidence interval. C) Top; mean spectrogram of remote trials (LE n = 594, RI n = 152), middle; recent trials (LE n = 605, RI n = 240), bottom; remote – recent difference spectrogram with the non-greyled region representing clusters with a difference of $p < 0.05$ in a cluster-based permutation test corrected for multiple comparisons. D) Top; mean spectrogram of remote trials in the hippocampus, bottom: recent. E-H same as A-D but for the last 1.5s before the end of remembered trials.

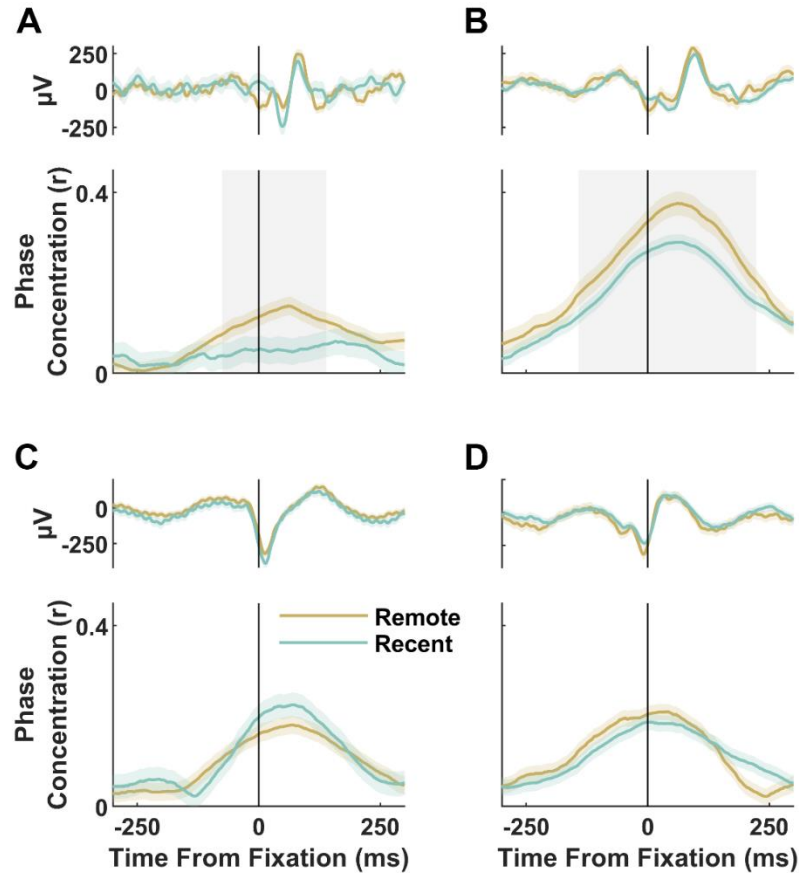


Figure 3. Eye movements on remembered remote trials are phase locked with the phase of retrosplenial cortex (RSC) theta oscillations. A) Top; mean LFP locked to fixations on remembered trials, bottom; mean phase concentration of RSC oscillations around fixations for monkey LE (remote $n = 2134$, recent $n = 1042$). Light shade around mean traces represent 95% bootstrapped confidence intervals. Grey shading represents $p < 0.05$ difference between remote and recent phase concentrations in a two-tailed cluster-based permutation test. B) same as A) but for animal RI (remote $n = 1267$, recent $n = 2921$). C) and D) are similar to A) and B) but for the hippocampus of each animal respectively (LE; remote $n = 2054$, recent $n = 1031$, RI; remote $n = 1297$, recent $n = 2972$).

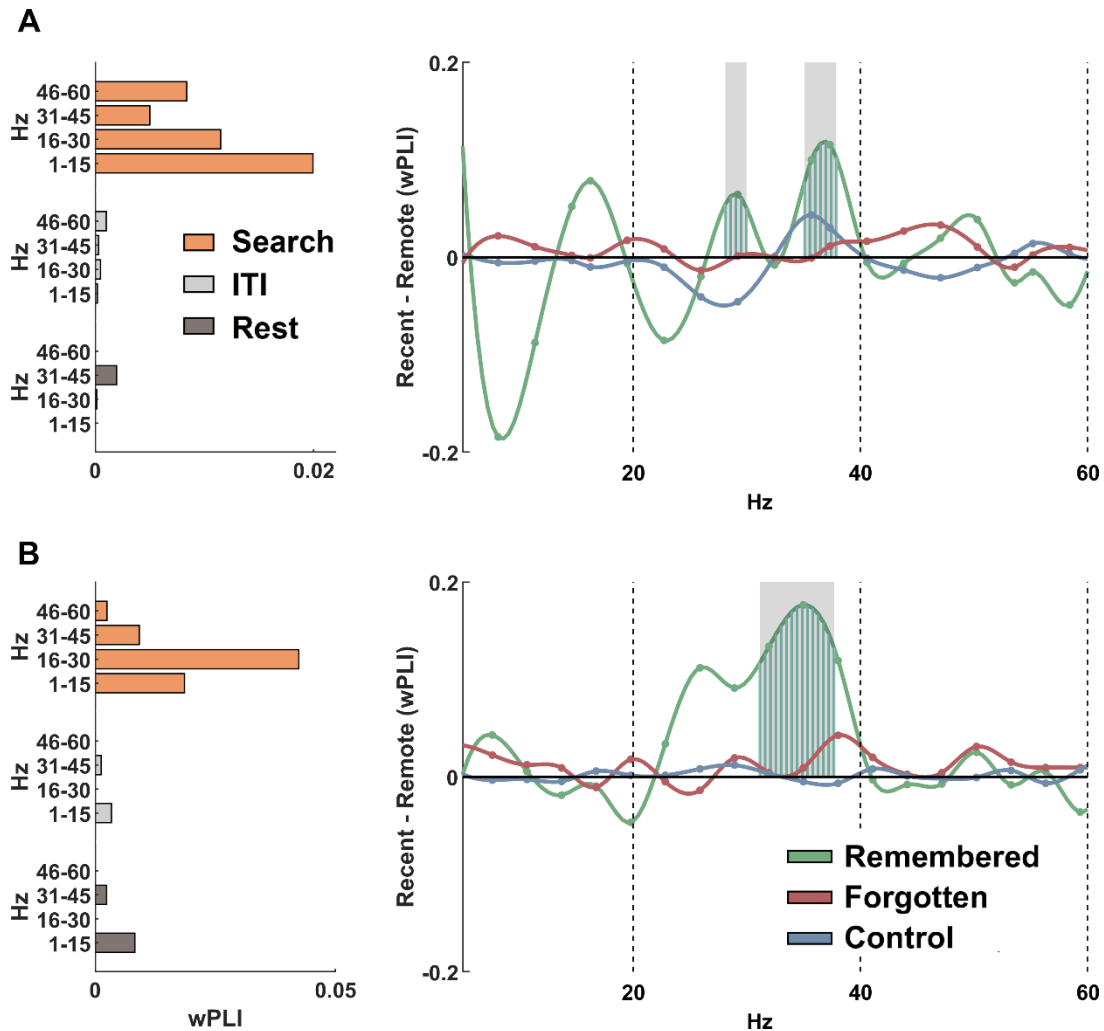
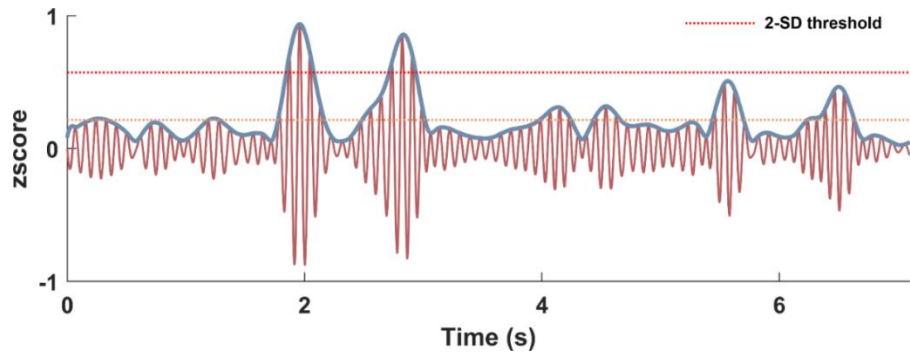
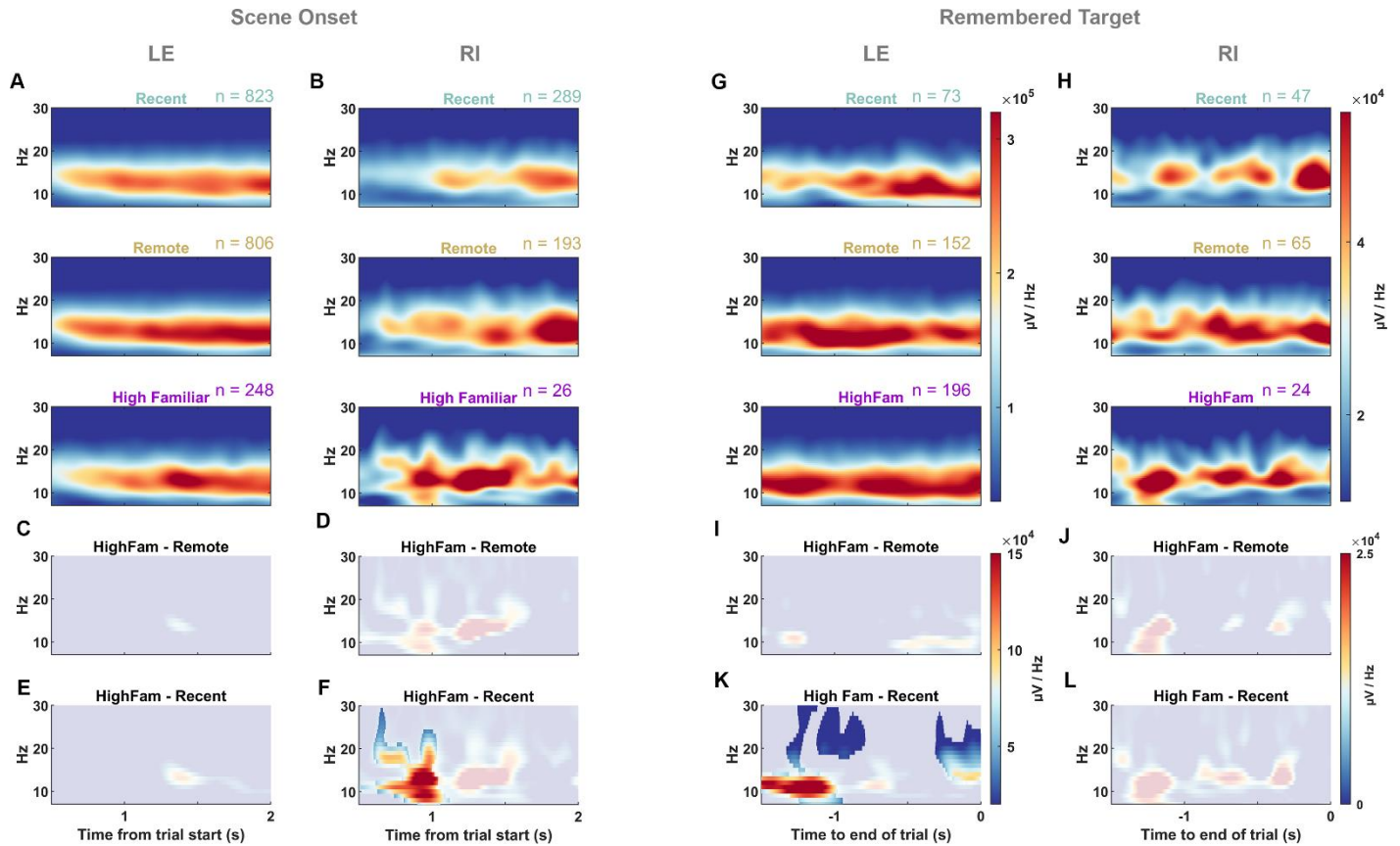


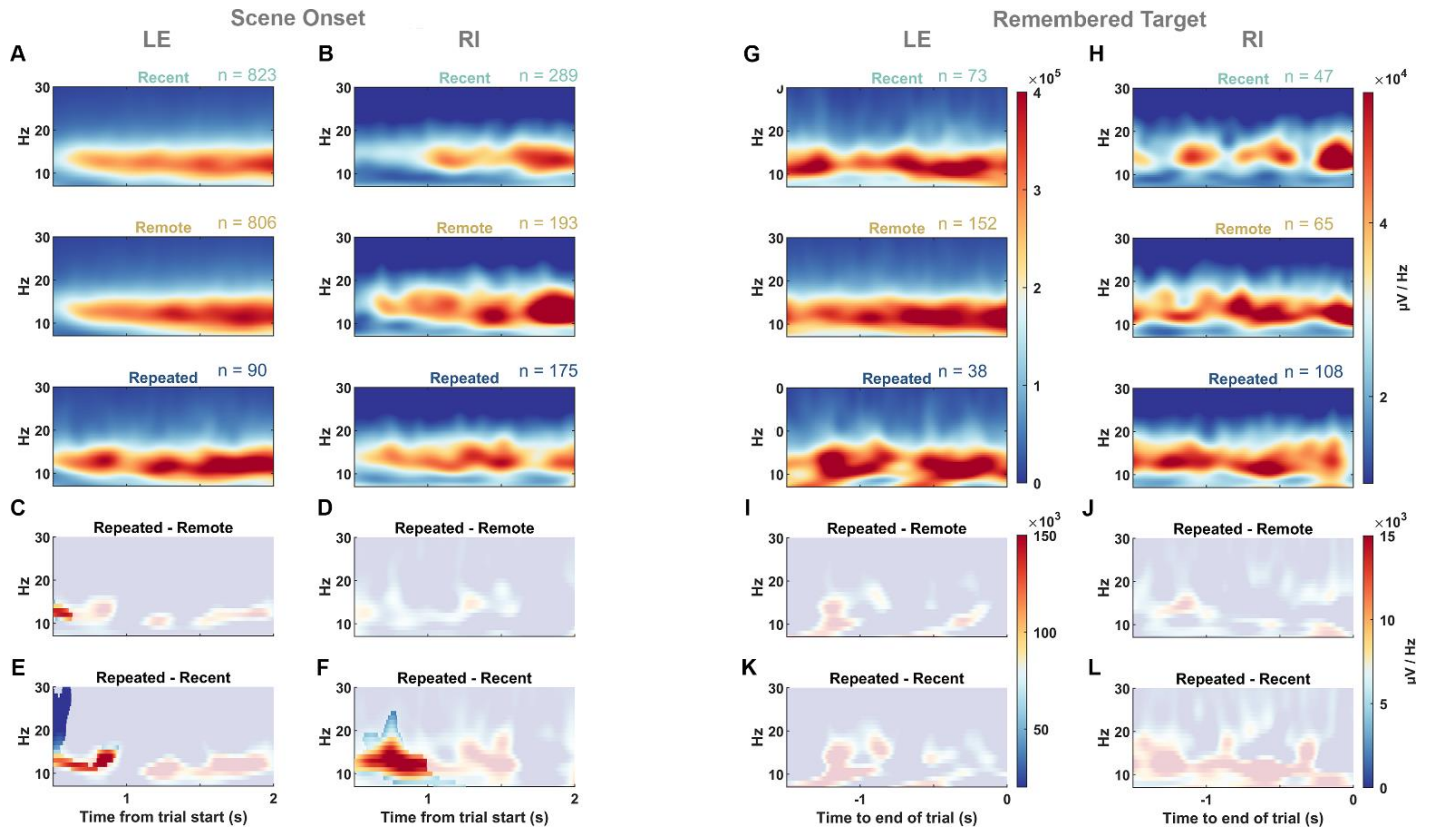
Figure 4. Greater retrosplenial hippocampal phase synchrony during remembered recent scenes. **A** *Left*; phase-locking (wPLI) by frequency during 10-15 Hz RSC bouts across rest ($n = 3346$), ITI ($n = 6423$), search ($n = 2384$) for LE. *Right*; difference in RSC-HPC phase-locking between bouts on recent and remote trials during remembered (recent = 112 bouts, remote = 204 bouts), forgotten (recent = 1159, remote = 909) and control (recent = 2937, remote = 2331) bouts. Vertical blue bars from zero indicate frequencies with a permutation test difference of $p < 0.05$. **B** Same as A but for animal RI, *left*; rest ($n = 2338$), ITI ($n = 1937$) and search ($n = 890$), *right*; remembered (recent = 106, remote = 176), forgotten (recent = 468, remote = 140) and control (recent = 1108, remote = 371). Grey shading indicates frequencies where the difference between recent and remote is $p < 0.05$ in a cluster-based permutation test.



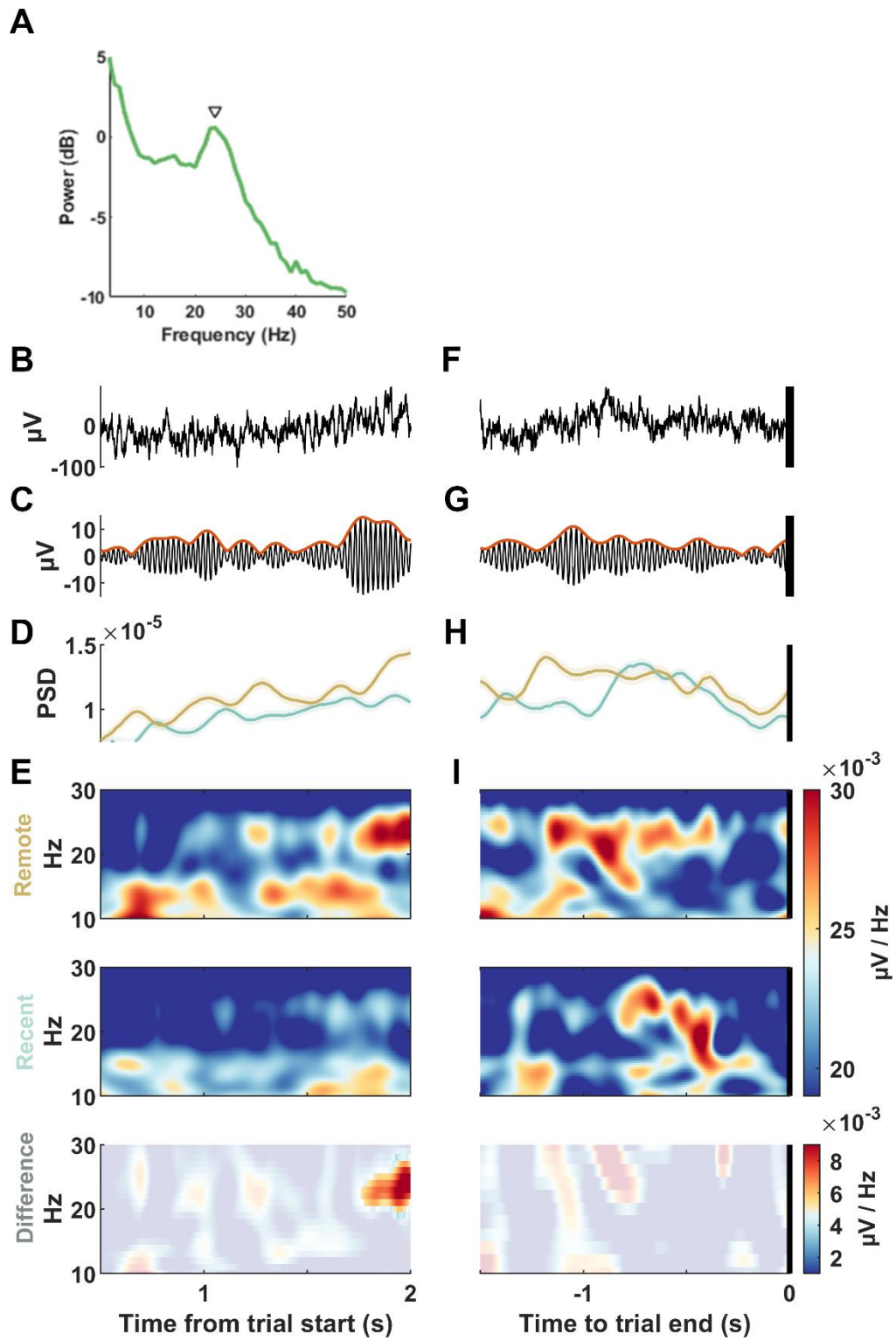
Supplemental Figure 1. Threshold-based bout detection example. Maroon trace is the 10-15 Hz filter of the broadband signal during a 7s trial. Purple trace is the upper bound envelope. Orange dotted line represents the mean of the envelope and the red dotted line represents the threshold at 2 standard deviations above the envelope mean. In this example trial, there are two threshold-crossing bouts detected.



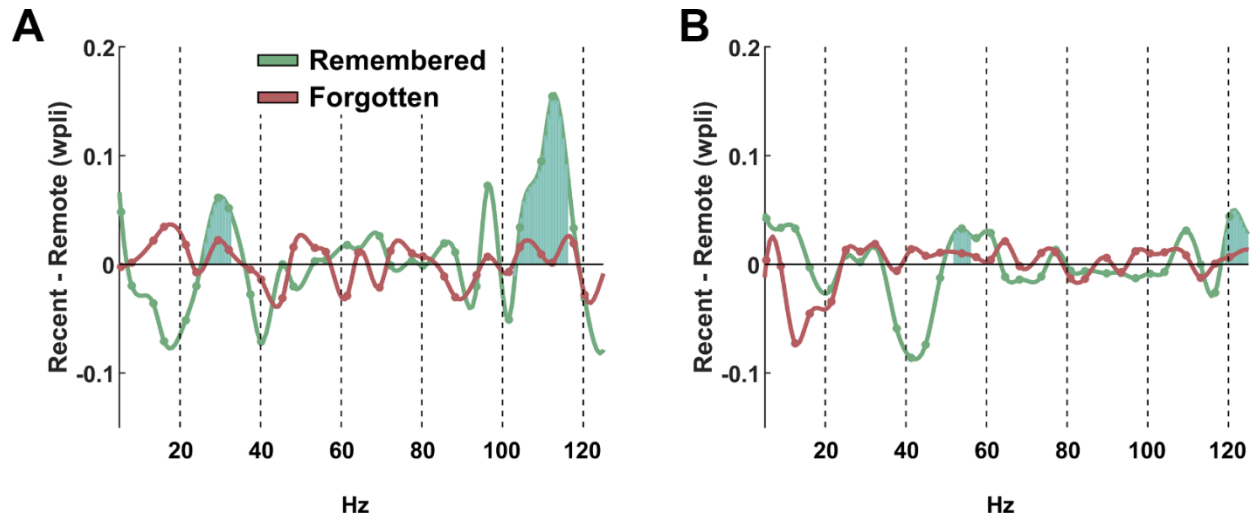
Supplemental Figure 2. Greater 10-15 Hz power in the retrosplenial cortex (RSC) during highly familiar scenes compared to recent scenes. A) *Top*; mean spectrogram of recent trials ($n=823$), *middle*; remote scenes ($n=806$), *bottom*; highly familiar scenes ($n=248$) for monkey LE. B) same as A) for monkey RI, recent $n = 289$, remote $n = 193$, highly familiar $n = 26$. C) Mean spectrogram difference between highly familiar and remote scenes. D) same as C) for monkey RI. E) Mean spectrogram difference between highly familiar and recent scenes. F) same as E) for monkey RI. G), I) and K) same as as A) C) and E) but for the trial end epoch of remembered trials, recent $n = 73$, remote $n = 152$, highly familiar $n = 196$. H), J) and L) same as G), I) and K) but for monkey RI, recent $n = 47$, remote $n = 65$, highly familiar $n = 24$.



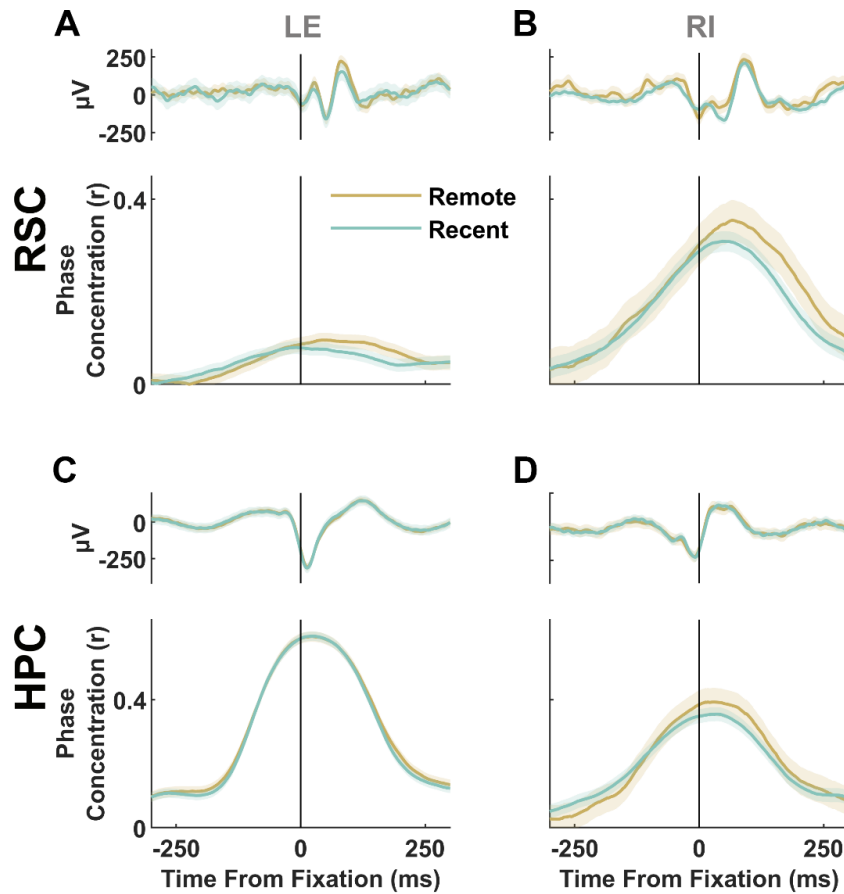
Supplemental Figure 3. Greater 10-15 Hz power in the retrosplenial cortex (RSC) during repeated recent scenes compared to recent scenes. A) *top*; mean spectrogram of recent trials (n=823), middle; remote scenes (n=806), *bottom*; repeated recent scenes (n=90) for monkey LE. B) same as A) for monkey RI, recent n = 289, remote n = 193, highly familiar n = 175. C) Mean spectrogram difference between repeated and remote scenes. D) same as C) for monkey RI. E) Mean spectrogram difference between repeated and recent scenes. F) same as E) for monkey RI. G), I) and K) same as as A) C) and E) but for the trial end epoch of remembered trials, recent n = 73, remote n = 152, highly familiar n = 38. H), J) and L) same as G), I) and K) but for monkey RI, recent n = 47, remote n = 65, highly familiar n = 108.



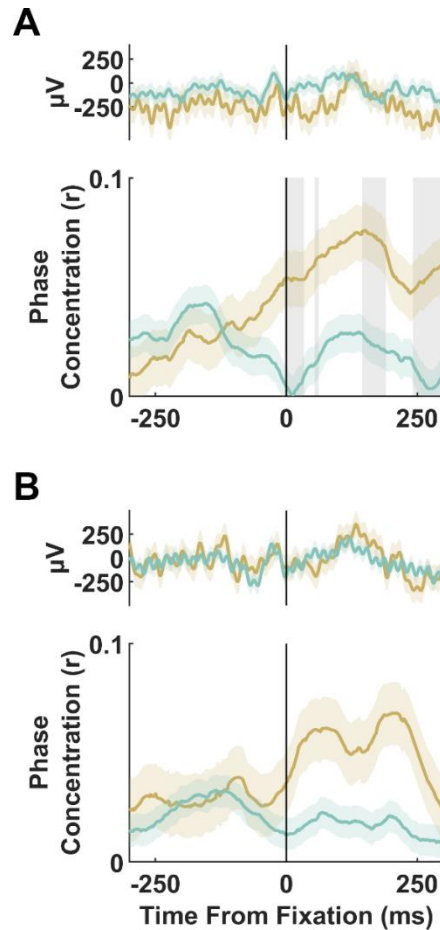
Supplemental Figure 4. Anterior cingulate cortex (ACC) exhibits greater 21-26 Hz power during remote scenes. A) Power across frequency during search showing a peak around ~23 Hz. B) Example broadband signal during first 2s after trial onset when a scene is presented. C) 21-26 Hz filter of signal above. D) mean power spectral density of 21-26 Hz band using 300ms windows in 1ms steps. Shading indicated 95% bootstrap confidence interval. E) Top; mean spectrogram of remote trials (n = 289), middle; recent trials (n = 193), bottom; remote – recent difference spectrogram with the non-greyed region representing clusters with a difference of $p < 0.05$ in a permutation test. F-I) same as B-E but for trial end epoch of remembered trials. Remote n = 45, recent n = 65.



Supplemental Figure 5. Greater anterior cingulate-hippocampal phase synchrony during remembered recent scenes. A) difference in ACC-HPC phase locking between bouts on recent and remote trials across remembered (recent = 111 bouts, remote = 194 bouts) and forgotten trials (recent = 530, remote = 142). Vertical blue bars from zero indicate frequencies with a permutation difference of $p < 0.05$. B) same as A) but for ACC-RSC synchrony.



Supplementary Figure 6. Eye movements are not preferentially locked to the phase of theta oscillations in the RSC during forgotten trials. A) Top; mean LFP locked to fixations on remembered trials, bottom; mean phase concentration of RSC oscillations around fixations for monkey LE (remote $n = 2134$, recent $n = 1042$). Light shade around mean traces represent 95% bootstrapped confidence intervals. B) same as A) but for animal RI (remote $n = 1267$, recent $n = 2921$). C) and D) are similar to A) and B) but for the hippocampus of each animal respectively.



Supplementary Figure 7. Eye movements on remembered remote trials are phase locked with the phase of anterior cingulate cortex (ACC) theta oscillations. A) Top; mean fixation-locked LFP signal on remembered trials, bottom; mean phase concentration of ACC theta oscillations around fixations for RI (remote $n = 1328$, recent $n = 2952$). Light shade around mean traces represent 95% bootstrapped confidence intervals. **B)** Same as A) but for forgotten trials.

Chapter 4: Conclusions

Neocortical activity during remote memory

Despite a torrent of studies on systems consolidation, little consensus exists regarding how memory representations reorganise with time. This state of disagreement is demonstrated by two recently proposed interpretations based on contrary lines of evidence (Yonelinas et al. 2019; Barry and Maguire 2019). Despite disagreements on a model for how memory reorganises with time, a clearer picture is emerging about memory representations in the brain more generally. This has been fueled in part by ensemble tagging techniques that allow for the permanent tagging and manipulation of neural populations active during an experience. For example, we now know that neural populations active during an experience need to be reactivated (or at least a subset of them) for successful recall of that experience, and that their inhibition impairs recall. This has been demonstrated in the DG, CA1 and CA3 of the hippocampus (Liu et al. 2012; Denny et al. 2014; Tanaka et al. 2014) and the retrosplenial cortex (Cowansage et al. 2014; de Sousa et al. 2019).

We now also know that neocortical memory representations form rapidly during learning, require time to develop and are stable over time. This has been observed as a gradual increase in spine density after learning in the ACC (Restivo et al. 2009; Vetere et al. 2011; Bero et al. 2014; Kitamura et al. 2017; Abate et al. 2018; Matos et al. 2019), prefrontal cortex (Tse et al. 2011), orbitofrontal cortex (Lesburguères et al. 2011), and RSC (Cowansage et al. 2014). These neocortical representations active during learning are reactivated during retrieval weeks later as demonstrated recently in the mPFC where tagged ensembles were five times more likely to fire during retrieval (Matos et al. 2019). In the RSC, tagged ensembles during a spatial

learning task become more stable with training, can be maintained for several weeks and their stability predicts memory retention (Milczarek et al. 2018). We found that recall of stimuli learned one year earlier was associated with greater engagement in the RSC and ACC, suggesting that neocortical memory representations are stable for at least one year in primates. We observed that eye movements were temporally coordinated with the phase of the neocortical oscillations during remembered remote scenes. Such coordination between eye movements and brain oscillations has been observed in visual areas (Montemurro et al. 2008; Bosman et al. 2009; Ito et al. 2011), and the hippocampus (Bartlett et al. 2011; Hoffman et al. 2013), but to our knowledge this is the first report of such locking occurring with RSC and ACC oscillations. This coordination may reflect a memory-to-vision guidance mechanism that allows pertinent memory - for example of the location of rewarding objects - to influence how organisms visually sample their environment and subsequently make decisions. Whether the RSC representations are necessary for remote recall remains to be tested.

Stronger cortical engagement was observed as enhanced beta power in the RSC and ACC during remote memory. This power band in cortical areas is known to be generated and entrained by somatostatin-expressing (SOM) and parvalbumin-expressing (PV) interneurons. Evidence of this comes from optogenetic studies that silence different interneuron types and observe the effects on different rhythm bands (Chen et al. 2017; Veit et al. 2017; Cardin 2018). Testing the importance of this rhythm for remote memory recall could be achieved through silencing or modulating SOM and PV interneurons through neuromodulatory techniques such as optogenetics or ultrasonic neuromodulation and examining whether the abolishment of the rhythm would affect recall.

RSC role in memory

The greater recruitment of RSC coupled with synchrony to eye movements during remote memory raises a question about how the RSC contributes to performance in our task. In Chapter 1, I reviewed evidence that the RSC is necessary for remote spatial memory for objects-in-scenes in primates (Buckley and Mitchell 2016), or rewards-in-mazes in rodents (Czajkowski et al. 2014). Longitudinal observations of RSC ensembles during spatial learning show that tagged ensembles stabilise over weeks during training and that their stability predicts memory retention (Milczarek et al. 2018). Decoding of cell spiking activity shows that RSC neurons code for contexts associated with rewards (Smith et al. 2012), cues associated with reward locations (Vedder et al. 2017) and egocentric reward-associated trajectories at decision points that possibly inform the animal about which path to traverse (Alexander and Nitz 2017; Miller et al. 2019). In our visual search task, this would be equivalent to coding for visual trajectories in the naturalistic scenes that lead to rewarding targets. In addition to place cells, primates are known to have view cells which have evolved in response to the primate dependence on the visual sensory modality to navigate in the world (Meister and Buffalo 2016). It is therefore plausible that the primate RSC codes for rewarded objects in visual scenes which provides useful information during navigation. One of the main symptoms of RSC damage in humans is an inability to use familiar landmarks to navigate, and an inability to learn new navigation routes (Maguire 2001).

Generalising from rodent decoding studies, if RSC neurons code for “*turn left at the bakery with the blue door to reach home*” in primates, it would explain why an individual is unable to use *the bakery with the blue door* to navigate their way home after RSC damage. Accordingly, the RSC is an integration site that contains visual trajectories based on objects in the environment in ensemble spiking sequences. This would explain why the RSC is strongly recruited when

macaques view remote scenes. RSC ensembles coding for the visual trajectory towards rewarding targets become reactivated and locally synchronised leading to the detection of enhanced power in the beta band. This would also explain why eye movements are synchronised with the phase of the RSC oscillation. Testing the necessity of the RSC for remote memory recall could be conducted using closed-loop stimulation to disrupt supra-threshold 10-15 Hz bouts of oscillatory activity during recall.

Hippocampal role in neocortical representations

There is now also evidence for the long-theorised role of the hippocampus as an index of neocortical neural populations active during an experience (Teyler and DiScenna 1986). This has been demonstrated by studies where inhibiting tagged hippocampal cells (cells active during learning) not only impairs recall, but also inhibits the reactivation of tagged ensembles in the neocortical areas such as the entorhinal, perirhinal and retrosplenial cortices (Tanaka et al. 2014; Guskjolen et al. 2018). The *indexing* role of the hippocampus that can bring about reactivation of neocortical traces is thought to underlie the stabilisation of neocortical memory representations. Evidence for this guiding role comes from studies showing that hippocampal lesions (Restivo et al. 2009), protein synthesis inhibition (Abate et al. 2018) and optogenetic silencing (Kitamura et al. 2017) disrupt learning-associated spine growth in neocortical areas. The functional effect of increasingly stable neocortical representations is increased firing selectivity for learned associations over weeks but not immediately after learning (Takehara-Nishiuchi and McNaughton 2008; Morrissey et al. 2017; Kitamura et al. 2017).

Therefore, during recall of recent memory, tagged hippocampal ensembles appear to trigger the reactivation of neocortical neurons active during learning. The functional relevance of this reactivation could be to aid in recall, strengthen the neocortical memory representation or

both. Our finding of greater synchrony between the hippocampus and the RSC/ACC during recall of recent memory is consistent with these findings, although we were unable to assert the functional relevance of such synchronisation other than note that it occurs only during remembered trials. If this synchrony supports further neocortical pattern strengthening for the purpose of creating stable remote representations, then disrupting it (optogenetically or through closed-loop stimulation) should impair recall at a remote time point. If this synchrony supports recent recall, then disrupting it should impair recall during recent probes. This prediction is based on the finding that interrupting a recently formed RSC memory representation impairs recall (Cowansage et al. 2014). We found hippocampal-neocortical synchrony in the gamma band (>20 Hz) which is ideally suited for ensuring effective communication between distant brain areas. Gamma band synchronization allows spikes from distant areas to arrive in a temporally coordinated manner allowing for more effective communication between areas (Fries 2015; Hahn et al. 2019).

Mechanism by which hippocampus guides neocortical stabilisation

One of the mechanisms by which the hippocampus guides the maturation of neocortical memory representations is thought to be neurophysiological coupling during sharp-wave ripples. The macaque hippocampus is reciprocally connected to the RSC which itself is reciprocally connected to the ACC and is thought to act as a conduit for information flow between the HPC and ACC. In the rodent brain, the HPC is monosynaptically connected to the ACC through sparse projections though a similar projection has yet to be shown in primates (Figure 1) ((Kobayashi and Amaral 2000; Kobayashi and Amaral 2003; Kobayashi and Amaral 2007; Cenquizca and Swanson 2007; Rajasethupathy et al. 2015).

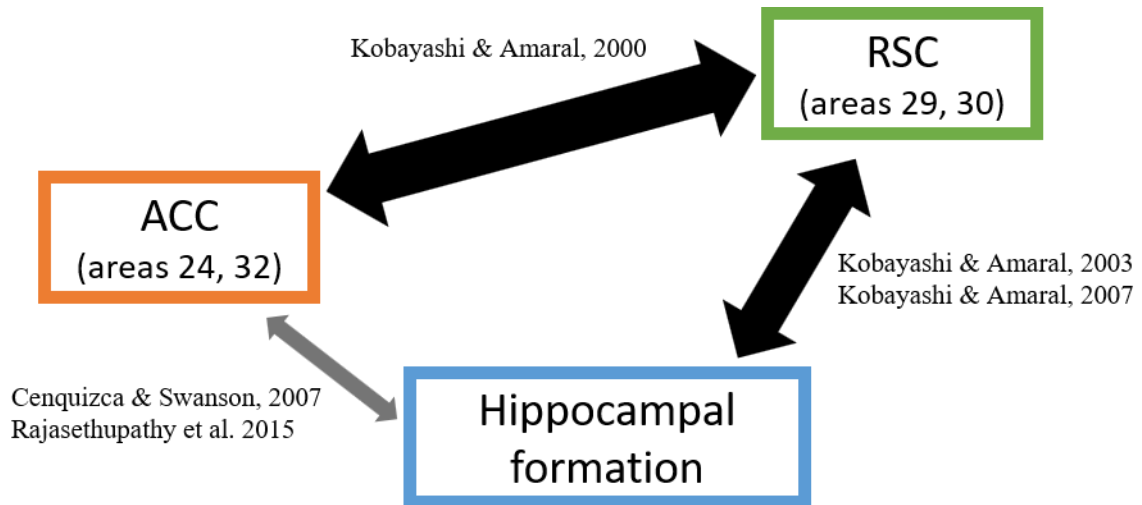


Figure 1. Hippocampal-neocortical connections. The hippocampal formation (subiculum, presubiculum, parasubiculum) and the parahippocampal region including the entorhinal cortex are reciprocally connected to the RSC, and the RSC is reciprocally connected to the ACC which may serve as an indirect HPC-ACC route.

As described earlier, replay of earlier spiking sequences occurs during hippocampal ripples (Nádasy et al. 1999; Lee and Wilson 2002; Foster and Wilson 2006; Csicsvari et al. 2007; Diba and Buzsáki 2007; Ji and Wilson 2007) and sees associated replay activity throughout the brain (Qin et al. 1997; Pennartz et al. 2004; Ji and Wilson 2007; Peyrache et al. 2009; Gomperts et al. 2015). This distributed and widespread repetition of earlier neuronal activity patterns during ripples is thought to promote the consolidation of earlier experiences into stable, long-term memory representations in the neocortex (Carr et al. 2011; Girardeau and Zugaro 2011; Sadowski et al. 2011; Roumis and Frank 2015; Buzsáki 2015). Recent evidence of this role shows that when ripple-spindle coupling following learning is disrupted, memory is impaired at a remote time point (Xia et al. 2017). Consistently, when ripple-spindle coupling is increased through closed-loop electrical stimulation during sleep after learning, memory

consolidation is enhanced as evidenced by improved memory performance (Maingret et al. 2016). This evidence suggests that during ripples the hippocampus induces a strengthening of neocortical representations in a way that facilitates the development of enduring memory representations.

Besides their widely hypothesised role in memory consolidation, ripples have recently garnered strong evidence suggesting they also play a role in retrieval (Jadhav et al. 2012; Leonard and Hoffman 2017; Wu et al. 2017; Norman et al. 2019; Vaz et al. 2019; Vaz et al. 2020). In a decoding study of awake ripples, ripples occurring at decision point in a memory task replayed activity patterns representing trajectories towards rewarded location in a maze (Wu et al. 2017). This suggests that ripples at the decision point brought about recall of memories that can guide the animal's decision. In a similar study in humans, performance in a verbal word associated memory task was predicted by ripples occurring just before verbal response initiating replay of spiking sequences in the temporal cortex that had occurred during the learning phase of the task (Vaz et al. 2020). These findings suggest that the hippocampus initiates retrieval of memory representations in neocortical areas during recall of recent memory through sharp-wave ripples. Whether such replay occurs during recall of remote memory has not yet been tested but would be a strong demonstration of remote memory dependence on the hippocampus or the neocortex. One of the main limitations of the experiment in Chapter 3 of this dissertation was our inability to observe ripples in both animals. The reason for this failure to detect is likely related to the size of the primate hippocampus and the low density of its neurons in comparison to the rodent hippocampus. The size and sparsity properties create a situation that can benefit from modifying recording locations until ripples are detected. In Chapter 2 for example, we used adjustable tetrodes which were inserted at the top of the hippocampus, then lowered

incrementally in daily sessions until ripples were detected. In the recordings from Chapter 3, the electrodes were chronically implanted during surgery targeting the anterior hippocampus and their location was not adjustable. This inflexibility to lower the electrodes and search for ripples naturally lowered the probability that they would be detected. Had we detected ripples, even without decoding spiking sequences, we may have been able to make inferences on hippocampal-neocortical communication during remote memory recall by examining ripple-associated activity in neocortical areas.

As reviewed above, replay comes in more flavours than initially thought. During waking ripples for example, replay occurs in reverse order, and a type of replay often called pre-play occurs before a rat traverses a maze containing possible future trajectories. Yet, despite a significant shift in our understanding of the ripple and replay phenomena, we still largely lack a solid understanding of the difference between ripples in different states, how different cell types contribute to replay and how different kinds of replay contribute to memory consolidation and recall (de la Prida 2020). These questions currently motivate an active and exciting area of memory research in rodents, and increasingly in primates where the ripple and hippocampal cell type literature is particularly scarce. Examinations of the rodent hippocampus – a relatively simple brain area – reveal a rich diversity even within classical cell types. It follows that the relatively more complex primate brain contains a potentially more diverse within cell-type heterogeneity that is yet to be explored (Cembrowski and Spruston 2019).

In Chapter 2, we attempted to contribute to answering the following question: if ripples occur in different states with potentially different types of replay, are the features of the ripples as commonly detected in the LFP also different? And if so, how do different cell types contribute to these differences in features? We examined how ripple features - such as amplitude and

duration - change with waking states and how four hippocampal cell types contribute to these features. We found that ripples during sleep have larger amplitude and larger post-ripple waves compared to waking ripples, and that ripples on remembered trials have larger amplitudes. We found that putative bursting pyramidal neurons and fast-spiking basket interneurons contribute to ripple amplitudes, while spiking by fast-spiking neurons was associated with the post-ripple wave. During search, ripple amplitude, which is larger for remembered trials, was associated with spiking from non-bursting putative pyramidal neurons. We hope this identification will aid in narrowing the focus on these cell types that participate in the ripple to identify replay patterns in macaques. We also hope this evidence can aid in targeting relevant cell types for manipulation with light-sensitive opsins that will allow for understanding their contribution to memory more directly.

We did not determine the content of ripples based on single-unit activity. However, based on changes we observed in ripple features with remembered trials, it is possible that underlying spiking reflects the task-relevant replay of spiking activity associated with the task. In our task, the animals were stationary and head-fixed, which rule out the involvement of place or head-direction cells in this task. It is more likely that spiking contained within ripples in our task reflects spatial view cell activity. These cells fire when the animals are looking at a particular area in their visual field and has been hypothesized to aid primates in representing the location of objects in space (Rolls et al. 1997; Rolls and Wirth 2018). Decoding this activity in our task would require the ability to record from a large number of single units and matching spatial view cells with their preferred fields by examining their spiking preferences as the animal searches the scene. The sequential activity of multiple spatial view cells during our task could be the neuronal activity that is replayed during ripples and whose replay during waking ripples facilitates recall.

Testing the causality that waking ripples facilitate recall in our task could be accomplished through closed-loop ripple interruption during recall. Testing the causality of quiescent ripples in consolidation could be accomplished through the real-time decoding and interruption of only ripples that contain spatial-view cell activity from earlier task periods while the subjects are quiescent.

Longevity of hippocampal representations

Whether the hippocampus continues to serve as a neocortical index for memories as they get older remains unclear and is perhaps the most heatedly debated tenet of systems consolidation. In one rodent study often used as physiological support for the idea that remote memory is hippocampus dependent, CA1 ensembles were tagged during contextual and cued fear conditioning (Goshen et al. 2011). Twelve weeks later, memory was probed while tagged cells were inhibited. Mice in the inhibited group displayed less freezing in the contextual but not cued conditioning group leading the authors to conclude that remote memory is hippocampus dependent. However, at the remote testing probes, both control and inhibited groups showed similar levels of memory decline (~30% reduction in freezing) making it unclear how much of the recall impairment is due to forgetting and how much was due to ensemble inhibition. Additionally, the impairments at remote time points were relatively modest compared to inhibition induced impairments at recent time points. This ambiguity also calls into question the prevalent use of contextual fear conditioning in ensemble manipulation experiments which use the rodent freezing response as an index of memory. Such an index which relies on the absence of behaviour makes it challenging to generalise findings to other kinds of memory and other species. We observed no changes in hippocampal spectral activity between recent and remote

memory, although we realise this is not conclusive evidence that the hippocampus plays no role during remote recall.

The standard model of systems consolidation suggests that the hippocampal index does not last long and that memory dependence shifts to the neocortex (Squire et al. 2015). The multiple trace model suggests that hippocampal traces are permanent and are recreated every time a memory is retrieved (Sekeres, Winocur and Moscovitch 2018). Contemporary evidence does not support the idea that hippocampal traces are permanent, but rather that they are highly transient and unstable. For example, longitudinal observations of neuronal ensembles show that populations firing in the same environment measured 5 and 30 days following initial exposure represent an overlap of ~10% between sessions, with about ~20% maintaining selectivity for a specific location across days (Ziv et al. 2013; Rubin et al. 2015). This decrease in overlap is not due to reduction in overall activity as equivalent numbers of cells participate in both events, suggesting that despite repeated exposure to the same location in an environment, earlier hippocampal representations are quickly replaced. Similarly unstable ensembles have been reported in CA1 and CA3 during reward-location tasks in two distinct virtual reality environments (Hainmueller and Bartos 2018). Longitudinal examinations of dendritic spines in the hippocampus show that they have considerably short lifespans of around 2 weeks (Attardo et al. 2015). Consistently, within 2 weeks after contextual fear conditioning, the spine density of DG tagged ensembles is significantly reduced, making it unlikely that these cells become reactivated during retrieval (Kitamura et al. 2017).

Adult neurogenesis provides further evidence for the transience of hippocampal memory representations. In rodents, new neurons reach structural and functional maturity after 1 month (Ge et al. 2007), while artificially increasing neurogenesis after a learning experience impairs

retrieval (Akers et al. 2014). When new granule cells are born in the DG, they develop dendrites and axons and form synapses with existing neurons. This process would naturally disrupt previously existing input-output relationships the hippocampal circuit (EC-DG-CA3) which would impede if not completely disrupt the reactivation of an earlier neural activity pattern involved in a memory representation due to natural cues converging via entorhinal inputs (Lledo et al. 2006; Frankland et al. 2013). While evidence of neurogenesis in humans is controversial (Eriksson et al. 1998; Boldrini et al. 2018; Sorrells et al. 2018), evidence shows a yearly exchange rate of 1.75% of hippocampal cells (Spalding et al. 2013). These converging lines of evidence makes it difficult to envisage how hippocampal memory representations could remain stable over time.

In summary, the current dissertation provides evidence for preferential recruitment of neocortical areas during recall of remote episodic-like memory. It also provides evidence for enhanced hippocampal-neocortical communication during recall of recent memory. Although this evidence could be interpreted to support the standard model of systems consolidation, we recognize that our findings are correlational and not causal. Without additional experiments testing causality by inhibiting activity or synchrony, it is not possible to conclude dependence of remote memory on neocortical areas or independence from the hippocampus. We hope this work - which characterizes for the first-time the spectral responses of multiple brain areas during a remote memory task in primates - is used as a steppingstone upon which causality testing experiments can be conducted in the future.

Bibliography

- Abate, G., Colazingari, S., Accoto, A., Conversi, D. and Bevilacqua, A. 2018. Dendritic spine density and EphrinB2 levels of hippocampal and anterior cingulate cortex neurons increase sequentially during formation of recent and remote fear memory in the mouse. *Behavioural Brain Research* 344, pp. 120–131.
- Abraham, W.C., Logan, B., Greenwood, J.M. and Dragunow, M. 2002. Induction and experience-dependent consolidation of stable long-term potentiation lasting months in the hippocampus. *The Journal of Neuroscience* 22(21), pp. 9626–9634.
- Addis, D.R., Moscovitch, M., Crawley, A.P. and McAndrews, M.P. 2004. Recollective qualities modulate hippocampal activation during autobiographical memory retrieval. *Hippocampus* 14(6), pp. 752–762.
- Aggleton, J.P., Wright, N.F., Vann, S.D. and Saunders, R.C. 2012. Medial temporal lobe projections to the retrosplenial cortex of the macaque monkey. *Hippocampus* 22(9), pp. 1883–1900.
- Aguirre, G.K. and D’Esposito, M. 1999. Topographical disorientation: a synthesis and taxonomy. *Brain: A Journal of Neurology* 122 (Pt 9), pp. 1613–1628.
- Ahissar, E., Vaadia, E., Ahissar, M., Bergman, H., Arieli, A. and Abeles, M. 1992. Dependence of cortical plasticity on correlated activity of single neurons and on behavioral context. *Science* 257(5075), pp. 1412–1415.
- Akers, K.G., Martinez-Canabal, A., Restivo, L., et al. 2014. Hippocampal neurogenesis regulates forgetting during adulthood and infancy. *Science* 344(6184), pp. 598–602.
- Alexander, A.S. and Nitz, D.A. 2015. Retrosplenial cortex maps the conjunction of internal and external spaces. *Nature Neuroscience* 18(8), pp. 1143–1151.
- Alexander, A.S. and Nitz, D.A. 2017. Spatially Periodic Activation Patterns of Retrosplenial Cortex Encode Route Sub-spaces and Distance Traveled. *Current Biology* 27(11), pp. 1551–1560.e4.
- Allen, T.A. and Fortin, N.J. 2013. The evolution of episodic memory. *Proceedings of the National Academy of Sciences of the United States of America* 110 Suppl 2, pp. 10379–10386.
- Anagnostaras, S.G., Maren, S. and Fanselow, M.S. 1999. Temporally graded retrograde amnesia of contextual fear after hippocampal damage in rats: within-subjects examination. *The Journal of Neuroscience* 19(3), pp. 1106–1114.
- Anastassiou, C.A., Perin, R., Buzsáki, G., Markram, H. and Koch, C. 2015. Cell type- and activity-dependent extracellular correlates of intracellular spiking. *Journal of Neurophysiology* 114(1), pp. 608–623.
- Andersen, Morris, Amaral, Bliss and O’Keefe 2006. *The Hippocampus Book*. Andersen, P., Morris, R., Amaral, D., Bliss, T., and O’Keefe, J. eds. Oxford University Press.

- Andrillon, T., Nir, Y., Cirelli, C., Tononi, G. and Fried, I. 2015. Single-neuron activity and eye movements during human REM sleep and awake vision. *Nature Communications* 6, p. 7884.
- Atherton, L.A., Dupret, D. and Mellor, J.R. 2015. Memory trace replay: the shaping of memory consolidation by neuromodulation. *Trends in Neurosciences* 38(9), pp. 560–570.
- Attardo, A., Fitzgerald, J.E. and Schnitzer, M.J. 2015. Impermanence of dendritic spines in live adult CA1 hippocampus. *Nature* 523(7562), pp. 592–596.
- Auger, S.D. and Maguire, E.A. 2013. Assessing the mechanism of response in the retrosplenial cortex of good and poor navigators. *Cortex* 49(10), pp. 2904–2913.
- Auger, S.D., Mullally, S.L. and Maguire, E.A. 2012. Retrosplenial cortex codes for permanent landmarks. *Plos One* 7(8), p. e43620.
- Axmacher, N., Elger, C.E. and Fell, J. 2008. Ripples in the medial temporal lobe are relevant for human memory consolidation. *Brain: A Journal of Neurology* 131(Pt 7), pp. 1806–1817.
- Babb, S.J. and Crystal, J.D. 2006. Episodic-like memory in the rat. *Current Biology* 16(13), pp. 1317–1321.
- Baddeley, A.D. and Warrington, E.K. 1970. Amnesia and the distinction between long- and short-term memory. *Journal of verbal learning and verbal behavior* 9(2), pp. 176–189.
- Bar, M. 2004. Visual objects in context. *Nature Reviews. Neuroscience* 5(8), pp. 617–629.
- Bar, M. and Aminoff, E. 2003. Cortical analysis of visual context. *Neuron* 38(2), pp. 347–358.
- Barry, D.N. and Maguire, E.A. 2019. Remote memory and the hippocampus: A constructive critique. *Trends in Cognitive Sciences* 23(2), pp. 128–142.
- Bartlett, A.M., Ovaysikia, S., Logothetis, N.K. and Hoffman, K.L. 2011. Saccades during object viewing modulate oscillatory phase in the superior temporal sulcus. *The Journal of Neuroscience* 31(50), pp. 18423–18432.
- Battaglia, F.P., Sutherland, G.R. and McNaughton, B.L. 2004. Hippocampal sharp wave bursts coincide with neocortical “up-state” transitions. *Learning & Memory* 11(6), pp. 697–704.
- Bauer, E.P., LeDoux, J.E. and Nader, K. 2001. Fear conditioning and LTP in the lateral amygdala are sensitive to the same stimulus contingencies. *Nature Neuroscience* 4(7), pp. 687–688.
- Bayley, P.J., Hopkins, R.O. and Squire, L.R. 2003. Successful recollection of remote autobiographical memories by amnesic patients with medial temporal lobe lesions. *Neuron* 38(1), pp. 135–144.
- Belluscio, M.A., Mizuseki, K., Schmidt, R., Kempster, R. and Buzsáki, G. 2012. Cross-frequency phase-phase coupling between θ and γ oscillations in the hippocampus. *The Journal of Neuroscience* 32(2), pp. 423–435.

- Benuzzi, F., Ballotta, D., Handjaras, G., et al. 2018. Eight Weddings and Six Funerals: An fMRI Study on Autobiographical Memories. *Frontiers in Behavioral Neuroscience* 12, p. 212.
- Berens, P. 2009. circstat : a *MATLAB* toolbox for circular statistics. *Journal of statistical software* 31(10).
- Bero, A.W., Meng, J., Cho, S., et al. 2014. Early remodeling of the neocortex upon episodic memory encoding. *Proceedings of the National Academy of Sciences of the United States of America* 111(32), pp. 11852–11857.
- Bliss, T.V. and Collingridge, G.L. 1993. A synaptic model of memory: long-term potentiation in the hippocampus. *Nature* 361(6407), pp. 31–39.
- Bliss, T.V. and Lomo, T. 1973. Long-lasting potentiation of synaptic transmission in the dentate area of the anaesthetized rabbit following stimulation of the perforant path. *The Journal of Physiology* 232(2), pp. 331–356.
- Boldrini, M., Fulmore, C.A., Tartt, A.N., et al. 2018. Human Hippocampal Neurogenesis Persists throughout Aging. *Cell Stem Cell* 22(4), pp. 589–599.e5.
- Bonnici, H.M., Chadwick, M.J., Lutti, A., Hassabis, D., Weiskopf, N. and Maguire, E.A. 2012. Detecting representations of recent and remote autobiographical memories in vmPFC and hippocampus. *The Journal of Neuroscience* 32(47), pp. 16982–16991.
- Bontempi, B., Laurent-Demir, C., Destrade, C. and Jaffard, R. 1999. Time-dependent reorganization of brain circuitry underlying long-term memory storage. *Nature* 400(6745), pp. 671–675.
- Bosch, M. and Hayashi, Y. 2012. Structural plasticity of dendritic spines. *Current Opinion in Neurobiology* 22(3), pp. 383–388.
- Bosman, C.A., Womelsdorf, T., Desimone, R. and Fries, P. 2009. A microsaccadic rhythm modulates gamma-band synchronization and behavior. *The Journal of Neuroscience* 29(30), pp. 9471–9480.
- Bragin, A., Engel, J., Wilson, C.L., Fried, I. and Buzsáki, G. 1999. High-frequency oscillations in human brain. *Hippocampus* 9(2), pp. 137–142.
- Broadbent, N.J. and Clark, R.E. 2013. Remote context fear conditioning remains hippocampus-dependent irrespective of training protocol, training-surgery interval, lesion size, and lesion method. *Neurobiology of Learning and Memory* 106, pp. 300–308.
- Brooks, D.N. and Baddeley, A.D. 1976. What can amnesic patients learn? *Neuropsychologia* 14(1), pp. 111–122.
- Buchanan, T.W., Tranel, D. and Adolphs, R. 2005. Emotional autobiographical memories in amnesic patients with medial temporal lobe damage. *The Journal of Neuroscience* 25(12), pp. 3151–3160.

- Buckley, M.J. and Mitchell, A.S. 2016. Retrosplenial cortical contributions to anterograde and retrograde memory in the monkey. *Cerebral Cortex* 26(6), pp. 2905–2918.
- Buckner, R.L., Wheeler, M.E. and Sheridan, M.A. 2001. Encoding processes during retrieval tasks. *Journal of Cognitive Neuroscience* 13(3), pp. 406–415.
- Buhusi, C.V. and Meck, W.H. 2005. What makes us tick? Functional and neural mechanisms of interval timing. *Nature Reviews. Neuroscience* 6(10), pp. 755–765.
- Burwell, R.D. 2000. The parahippocampal region: corticocortical connectivity. *Annals of the New York Academy of Sciences* 911, pp. 25–42.
- Buzsáki, G. 2015. Hippocampal sharp wave-ripple: A cognitive biomarker for episodic memory and planning. *Hippocampus* 25(10), pp. 1073–1188.
- Buzsáki, G., Anastassiou, C.A. and Koch, C. 2012. The origin of extracellular fields and currents--EEG, ECoG, LFP and spikes. *Nature Reviews. Neuroscience* 13(6), pp. 407–420.
- Buzsáki, G., Buhl, D.L., Harris, K.D., Csicsvari, J., Czeh, B. and Morozov, A. 2003. Hippocampal network patterns of activity in the mouse. *Neuroscience* 116(1), pp. 201–211.
- Buzsáki, G., Haas, H.L. and Anderson, E.G. 1987. Long-term potentiation induced by physiologically relevant stimulus patterns. *Brain Research* 435(1-2), pp. 331–333.
- Buzsáki, G., Leung, L.W. and Vanderwolf, C.H. 1983. Cellular bases of hippocampal EEG in the behaving rat. *Brain Research* 287(2), pp. 139–171.
- Camille, N., Tsuchida, A. and Fellows, L.K. 2011. Double dissociation of stimulus-value and action-value learning in humans with orbitofrontal or anterior cingulate cortex damage. *The Journal of Neuroscience* 31(42), pp. 15048–15052.
- Cardin, J.A. 2018. Inhibitory interneurons regulate temporal precision and correlations in cortical circuits. *Trends in Neurosciences* 41(10), pp. 689–700.
- Carr, M.F., Jadhav, S.P. and Frank, L.M. 2011. Hippocampal replay in the awake state: a potential substrate for memory consolidation and retrieval. *Nature Neuroscience* 14(2), pp. 147–153.
- Cembrowski, M.S. and Spruston, N. 2019. Heterogeneity within classical cell types is the rule: lessons from hippocampal pyramidal neurons. *Nature Reviews. Neuroscience* 20(4), pp. 193–204.
- Cenquizca, L.A. and Swanson, L.W. 2007. Spatial organization of direct hippocampal field CA1 axonal projections to the rest of the cerebral cortex. *Brain Research Reviews* 56(1), pp. 1–26.
- Chau, V.L., Murphy, E.F., Rosenbaum, R.S., Ryan, J.D. and Hoffman, K.L. 2011. A Flicker Change Detection Task Reveals Object-in-Scene Memory Across Species. *Frontiers in Behavioral Neuroscience* 5, p. 58.

- Chen, G., Zhang, Y., Li, X., et al. 2017. Distinct Inhibitory Circuits Orchestrate Cortical beta and gamma Band Oscillations. *Neuron* 96(6), pp. 1403–1418.e6.
- Chen, L.L., Lin, L.H., Green, E.J., Barnes, C.A. and McNaughton, B.L. 1994. Head-direction cells in the rat posterior cortex. I. Anatomical distribution and behavioral modulation. *Experimental Brain Research* 101(1), pp. 8–23.
- Cho, J. and Sharp, P.E. 2001. Head direction, place, and movement correlates for cells in the rat retrosplenial cortex. *Behavioral Neuroscience* 115(1), pp. 3–25.
- Chrobak, J.J. and Buzsáki, G. 1994. Selective activation of deep layer (V-VI) retrohippocampal cortical neurons during hippocampal sharp waves in the behaving rat. *The Journal of Neuroscience* 14(10), pp. 6160–6170.
- Citri, A. and Malenka, R.C. 2008. Synaptic plasticity: multiple forms, functions, and mechanisms. *Neuropsychopharmacology* 33(1), pp. 18–41.
- Clark, R.E., Broadbent, N.J. and Squire, L.R. 2005. Impaired remote spatial memory after hippocampal lesions despite extensive training beginning early in life. *Hippocampus* 15(3), pp. 340–346.
- Clayton, N.S. and Dickinson, A. 1998. Episodic-like memory during cache recovery by scrub jays. *Nature* 395(6699), pp. 272–274.
- Clayton, N.S., Griffiths, D.P., Emery, N.J. and Dickinson, A. 2001. Elements of episodic-like memory in animals. *Philosophical Transactions of the Royal Society of London. Series B, Biological Sciences* 356(1413), pp. 1483–1491.
- Cohen, M.X. 2018. Using spatiotemporal source separation to identify prominent features in multichannel data without sinusoidal filters. *The European Journal of Neuroscience* 48(7), pp. 2454–2465.
- Cohen, N.J. and Squire, L.R. 1980. Preserved learning and retention of pattern-analyzing skill in amnesia: dissociation of knowing how and knowing that. *Science* 210(4466), pp. 207–210.
- Colgin, L.L. 2016. Rhythms of the hippocampal network. *Nature Reviews. Neuroscience* 17(4), pp. 239–249.
- Constantinou, M., Gonzalo Cogno, S., Elijah, D.H., et al. 2016. Bursting neurons in the hippocampal formation encode features of LFP rhythms. *Frontiers in Computational Neuroscience* 10, p. 133.
- Cooper, B.G., Manka, T.F. and Mizumori, S.J.Y. 2001. Finding your way in the dark: The retrosplenial cortex contributes to spatial memory and navigation without visual cues. *Behavioral Neuroscience* 115(5), pp. 1012–1028.
- Cooper, B.G. and Mizumori, S.J. 1999. Retrosplenial cortex inactivation selectively impairs navigation in darkness. *Neuroreport* 10(3), pp. 625–630.

- Corcoran, K.A., Donnan, M.D., Tronson, N.C., et al. 2011. NMDA receptors in retrosplenial cortex are necessary for retrieval of recent and remote context fear memory. *The Journal of Neuroscience* 31(32), pp. 11655–11659.
- Corkin, S. 2002. What's new with the amnesic patient H.M.? *Nature Reviews. Neuroscience* 3(2), pp. 153–160.
- Corkin, S., Amaral, D.G., González, R.G., Johnson, K.A. and Hyman, B.T. 1997. H. M.'s medial temporal lobe lesion: findings from magnetic resonance imaging. *The Journal of Neuroscience* 17(10), pp. 3964–3979.
- Cowansage, K.K., Shuman, T., Dillingham, B.C., Chang, A., Golshani, P. and Mayford, M. 2014. Direct reactivation of a coherent neocortical memory of context. *Neuron* 84(2), pp. 432–441.
- Csicsvari, J., Hirase, H., Czurkó, A., Mamiya, A. and Buzsáki, G. 1999. Oscillatory coupling of hippocampal pyramidal cells and interneurons in the behaving Rat. *The Journal of Neuroscience* 19(1), pp. 274–287.
- Csicsvari, J., Hirase, H., Mamiya, A. and Buzsáki, G. 2000. Ensemble patterns of hippocampal CA3-CA1 neurons during sharp wave-associated population events. *Neuron* 28(2), pp. 585–594.
- Csicsvari, J., O'Neill, J., Allen, K. and Senior, T. 2007. Place-selective firing contributes to the reverse-order reactivation of CA1 pyramidal cells during sharp waves in open-field exploration. *The European Journal of Neuroscience* 26(3), pp. 704–716.
- Czajkowski, R., Jayaprakash, B., Wiltgen, B., et al. 2014. Encoding and storage of spatial information in the retrosplenial cortex. *Proceedings of the National Academy of Sciences of the United States of America* 111(23), pp. 8661–8666.
- Day, J.J. and Sweatt, J.D. 2011. Epigenetic modifications in neurons are essential for formation and storage of behavioral memory. *Neuropsychopharmacology* 36(1), pp. 357–358.
- Day, M., Langston, R. and Morris, R.G.M. 2003. Glutamate-receptor-mediated encoding and retrieval of paired-associate learning. *Nature* 424(6945), pp. 205–209.
- de la Prida, L.M. 2020. Potential factors influencing replay across CA1 during sharp-wave ripples. *Philosophical Transactions of the Royal Society of London. Series B, Biological Sciences* 375(1799), p. 20190236.
- de Sousa, A.F., Cowansage, K.K., Zutshi, I., et al. 2019. Optogenetic reactivation of memory ensembles in the retrosplenial cortex induces systems consolidation. *Proceedings of the National Academy of Sciences of the United States of America* 116(17), pp. 8576–8581.
- Denny, C.A., Kheirbek, M.A., Alba, E.L., et al. 2014. Hippocampal memory traces are differentially modulated by experience, time, and adult neurogenesis. *Neuron* 83(1), pp. 189–201.

- Dere, E., Kart-Teke, E., Huston, J.P. and De Souza Silva, M.A. 2006. The case for episodic memory in animals. *Neuroscience and Biobehavioral Reviews* 30(8), pp. 1206–1224.
- Diba, K. and Buzsáki, G. 2007. Forward and reverse hippocampal place-cell sequences during ripples. *Nature Neuroscience* 10(10), pp. 1241–1242.
- Ding, H.K., Teixeira, C.M. and Frankland, P.W. 2008. Inactivation of the anterior cingulate cortex blocks expression of remote, but not recent, conditioned taste aversion memory. *Learning & Memory* 15(5), pp. 290–293.
- Dzhala, V.I. and Staley, K.J. 2004. Mechanisms of fast ripples in the hippocampus. *The Journal of Neuroscience* 24(40), pp. 8896–8906.
- Eacott, M.J., Easton, A. and Zinkivskay, A. 2005. Recollection in an episodic-like memory task in the rat. *Learning & Memory* 12(3), pp. 221–223.
- Ego-Stengel, V. and Wilson, M.A. 2010. Disruption of ripple-associated hippocampal activity during rest impairs spatial learning in the rat. *Hippocampus* 20(1), pp. 1–10.
- Eichenbaum, H. 2018. What Versus Where: Non-spatial Aspects of Memory Representation by the Hippocampus. *Current topics in behavioral neurosciences* 37, pp. 101–117.
- Eichenbaum, H., Yonelinas, A.P. and Ranganath, C. 2007. The medial temporal lobe and recognition memory. *Annual Review of Neuroscience* 30, pp. 123–152.
- Einarsson, E.Ö. and Nader, K. 2012. Involvement of the anterior cingulate cortex in formation, consolidation, and reconsolidation of recent and remote contextual fear memory. *Learning & Memory* 19(10), pp. 449–452.
- Einarsson, E.Ö., Pors, J. and Nader, K. 2015. Systems reconsolidation reveals a selective role for the anterior cingulate cortex in generalized contextual fear memory expression. *Neuropsychopharmacology* 40(2), pp. 480–487.
- Einevoll, G.T., Kayser, C., Logothetis, N.K. and Panzeri, S. 2013. Modelling and analysis of local field potentials for studying the function of cortical circuits. *Nature Reviews. Neuroscience* 14(11), pp. 770–785.
- Ellender, T.J., Nissen, W., Colgin, L.L., Mann, E.O. and Paulsen, O. 2010. Priming of hippocampal population bursts by individual perisomatic-targeting interneurons. *The Journal of Neuroscience* 30(17), pp. 5979–5991.
- English, D.F., Peyrache, A., Stark, E., et al. 2014. Excitation and inhibition compete to control spiking during hippocampal ripples: intracellular study in behaving mice. *The Journal of Neuroscience* 34(49), pp. 16509–16517.
- Epstein, R.A. 2008. Parahippocampal and retrosplenial contributions to human spatial navigation. *Trends in Cognitive Sciences* 12(10), pp. 388–396.
- Ergorul, C. and Eichenbaum, H. 2004. The hippocampus and memory for “what,” “where,” and “when”. *Learning & Memory* 11(4), pp. 397–405.

- Eriksson, P.S., Perfilieva, E., Björk-Eriksson, T., et al. 1998. Neurogenesis in the adult human hippocampus. *Nature Medicine* 4(11), pp. 1313–1317.
- Eschenko, O., Ramadan, W., Mölle, M., Born, J. and Sara, S.J. 2008. Sustained increase in hippocampal sharp-wave ripple activity during slow-wave sleep after learning. *Learning & Memory* 15(4), pp. 222–228.
- Esgளை, M., Daliri, M.R. and Treue, S. 2017. Local field potentials are induced by visually evoked spiking activity in macaque cortical area MT. *Scientific Reports* 7(1), p. 17110.
- Fink, G.R., Markowitsch, H.J., Reinkemeier, M., Bruckbauer, T., Kessler, J. and Heiss, W.D. 1996. Cerebral representation of one's own past: neural networks involved in autobiographical memory. *The Journal of Neuroscience* 16(13), pp. 4275–4282.
- Foster, D.J. and Wilson, M.A. 2006. Reverse replay of behavioural sequences in hippocampal place cells during the awake state. *Nature* 440(7084), pp. 680–683.
- Frankland, P.W., Bontempi, B., Talton, L.E., Kaczmarek, L. and Silva, A.J. 2004. The involvement of the anterior cingulate cortex in remote contextual fear memory. *Science* 304(5672), pp. 881–883.
- Frankland, P.W., Köhler, S. and Josselyn, S.A. 2013. Hippocampal neurogenesis and forgetting. *Trends in Neurosciences* 36(9), pp. 497–503.
- Fries, P. 2015. Rhythms for Cognition: Communication through Coherence. *Neuron* 88(1), pp. 220–235.
- Furman, O., Mendelsohn, A. and Dudai, Y. 2012. The episodic engram transformed: Time reduces retrieval-related brain activity but correlates it with memory accuracy. *Learning & Memory* 19(12), pp. 575–587.
- Gaffan, D. 1994a. Dissociated effects of perirhinal cortex ablation, fornix transection and amygdectomy: evidence for multiple memory systems in the primate temporal lobe. *Experimental Brain Research* 99(3), pp. 411–422.
- Gaffan, D. 1994b. Scene-specific memory for objects: a model of episodic memory impairment in monkeys with fornix transection. *Journal of Cognitive Neuroscience* 6(4), pp. 305–320.
- Gan, J., Weng, S.-M., Pernía-Andrade, A.J., Csicsvari, J. and Jonas, P. 2017. Phase-Locked Inhibition, but Not Excitation, Underlies Hippocampal Ripple Oscillations in Awake Mice In Vivo. *Neuron* 93(2), pp. 308–314.
- Ge, S., Yang, C.-H., Hsu, K.-S., Ming, G.-L. and Song, H. 2007. A critical period for enhanced synaptic plasticity in newly generated neurons of the adult brain. *Neuron* 54(4), pp. 559–566.
- Gilbert, P.E. and Kesner, R.P. 2003a. Localization of function within the dorsal hippocampus: the role of the CA3 subregion in paired-associate learning. *Behavioral Neuroscience* 117(6), pp. 1385–1394.

- Gilbert, P.E. and Kesner, R.P. 2003b. Recognition memory for complex visual discriminations is influenced by stimulus interference in rodents with perirhinal cortex damage. *Learning & Memory* 10(6), pp. 525–530.
- Gilboa, A., Winocur, G., Grady, C.L., Hevenor, S.J. and Moscovitch, M. 2004. Remembering our past: functional neuroanatomy of recollection of recent and very remote personal events. *Cerebral Cortex* 14(11), pp. 1214–1225.
- Girardeau, G., Benchenane, K., Wiener, S.I., Buzsáki, G. and Zugaro, M.B. 2009. Selective suppression of hippocampal ripples impairs spatial memory. *Nature Neuroscience* 12(10), pp. 1222–1223.
- Girardeau, G. and Zugaro, M. 2011. Hippocampal ripples and memory consolidation. *Current Opinion in Neurobiology* 21(3), pp. 452–459.
- Gomperts, S.N., Kloosterman, F. and Wilson, M.A. 2015. VTA neurons coordinate with the hippocampal reactivation of spatial experience. *eLife* 4.
- Goshen, I., Brodsky, M., Prakash, R., et al. 2011. Dynamics of retrieval strategies for remote memories. *Cell* 147(3), pp. 678–689.
- Guskjolen, A., Kenney, J.W., de la Parra, J., Yeung, B.-R.A., Josselyn, S.A. and Frankland, P.W. 2018. Recovery of “lost” infant memories in mice. *Current Biology* 28(14), pp. 2283–2290.e3.
- Hahn, G., Ponce-Alvarez, A., Deco, G., Aertsen, A. and Kumar, A. 2019. Portraits of communication in neuronal networks. *Nature Reviews. Neuroscience* 20(2), pp. 117–127.
- Haijima, A. and Ichitani, Y. 2008. Anterograde and retrograde amnesia of place discrimination in retrosplenial cortex and hippocampal lesioned rats. *Learning & Memory* 15(7), pp. 477–482.
- Hainmueller, T. and Bartos, M. 2018. Parallel emergence of stable and dynamic memory engrams in the hippocampus. *Nature* 558(7709), pp. 292–296.
- Hájos, N., Karlócai, M.R., Németh, B., et al. 2013. Input-output features of anatomically identified CA3 neurons during hippocampal sharp wave/ripple oscillation in vitro. *The Journal of Neuroscience* 33(28), pp. 11677–11691.
- Harker, K.T. and Whishaw, I.Q. 2004. A reaffirmation of the retrosplenial contribution to rodent navigation: reviewing the influences of lesion, strain, and task. *Neuroscience and Biobehavioral Reviews* 28(5), pp. 485–496.
- Hebb, D.O. 1949. *The Organization of Behavior*. London: Routledge.
- Hemond, P., Epstein, D., Boley, A., Migliore, M., Ascoli, G.A. and Jaffe, D.B. 2008. Distinct classes of pyramidal cells exhibit mutually exclusive firing patterns in hippocampal area CA3b. *Hippocampus* 18(4), pp. 411–424.
- Henze, D.A., Borhegyi, Z., Csicsvari, J., Mamiya, A., Harris, K.D. and Buzsáki, G. 2000. Intracellular features predicted by extracellular recordings in the hippocampus in vivo. *Journal of Neurophysiology* 84(1), pp. 390–400.

- Hindley, E.L., Nelson, A.J.D., Aggleton, J.P. and Vann, S.D. 2014. Dysgranular retrosplenial cortex lesions in rats disrupt cross-modal object recognition. *Learning & Memory* 21(3), pp. 171–179.
- Hoffman, K.L., Dragan, M.C., Leonard, T.K., Micheli, C., Montefusco-Siegmund, R. and Valiante, T.A. 2013. Saccades during visual exploration align hippocampal 3-8 Hz rhythms in human and non-human primates. *Frontiers in Systems Neuroscience* 7, p. 43.
- Hoffman, M.L., Beran, M.J. and Washburn, D.A. 2009. Memory for “what”, “where”, and “when” information in rhesus monkeys (*Macaca mulatta*). *Journal of Experimental Psychology. Animal Behavior Processes* 35(2), pp. 143–152.
- Holland, S.M. and Smulders, T.V. 2011. Do humans use episodic memory to solve a What-Where-When memory task? *Animal Cognition* 14(1), pp. 95–102.
- Hulse, B.K., Moreaux, L.C., Lubenov, E.V. and Siapas, A.G. 2016. Membrane Potential Dynamics of CA1 Pyramidal Neurons during Hippocampal Ripples in Awake Mice. *Neuron* 89(4), pp. 800–813.
- Ino, T., Doi, T., Hirose, S., Kimura, T., Ito, J. and Fukuyama, H. 2007. Directional disorientation following left retrosplenial hemorrhage: a case report with fMRI studies. *Cortex* 43(2), pp. 248–254.
- Isomura, Y., Sirota, A., Ozen, S., et al. 2006. Integration and segregation of activity in entorhinal-hippocampal subregions by neocortical slow oscillations. *Neuron* 52(5), pp. 871–882.
- Ito, J., Maldonado, P., Singer, W. and Grün, S. 2011. Saccade-related modulations of neuronal excitability support synchrony of visually elicited spikes. *Cerebral Cortex* 21(11), pp. 2482–2497.
- Izquierdo, I., Quillfeldt, J.A., Zannata, M.S., et al. 1997. Sequential role of hippocampus and amygdala, entorhinal cortex and parietal cortex in formation and retrieval of memory for inhibitory avoidance in rats. *The European Journal of Neuroscience* 9(4), pp. 786–793.
- Jadhav, S.P., Kemere, C., German, P.W. and Frank, L.M. 2012. Awake hippocampal sharp-wave ripples support spatial memory. *Science* 336(6087), pp. 1454–1458.
- Ji, D. and Wilson, M.A. 2007. Coordinated memory replay in the visual cortex and hippocampus during sleep. *Nature Neuroscience* 10(1), pp. 100–107.
- Jiang, M.Y., DeAngeli, N.E., Bucci, D.J. and Todd, T.P. 2018. Retrosplenial cortex has a time-dependent role in memory for visual stimuli. *Behavioral Neuroscience* 132(5), pp. 396–402.
- Joo, H.R. and Frank, L.M. 2018. The hippocampal sharp wave-ripple in memory retrieval for immediate use and consolidation. *Nature Reviews. Neuroscience* 19(12), pp. 744–757.
- Jutras, M.J., Fries, P. and Buffalo, E.A. 2009. Gamma-band synchronization in the macaque hippocampus and memory formation. *The Journal of Neuroscience* 29(40), pp. 12521–12531.

- Kandel, E.R., Dudai, Y. and Mayford, M.R. 2014. The molecular and systems biology of memory. *Cell* 157(1), pp. 163–186.
- Kapur, N. and Brooks, D.J. 1999. Temporally-specific retrograde amnesia in two cases of discrete bilateral hippocampal pathology. *Hippocampus* 9(3), pp. 247–254.
- Kart-Teke, E., De Souza Silva, M.A., Huston, J.P. and Dere, E. 2006. Wistar rats show episodic-like memory for unique experiences. *Neurobiology of Learning and Memory* 85(2), pp. 173–182.
- Katche, C., Dorman, G., Gonzalez, C., et al. 2013. On the role of retrosplenial cortex in long-lasting memory storage. *Hippocampus* 23(4), pp. 295–302.
- Katche, C., Dorman, G., Slipczuk, L., Cammarota, M. and Medina, J.H. 2013. Functional integrity of the retrosplenial cortex is essential for rapid consolidation and recall of fear memory. *Learning & Memory* 20(4), pp. 170–173.
- Katche, C. and Medina, J.H. 2017. Requirement of an Early Activation of BDNF/c-Fos Cascade in the Retrosplenial Cortex for the Persistence of a Long-Lasting Aversive Memory. *Cerebral Cortex* 27(2), pp. 1060–1067.
- Katz, C., Patel, K., Talakoub, O., Groppe, D., Hoffman, K. and Valiante, T.A. 2018. Differential generation of saccade, fixation and image onset event-related potentials in the human mesial temporal lobe. *BioRxiv*.
- Keene, C.S. and Bucci, D.J. 2008a. Involvement of the retrosplenial cortex in processing multiple conditioned stimuli. *Behavioral Neuroscience* 122(3), pp. 651–658.
- Keene, C.S. and Bucci, D.J. 2008b. Neurotoxic lesions of retrosplenial cortex disrupt signaled and unsignaled contextual fear conditioning. *Behavioral Neuroscience* 122(5), pp. 1070–1077.
- Kim, J.J. and Fanselow, M.S. 1992. Modality-specific retrograde amnesia of fear. *Science* 256(5057), pp. 675–677.
- Kirwan, C.B., Bayley, P.J., Galván, V.V. and Squire, L.R. 2008. Detailed recollection of remote autobiographical memory after damage to the medial temporal lobe. *Proceedings of the National Academy of Sciences of the United States of America* 105(7), pp. 2676–2680.
- Kitamura, T., Ogawa, S.K., Roy, D.S., et al. 2017. Engrams and circuits crucial for systems consolidation of a memory. *Science* 356(6333), pp. 73–78.
- Klausberger, T., Magill, P.J., Márton, L.F., et al. 2003. Brain-state- and cell-type-specific firing of hippocampal interneurons in vivo. *Nature* 421(6925), pp. 844–848.
- Klausberger, T., Márton, L.F., Baude, A., Roberts, J.D.B., Magill, P.J. and Somogyi, P. 2004. Spike timing of dendrite-targeting bistratified cells during hippocampal network oscillations in vivo. *Nature Neuroscience* 7(1), pp. 41–47.
- Klausberger, T. and Somogyi, P. 2008. Neuronal diversity and temporal dynamics: the unity of hippocampal circuit operations. *Science* 321(5885), pp. 53–57.

Knierim, J.J., Neunuebel, J.P. and Deshmukh, S.S. 2014. Functional correlates of the lateral and medial entorhinal cortex: objects, path integration and local-global reference frames. *Philosophical Transactions of the Royal Society of London. Series B, Biological Sciences* 369(1635), p. 20130369.

Kobayashi, Y. and Amaral, D.G. 2000. Macaque monkey retrosplenial cortex: I. three-dimensional and cytoarchitectonic organization. *The Journal of Comparative Neurology* 426(3), pp. 339–365.

RESEARCH ARTICLE

Sharp-wave ripple features in macaques depend on behavioral state and cell-type specific firing

Ahmed T. Hussin¹ | Timothy K. Leonard² | Kari L. Hoffman^{2,3} 

¹Department of Biology, Centre for Vision Research, York University, Toronto, Ontario, Canada

²Department of Psychology, Centre for Vision Research, York University, Toronto, Ontario, Canada

³Department of Psychology, Center for Integrative and Cognitive Neuroscience, Vanderbilt Vision Research Center, Vanderbilt Brain Institute, Vanderbilt University, Nashville, Tennessee

Correspondence

Kari L. Hoffman, Department of Psychology, Center for Integrative and Cognitive Neuroscience, Vanderbilt Vision Research Center, Vanderbilt Brain Institute, Vanderbilt University, Nashville, Tennessee.
Email: kari.hoffman@vanderbilt.edu

Funding information

Alzheimer's Society of Canada Doctoral Award; National Science and Engineering Research Council (NSERC) Discovery Grant, NSERC CREATE Vision Science and Applications; Brain Canada Multi-Investigator Research Initiative; the Krembil Foundation; Canada Foundation for Innovation; Alfred P. Sloan Foundation

Abstract

Sharp-wave ripples (SWRs) are spontaneous, synchronized neural population events in the hippocampus widely thought to play a role in memory consolidation and retrieval. They occur predominantly in sleep and quiet immobility, and in primates, they also appear during active visual exploration. Typical measures of SWRs in behaving rats include changes in the rate of occurrence, or in the incidence of specific neural ensemble activity contained within the categorical SWR event. Much less is known about the relevance of spatiotemporal SWR features, though they may index underlying activity of specific cell types including ensemble-specific internally generated sequences. Furthermore, changes in SWR features during active exploratory states are unknown. In this study, we recorded hippocampal local-field potentials and single-units during periods of quiescence and as macaques performed a memory-guided visual search task. We observed that (a) ripples during quiescence have greater amplitudes and larger postripple waves (PRW) compared to those in task epochs, and (b) during “remembered” trials, ripples have larger amplitudes than during “forgotten” trials, with no change in duration or PRWs. We further found that spiking activity influences SWR features as a function of cell type and ripple timing. As expected, larger ripple amplitudes were associated with putative pyramidal or putative basket interneuron (IN) activity, even when the spikes in question exceed the duration of the ripple. In contrast, the PRW was attenuated with activity from low firing rate cells and enhanced with activity from high firing rate cells, with putative IN spikes during ripples leading to the most prominent PRW peaks. The selective changes in SWR features as a function of time window, cell type, and cognitive/vigilance states suggest that this mesoscopic field event can offer additional information about the local network and animal's state than would be appreciated from SWR event rates alone.

KEYWORDS

bursting, electrophysiology, hippocampus, local field potential, memory, nonhuman primate

1 | INTRODUCTION

The sharp-wave ripple (SWR) is a highly synchronized neural population event in the hippocampus that is widely thought to support memory. Ripples are typically detected in the hippocampal local field potential (LFP) arising from synaptic and spiking activity in local neuronal populations (Buzsáki, 2015; Schomburg, Anastassiou, Buzsáki, & Koch, 2012). Ripples occur most frequently during non-REM sleep, where they are important for memory consolidation (Ego-Stengel & Wilson, 2010; Girardeau, Benchenane, Wiener, Buzsáki, & Zugaro, 2009; Nokia, Mikkonen, Penttonen, & Wikgren, 2012), and less

frequently during waking, where they appear to be important for memory-based decision-making (Jadhav, Kemere, German, & Frank, 2012; Leonard & Hoffman, 2017; Wu, Haggerty, Kemere, & Ji, 2017). During ripples, firing sequences observed during earlier waking periods are replayed among local populations within the hippocampus (Csicsvari, O'Neill, Allen, & Senior, 2007; Diba & Buzsáki, 2007; Foster & Wilson, 2006; Ji & Wilson, 2007; Lee & Wilson, 2002; Nadásdy, Hirase, Czurko, Csicsvari, & Buzsáki, 1999), and at distant neocortical (Ji & Wilson, 2007; Peyrache, Khamassi, Benchenane, Wiener, & Battaglia, 2009; Qin, McNaughton, Skaggs, & Barnes, 1997) and subcortical (Gomperts, Kloosterman, & Wilson, 2015;

Pennartz et al., 2004) sites. This “replay” phenomenon is thought to involve the synaptic modifications of relevant neural ensembles, supporting theories about the role of ripples in memory consolidation (Buzsáki, 2015; Carr, Jadhav, & Frank, 2011; Girardeau & Zugaro, 2011; Roumis & Frank, 2015; Sadowski, Jones, & Mellor, 2011). When ripples are disrupted, memory is impaired, suggesting a causal role for the neural activity occurring during ripples in memory formation (Ego-Stengel & Wilson, 2010; Girardeau et al., 2009; Jadhav et al., 2012; Nokia et al., 2012).

Because the ripple mean field potential (or ripple-LFP) arises from the synchronous activity of neuronal ensembles thought to be critical for memory formation, it is important to understand how the activity of local cell populations shapes the ripple-LFP. Following a ripple, a brief period of hyperpolarization ensues where spikes are suppressed (English et al., 2014; Hulse, Moreaux, Lubenov, & Siapas, 2016). This period, which is observed in the ripple-LFP as a positive polarity deflection (or postripple wave, PRW), may be additionally valuable in decoding local circuit activity immediately prior to and during the ripple. In general, neuronal firing rate and/or phase-locked firing are associated with high frequency (>50 Hz) LFP (Anastassiou, Perin, Buzsáki, Markram, & Koch, 2015; Belluscio, Mizuseki, Schmidt, Kempter, & Buzsáki, 2012; Montefusco-Siegmund, Leonard, & Hoffman, 2017; Ray, Crone, Niebur, Franaszczuk, & Hsiao, 2008; Scheffer-Teixeira, Belchior, Leão, Ribeiro, & Tort, 2013). More specifically, the spatio-temporal features of the ripple-LFP can vary according to the specific neural ensembles active during the ripple. This relationship has been used to decode replay spiking content based on the similarity of ripple features alone (Taxidis, Anastassiou, Diba, & Koch, 2015).

The relationship between spiking activity and ripple features becomes more complicated when considering different vigilance states and corresponding changes in neuromodulatory tone (Atherton, Dupret, & Mellor, 2015). Despite numerous reports measuring ripple occurrence, few studies have investigated how ripple-LFP features vary with learning. In one study, ripple amplitude was observed to be greater during sleep when followed by learning (Eschenko, Ramadan, Molle, Born, & Sara, 2008). Sharp-wave amplitude during sleep has also been shown to be greater than in waking (Buzsáki, 2015; O'Neill, Senior, & Csicsvari, 2006). Other investigations into the variance in ripple amplitude found a positive correlation with spiking activity of a cell class in the cingulate cortex, suggesting that ripple-LFP features can predict spiking activity not only locally in the hippocampus but also even in distal neocortical areas (Wang & Ikemoto, 2016).

Characterization of cell-type specific firing during ripples and their relation to SWR features is especially lacking in behaving primates where ripple physiology seems to be generally complementary to that observed in rats and mice (Bragin et al., 1999; Skaggs et al., 2007; Le Van Quyen et al., 2008; Logothetis et al., 2012; Leonard et al., 2015; Leonard & Hoffman, 2017). Despite the many similarities, a key difference is that ripples occur not only during awake immobility in primates but also during active visual exploration (Leonard et al., 2015; Leonard & Hoffman, 2017). To date, the only features measured during exploratory SWRs were their rate of occurrence and peak frequency, which did not differ by state.

In this study, we examined how three ripple-LFP features vary across waking states and as a function of learning, in addition to their modulation by spiking activity (single-unit activity, SUA). We found

that ripple and PRW amplitude in macaques are greater during quiescence than waking and that on remembered trials in a visual-search memory task, ripple amplitude is increased, with no change to duration or PRWs. We also describe the SWR modulation by cell types, classified by burstiness and firing rate, finding that low-firing rate cells (putative principal cells) are associated with enhanced ripple amplitude and attenuated postripple amplitude, whereas high-firing bursting and nonbursting cell types (putative basket interneurons) are associated with enhanced ripple and PRW amplitudes.

2 | MATERIALS AND METHODS

2.1 | Subjects and experimental design

Two adult female macaques (*Macaca mulatta*, named LU and LE) completed a visual target-detection task that requires hippocampal function in primates (Chau, Murphy, Rosenbaum, Ryan, & Hoffman, 2011), during daily recording sessions (this data set was used in Leonard et al. (2015) and Leonard and Hoffman (2017)). The flicker change-detection task [previously described in Leonard et al. (2015) and Leonard and Hoffman (2017)] required the animals to find and select a target object from nontargets in unique visual scenes for fluid reward (Figure 1a). Selection of a scene-unique target object was accomplished by holding gaze in the target region for a prolonged (≥ 800 ms) duration. The target object was defined as a changing item in a natural scene image, where the original and changed images were presented in alternation, each lasting 500 ms, with a brief grey-screen (50 ms) shown between image presentations. Displayed this way, detection of the changing part of the scene requires an effortful search in humans and macaques (Chau et al., 2011). An inter-trial interval (ITI) of 2–20 s followed each trial. The daily sessions began and ended with a period of at least 10 min when no stimulus was presented within the darkened booth and animals were allowed to sleep or sit quietly (quiescent period). Eye movements were recorded using video-based eye tracking (iViewX Hi-Speed Primate remote infrared eye tracker). All experimental protocols were conducted with approval from the local ethics and animal care authorities (Animal Care Committee, Canadian Council on Animal Care).

2.2 | Electrophysiological recordings

Both animals were chronically implanted with independently moveable platinum/tungsten multicore tetrodes (96 μm outer diameter; Thomas Recordings) lowered into hippocampal CA3/DG regions. Animal LE had a 9-tetrode bundle centered at AP +11 mm verified post-implant with MRI. For this study we analyzed activity from the 4/9 tetrodes placed to optimize ripple and unit responses; these tetrodes were separated by <600 μm in the bundle. Animal LU had 8 tetrodes divided into two bundles: one at AP +11 mm and the other at AP +8 mm verified with postoperative CT co-registration to MRI. Based on ripple and unit activity we analyzed 3 tetrodes from each bundle, with separation <500 μm in the bundles). LFPs were digitally sampled at 32 kHz using a Digital Lynx acquisition system (Neuralynx) and filtered between 0.5 Hz and 2 kHz. Single-unit activity was sampled at

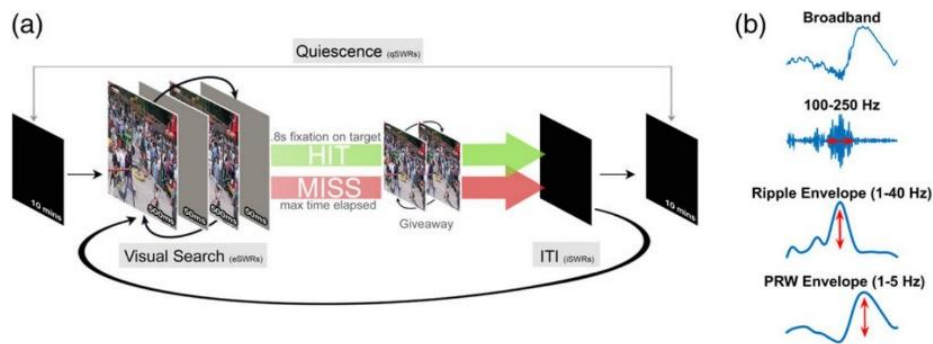


FIGURE 1 Experimental design of memory-guided visual search task and signal processing. (a) An original and modified scene is presented in alternation, interleaved with a brief grey mask, requiring an effortful search to detect the changing target. A trial ends with a 0.8 s fixation on the target for which a fluid reward is delivered (HIT), or when the maximum trial time is reached (MISS). A “giveaway” then follows in which the two scenes are displayed without a mask, revealing the target location. A trial ends with a black screen inter-trial-interval (ITI) of 2–22 s before the next trial is presented. During daily recording sessions, scenes are presented in blocks of 30 and the task is bookended with two rest periods (quiescence; ≥ 10 min) where a black screen is presented and animals sleep. See *Materials and Methods* for more details. (b) The broadband LFP signal is bandpass filtered in the ripple band (100–250 Hz), z-scored, rectified and then low pass filtered (1–40 Hz) to create the ripple envelope whose maximum value represents the ripple amplitude. The PRW envelope is a low pass filter (1–5 Hz) of the broadband signal and its peak represents the PRW amplitude [Color figure can be viewed at wileyonlinelibrary.com]

32 kHz and filtered between 600 Hz and 6 kHz, recording the waveform for 1 ms around a threshold triggered spike events. Single units were isolated using MClust based on wave-shape principle components, energy and peak/valley across channels. Only well-isolated cells were included, based on $< 1\%$ interspike intervals (ISIs) within 2 ms and cross-correlograms between bursting cell pairs that had to be free of burst-latency peaks (asymmetric, < 10 ms peak that could indicate the erroneous splitting of one CS unit into two; Harris, Henze, Csicsvari, Hirase, & Buzsáki, 2000). Units were classified as putative principal units (PR) if they had a burst firing mode (ISI mode peak, < 10 ms, comprising $\geq 10\%$ of ISIs) and under < 1 Hz overall firing rate. Units were classified as putative interneurons (IN) if they had no burst firing mode (> 10 ms ISI) and a firing rate > 1 Hz. The remaining two possible categories were the burst firing mode with > 1 Hz firing rate (BHF), and nonburst firing mode with < 1 Hz spiking rate (NBLF). Waveshape parameters such as spike width and peak-trough asymmetry can vary as a function of recording location relative to the cell body and not only by cell type (Henze et al., 2000, figure 8), therefore these wave-shape measures were not used for cell type classification in this study.

2.3 | SWR detection and feature estimation

SWR events were detected using the tetrode channel with the most visibly apparent ripple activity. The LFP signal was bandpass filtered (100–250 Hz), transformed into z-scores, rectified and then low pass filtered (1–40 Hz). Ripple events were defined as threshold crossings 3 SDs above the mean, with a minimum duration of 50 ms beginning and ending at 1 SD. This time period also defined the ripple duration. SWR amplitude was defined as the maximum peak of the ripple envelope (z-score). The amplitude of the PRW was defined as the maximum peak (z-score) of a narrower lowpass filter (1–5 Hz, Figure 1b). SWR amplitude, duration and PRW amplitude values were then normalized per tetrode for each animal. The use of the z transformation preserved the shape of the distributions (i.e., the relative magnitude differences from the mean) that would be lost with percentile/rank order, while ensuring an even scaling across tetrodes in case of overall

differences in ripple amplitude. Each feature of the SWR (ripple duration, amplitude, and PRW amplitude) was then compared across different states and task epochs.

2.4 | SWR features across behavioral epochs

SWRs were clustered depending on time of occurrence into three behavioral epochs; quiescence (10 min dark-booth time period at the beginning and end of every session, qSWR), ITI (2–22 s interval between scene presentations representing quiet waking “inactive” states, iSWR), and exploratory search (during “active” visual search, eSWR). We excluded search ripples that occurred while the monkey fixated off-screen, and during search trials where the monkey spent $> 40\%$ of trial time fixating off-screen. Task SWRs were further clustered by stimulus repetition into novel (scene repetition number = 0) and repeated trials (scene repetition number > 0), and repeated trial ripples were further clustered into ripples occurring during trials where the target was successfully found (HIT), and when the target was not (MISS).

2.5 | Statistical analysis

Ripple features across waking state and task epochs were compared using the Wilcoxon rank-sum test and the Kolmogorov–Smirnov (K–S) test. For the single-unit and ripple-LFP waveform analysis, a Kruskal–Wallis test was conducted with a Bonferroni correction for multiple comparisons.

3 | RESULTS

Based on SWR clustering described above, we detected 2,526 qSWRs (LU = 1866, LE = 660), 536 iSWRs (LU = 340, LE = 196), and 664 eSWRs (LU = 462, LE = 202) from a total of 77 recording sessions (LU = 45, LE = 32). Based on unit clustering described earlier,

we recorded from a total of 509 units: 242 PRs, 133 NBLFs, 48 BHF and 86 INs.

3.1 | SWR features across states

We first examined SWR duration, amplitude and PRW amplitude across the different states (qSWR, iSWR, and eSWR; Figure 2). SWR duration was not different across states (rank sum and K-S test $p > .5$; Figure 2a), whereas ripple amplitude was greater during qSWRs compared to eSWRs (rank sum $z = 2.48$, $p = 1.31 \times 10^{-2}$; K-S $d = 8.0 \times 10^{-2}$, $p = 8.4 \times 10^{-3}$, Figure 2b), and PRW amplitude was greater in qSWRs compared to iSWRs (rank sum: $z = 2.79$, $p = 5.30 \times 10^{-3}$, K-S $d = 7.0 \times 10^{-2}$, $p = 2.3 \times 10^{-2}$) and eSWRs (rank-sum: $z = 3.33$, $p = 8.63 \times 10^{-4}$, K-S $d = 9.1 \times 10^{-2}$, $p = 2.0 \times 10^{-3}$, Figure 2c).

3.2 | SWR features during recognition memory task

Previously, we found that ripples occur more frequently and closer to a visual target with learning (Leonard & Hoffman, 2017). We therefore asked whether ripples that occur on repeated trials are different in duration or amplitude. First, we examined whether features vary by scene repetition by splitting ripples into novel (repetitions = 0) and repeated (repetitions > 0), but found no differences in ripple duration, amplitude, or PRW amplitude between novel and repeated trials (rank sum and K-S tests $p > .05$). Next, we split repeated trials into trials where the target was successfully found (indicating memory for the target location), and not found (indicating forgetting). Ripple duration (Figure 3a) and PRW amplitude (Figure 3c) were not different between remembered and forgotten trials (rank sum and K-S tests $p > .5$). During remembered trials ($n = 112$) ripple amplitude was larger than forgotten trials ($n = 220$) (rank sum $z = 2.11$, $p = 3.5 \times 10^{-2}$, K-S test $d = 0.16$, $p = 3.6 \times 10^{-2}$, Figure 3b). Because we had

observed a greater ripple amplitude during quiescence compared to search, we compared ripple amplitude on remembered trials and quiescence but found no difference (rank sum: $z = 0.59$, $p = .55$, K-S $d = 8.5 \times 10^{-2}$, $p = .41$).

3.3 | SUA analysis

Next, we examined local cell-type specific firing underlying ripples. Spikes occurring in a 400 ms time window centered around the peak of the ripple envelope were clustered based on spike-timing relative to the ripple event. Spikes were clustered into *preripple*, if they occurred before the ripple, *ripple*; if they occurred during the ripple or *postripple*; if they occurred after the ripple (during the PRW). For each functional-unit type, the average ripple-LFP waveform was calculated based on the window of spike-times aligned to ripple peak (Figure 4). Also calculated for each unit is the average ripple waveform where no spikes were observed (Null), and below each waveform plot is the normalized spike count distribution for each unit class in the ripple window clustered by spike-timing (*preripple*, *ripple*, and *postripple*).

3.4 | SUA effects on ripple trough

We observed different effects on the magnitude of the ripple trough (defined as nearest trough to ripple peak) based on spike-time occurrence for PR (Figure 4a, $H[3] = 78.65$, $p = 5.99 \times 10^{-17}$), NBLF (Figure 4b, $H[3] = 141.10$, $p = 2.2 \times 10^{-30}$), IN (Figure 4d, $H[3] = 360.89$, $p = 6.53 \times 10^{-78}$), but not BHF cells (Figure 4c, $H[3] = 5.19$, $p = .16$). In PR cells, spiking in any of the time windows (*preripple*, *ripple*, or *postripple*) was associated with a larger trough compared to no spikes ($p < .05$, Bonferroni post hoc test; mean LE-PR-ripple = $-1.79z$, LE-PR-null = -1.59 , LU-PR-ripple = $-2.74z$, LU-PR-null = $-1.58z$). In NBLF cells, spiking in the ripple window was

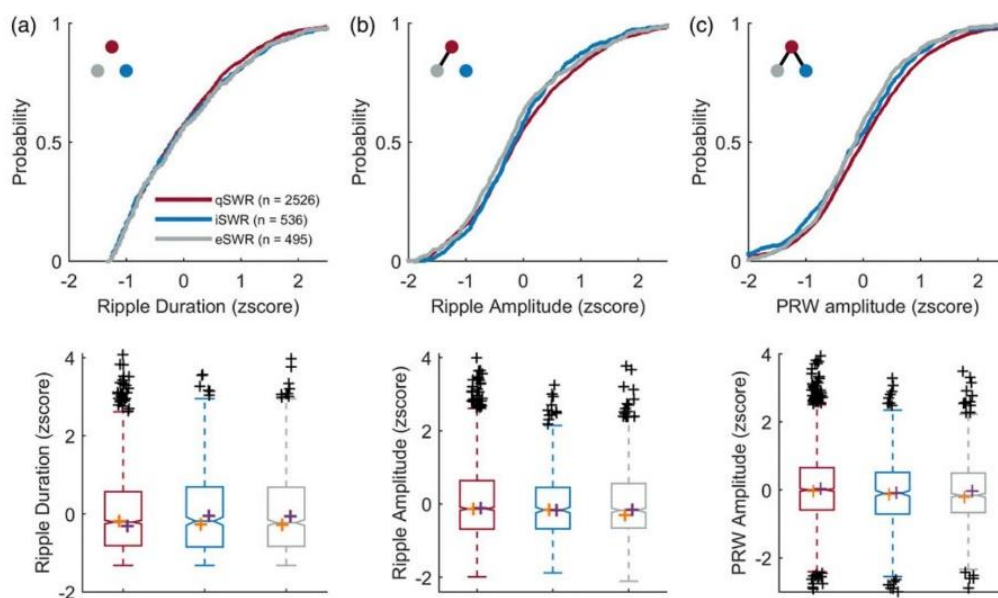


FIGURE 2 Ripple and PRW amplitudes are greater during qSWRs than iSWRs and eSWRs. *Top*: cumulative probability distribution. Blackline connecting dots in the top left inset of top panels indicates $p < .05$ between groups, as represented by dot color. *Bottom*: boxplots of corresponding distributions above with median values for each animal plotted in orange (for LU) and purple (for LE) crosses, for SWR duration (a), amplitude (b) and PRW amplitude (c) across qSWRs ($n = 2,526$), iSWRs ($n = 536$), and eSWRs ($n = 495$) [Color figure can be viewed at wileyonlinelibrary.com]

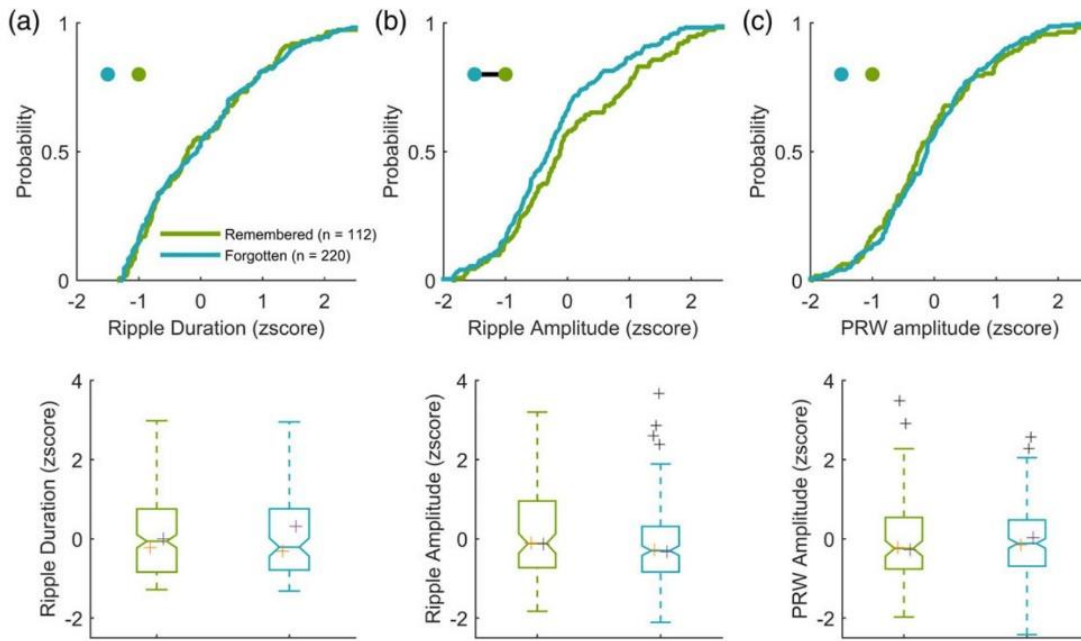


FIGURE 3 SWR amplitude, but not duration or PRW amplitude, is greater during remembered trials during the goal-directed visual search. *Top*: cumulative probability distribution. Blackline connecting dots in the top left inset of top panels indicates $p < .05$ between groups, as represented by dot color. *Bottom*: boxplots of corresponding distributions above. Median values for each animal are plotted in orange (LU) and purple (LE) crosses for SWR duration (a), amplitude (b), and PRW amplitude (c) during remembered ($n = 220$) and forgotten ($n = 112$) trials [Color figure can be viewed at wileyonlinelibrary.com]

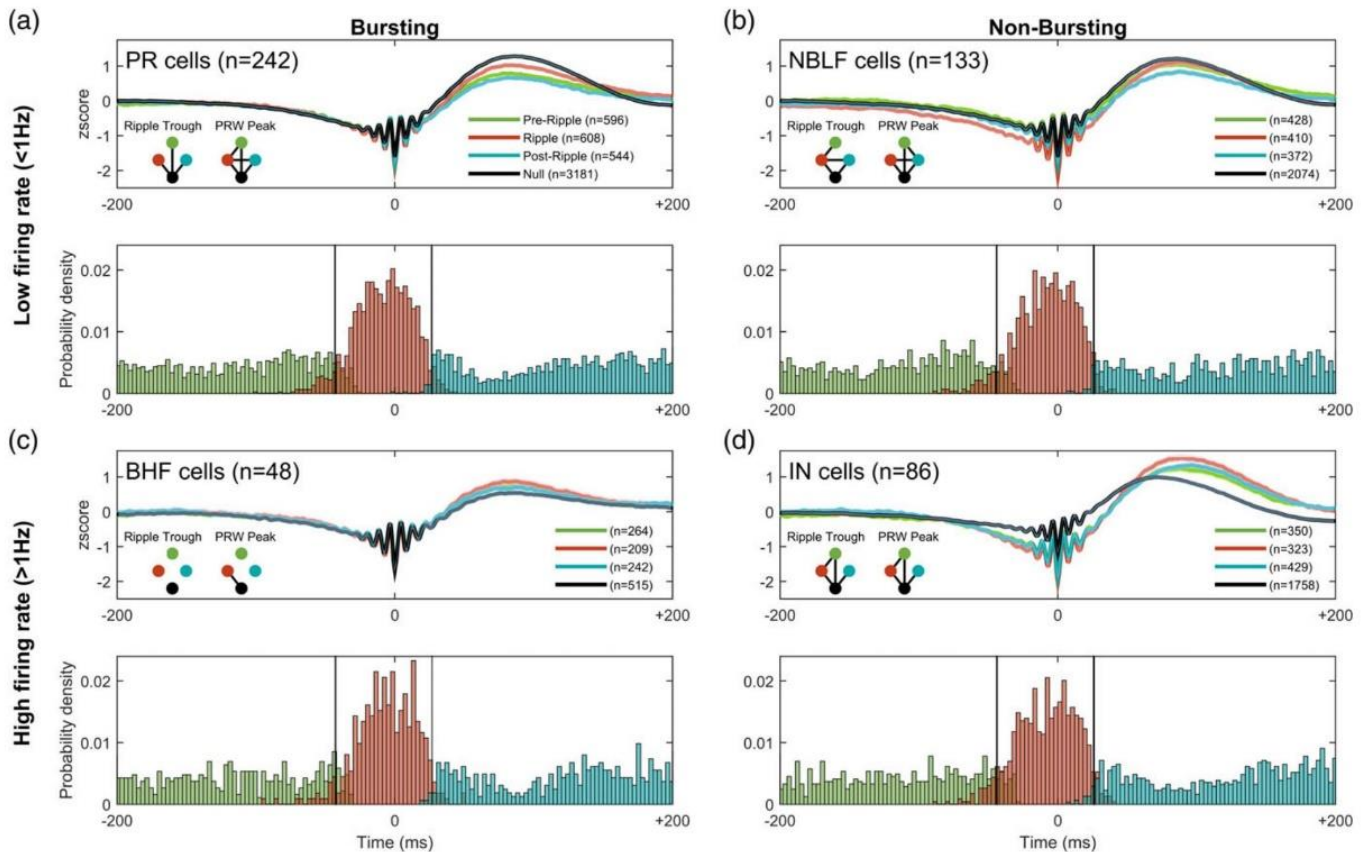


FIGURE 4 Ripple waveform varies by cell-type activity and spike timing relative to the SWR event. (A) *Top*: mean \pm 95% confidence intervals of broadband SWRs grouped by putative principal cells' spike-timing into preripple, ripple, PRW, and null. Blackline connecting dots in the lower left inset of top panel indicates $p < .05$ between groups, as represented by dot color, for respective ripple feature. *Bottom*: probability density histogram of spike counts in a ± 200 ms window centered around the maximum ripple amplitude for putative principal units. The ripple window membership (pre, ripple, post) is indicated by the color of the histogram bar. (b) as in (a) but for nonbursting low-firing rate units; (c) for bursting high-firing rate, and (d) for putative interneuron units [Color figure can be viewed at wileyonlinelibrary.com]

associated with a greater trough compared to spiking in preripple and postripple windows, as well as no spiking ($p < .05$, Bonferroni post hoc; mean LE-NBLF-ripple = $-1.92z$, LE-NBLF-null = $-1.61z$; LU-NBLF-ripple = $-2.75z$, LU-NBLF-null = $-1.54z$). In IN cells, a similar pattern followed whereby ripple spikes were associated with a larger trough compared to preripple and no spikes ($p < .05$, Bonferroni post hoc; LE-INT-ripple = $-1.73z$, LE-INT-null = $-1.59z$; LU-INT-ripple = $-2.3z$, LU-INT-null = $-1.04z$). Interestingly, for nonbursting low firing rate cells that fired during the ripple, the LFP showed slow negative deflections in the ~ 200 ms leading up to the ripple event.

3.5 | SUA effects on the PRW

The peak magnitude of the PRW in the broadband signal varied according to spike-time occurrence and as a function of cell type, among PR ($H[3] = 693.67$, $p = 4.94 \times 10^{-150}$), NBLF ($H[3] = 150.59$, $p = 1.96 \times 10^{-32}$), IN ($H[3] = 25.10$, $p = 1.47 \times 10^{-5}$), and BHF cells ($H[3] = 11.90$, $p = 7.7 \times 10^{-3}$). The spiking of low firing-rate cells (PR and NBLF cells, Figure 4a,b) during the ripple window was associated with smaller peaks compared to null spiking ($p < .05$, Bonferroni post hoc), whereas the opposite effect was seen with high firing-rate cells (BHF and IN cells, Figure 4c,d) where spiking was associated with a larger PRW ($p < .05$, Bonferroni post hoc). For low firing-rate cells (Figure 4a,b), spiking during the postripple window resulted in the smallest peak ($p < .05$, Bonferroni post hoc). For high firing-rate cells (Figure 4c,d), spiking during the ripple was associated with the largest peaks ($p < .05$, Bonferroni post hoc). The heightened modulation for both peaks and troughs found for the IN group suggests a stronger overall ripple amplitude, measured explicitly below.

3.6 | SUA effects on the amplitude of the ripple envelope

In the earlier analysis of SWR feature changes with behavioral state, the ripple amplitude envelope was greater during quiescence than search (Figure 2b), and larger during remembered compared to forgotten trials (Figure 3b). We therefore sought to examine how spiking in different time windows (preripple, ripple, and postripple) by different cell types affects ripple amplitude (Figure 5). We found that spiking by PR ($H[3] = 934.73$, $p = 2.60 \times 10^{-202}$), NBLF ($H[3] = 659.32$, $p = 1.39 \times 10^{-142}$), and IN cells ($H[3] = 613.21$, $p = 1.38 \times 10^{-132}$) during any period in the 400 ms ripple window was associated with an increase in ripple amplitude (Figure 5a,b,d), whereas spikes from BHF cells had no effect on amplitude (Figure 5c, $H[3] = 9.83$, $p = .20$; LE-BHF-ripple = $0.35z$, LE-BHF-null = $0.35z$, LU had no BHF cells). The contribution of PR and NBLF spiking to ripple amplitude based on spike-timing followed a similar trend where spiking during the ripple window yielded a larger ripple amplitude compared to the postripple window and null spiking (Figure 5a,b, $p < .05$, Bonferroni post hoc; LE-PR-ripple = $0.38z$, LE-PR-null = $0.25z$; LU-PR-ripple = $0.41z$, LU-PR-null = $0.25z$; LE-NBLF-ripple = $0.37z$, LE-NBLF-null = $0.33z$). With NBLF cells ripple-window amplitude was also different from preripple spikes ($p < .05$, Bonferroni post hoc). Ripple-aligned spikes from NBLF cells resulted in the largest ripple amplitude across all cell classes and spike-times ($p < .05$, Bonferroni post hoc). With IN cells,

spikes during the three time-windows yielded a larger amplitude compared to that seen without IN spiking (Figure 5d, $p > .05$, Bonferroni post hoc).

3.7 | SUA effects on the amplitude of the PRW envelope

All four cell classes showed differences in PRW amplitude based on spike-timing; PR ($H[3] = 600.57$, $p = 7.59 \times 10^{-130}$), NBLF ($H[3] = 111.86$, $p = 4.37 \times 10^{-24}$), BHF ($H[3] = 13.20$, $p = 4.20 \times 10^{-3}$) and IN cells ($H[3] = 17.98$, $p = 4.0 \times 10^{-4}$). Not surprisingly, the effects on PRW amplitude were similar to those reported earlier on the broadband signal. Spiking by low-spiking cells (PR and NBLF cells) was associated with smaller PRW amplitudes compared to no spikes (mean LE-PR-ripple = $0.96z$, LE-PR-null = $1.39z$, LU-PR-ripple = $0.77z$, LU-PR-null = $1.21z$, LE-NBLF-ripple = $1.11z$, LE-NBLF-null = $1.37z$, LU-NBLF-ripple = $0.94z$, LU-NBLF-null = $1.17z$), whereas spiking by high firing-rate cells (BHF and IN cells) was associated with larger PRW amplitudes (mean LE-BHF-ripple = $1.12z$, LE-BHF-null = $0.47z$; LU had no BHF units; LE-IN-ripple = $1.51z$, LE-IN-null = $0.92z$, LU-IN-ripple = $1.46z$, LU-IN-null = $1.12z$). In PR cells, null spiking was associated with the largest PRW amplitude, whereas spiking during the ripple resulted in a larger amplitude compared to preripple and postripple spikes (Figure 5a, $p < .05$, Bonferroni post hoc). For NBLF cells, although the pattern was similar to PR cells, the decrease in amplitude due to spiking in the window was not as profound (Figure 5b). Null spiking was associated with a larger PRW amplitude compared to spikes during the ripple, preripple, and postripple, and ripple spikes yielded a larger amplitude than postripple spikes ($p < .05$, Bonferroni post hoc). High firing rate cells had a similar trend to PRW amplitude by spike-time but with a different direction of magnitude. Spikes during the ripple by BHF cells resulted in larger PRW amplitude compared to no spikes (Figure 5c, $p < .05$, Bonferroni post hoc). But of all cell types, the IN group showed the most striking effects, with spiking during the ripple producing a larger PRW amplitude compared to preripple and no spikes (Figure 5d, $p < .05$, Bonferroni post hoc), as well the largest PRW amplitude compared to all other cell classes and spike times ($p < .05$, Bonferroni post hoc).

3.8 | Dependency of spiking across ripple time windows

The apparent relationship between spiking in one epoch and LFP/ripple feature in another epoch could in principle be due to joint spiking across epochs, and not to a true time-lagged modulation. For each unit of each cell type, we calculated the conditional probability of spiking in one time window given a spike from that cell during another window of a ripple event (pre, during, post). Across units from all cell types across all pairs of epochs, a spike in one window typically predicted the *absence* of spikes in the other ripple window. Median probabilities per cell type and window pair ranged from 0 to 0.33. Thus, LFP fluctuations that occur with a lag from the time of spikes do not appear to be an artifact of latent concurrent spiking.

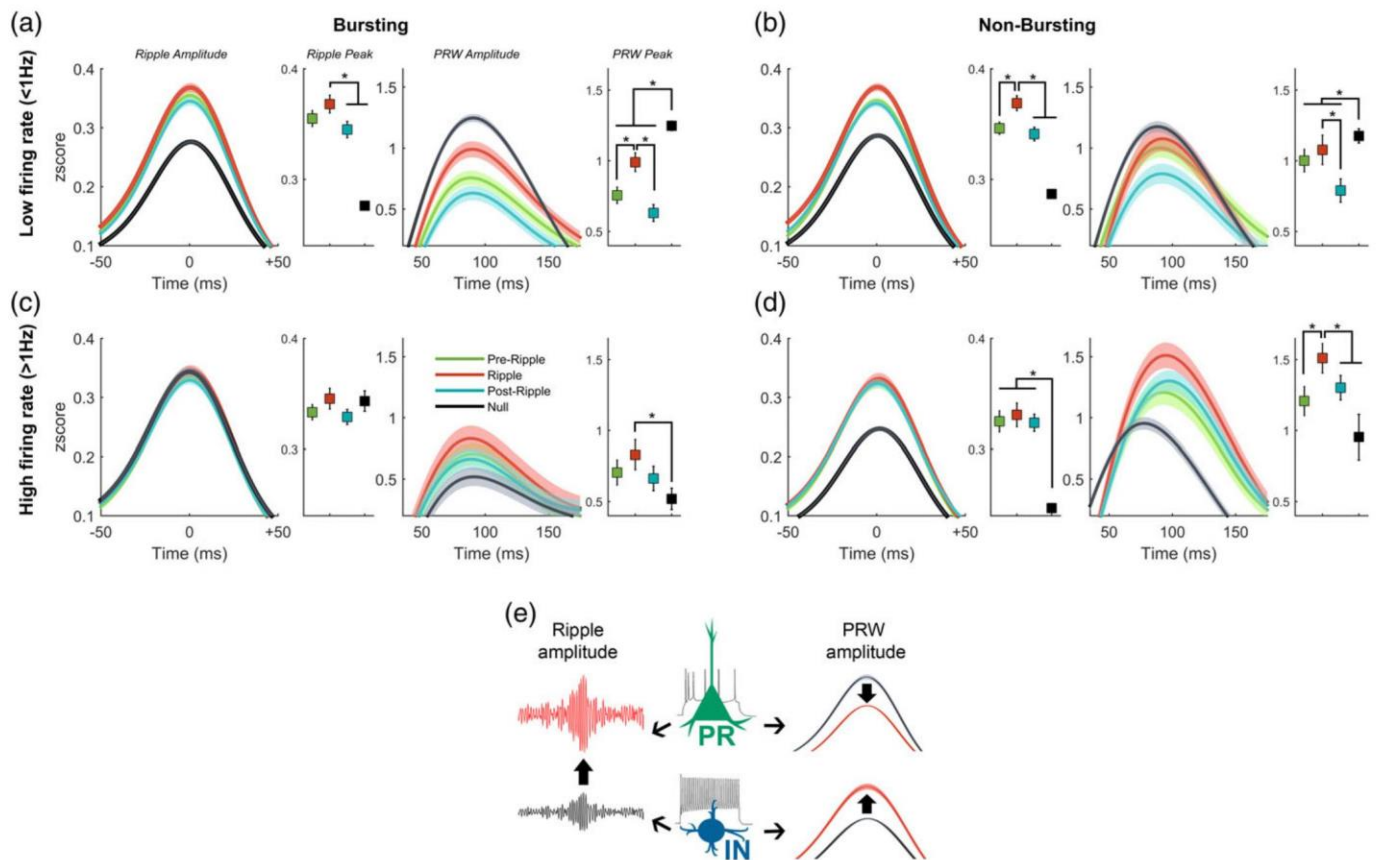


FIGURE 5 Ripple and PRW amplitudes vary by cell-type activity and spike-timing. Mean \pm 95% confidence intervals of ripple (left) and PRW (right) envelope amplitudes along with peak values with error bars indicating 95% confidence intervals for principal units (a), nonbursting low-firing units (b), bursting high-firing (c) and putative interneurons (d). Schematic of main effects; spikes from principal cells (PR) and interneurons (IN) are associated with greater ripple amplitude, PR spikes are associated with attenuated PRW while IN spikes are associated with enhanced PRW (e). * $p < .05$ [Color figure can be viewed at wileyonlinelibrary.com]

4 | DISCUSSION

In this study, we showed for the first time in primates that ripple features vary with waking state and memory. By comparing ripple events during quiescent and active periods, we observed that (a) quiescent ripples have larger amplitudes and larger PRWs. Further examination of awake ripples during the memory task revealed that (b) ripples during remembered trials have greater amplitudes compared to forgotten trials, with no change to duration or PRWs. By analyzing ripple-associated single-unit activity, we found that (c) ripple amplitude is associated with the activity of low-firing cells and putative interneurons, whereas the peak and elaboration of the PRW are enhanced by even coarsely timed activity from putative interneurons.

Ripple amplitude is a measure of the magnitude of the high-frequency ripple oscillation that is thought to reflect both postsynaptic currents and spiking activity by cells within a radius of ~ 100 – $200 \mu\text{m}$ around a recording electrode (Schomburg et al., 2012). The amplitude is dictated by the size and number of active neuronal ensembles that are made up of principal cells and interneurons (Csicsvari et al., 2000), and can be used to predict if similar ensembles are active across ripples (Taxidis et al., 2015).

We classified cells physiologically into four types using burst firing mode and firing rate, although additional functional cell type divisions

are possible. All four cell types showed positive modulation of firing rate during ripples, yet only the activity of low-firing cells and the non-bursting high-firing cells was associated with increasing ripple amplitude. Low-firing cells were associated with a decrease in PRW amplitude whereas high-firing cells showed the opposite effect. Critically, we found that spiking effects on ripple and PRW amplitude were strongest when spikes occurred within the ripple window, yet effects were also observable when spiking occurred within the preripple and postripple periods. This suggests that the effects of spiking on the ripple-LFP can be extended in time, consistent with previous reports showing similar delayed spike-LFP relationships (Esgkhaei et al., 2017). This time-offset cannot be explained by an increase in the conditional probability of spikes in the preripple or postripple window and spiking within the ripple as we observe that the probability stays the same. The low-firing cells are likely pyramidal cells, which in the rodent hippocampus are known to display bursting modes (Hemond et al., 2008), with a variable composition across and within subfields (Masukawa, Benardo, & Prince, 1982; Schwartzkroin, 1975). Whereas bursting pyramidal cells have been singled out as necessary for the fast oscillation of ripples (Dzhala & Staley, 2004) and for affecting LFP amplitude (Constantinou et al., 2016), our results suggest that non-bursting principal cells are also strongly associated with the amplitude of the fast ripple oscillation. This positive ripple-associated modulation

of principal cell activity is consistent with previous findings (Csicsvari et al., 1999; Csicsvari, Hirase, Mamiya, & Buzsáki, 2000; Hajos et al., 2013; Klausberger et al., 2003; Klausberger et al., 2004; Le Van Quyen et al., 2008). Most of our spikes and ripples (~92%) were detected on the same electrodes and so we were unable to systematically examine the dependence of the relationship spikes have on the ripple field potential as a function of distance. Although the bundled tetrode arrays used in this study are not ideal for spatial sampling along the septotemporal and transverse hippocampal axes, this is an interesting area for future investigation given the spatiotemporal spread of ripples along the septotemporal axis (Patel, Schomburg, Berenyi, Fujisawa, & Buzsáki, 2013).

The nonbursting high-firing cell type in our study is likely to contain parvalbumin-positive interneurons. Parvalbumin-positive (PV⁺) and bistratified cells show the greatest ripple-associated increase in spiking rate (Klausberger et al., 2003; Klausberger and Somogyi, 2008), with PV⁺ cells having the greatest excitatory conductance after the ripple peak (Hajos et al., 2013). Axo-axonic and O-LM cells typically display negative modulation where they cease to spike during ripples, whereas CCK⁺ interneurons appear to be unmodulated by ripples (Klausberger et al., 2003; Klausberger and Somogyi, 2008). Of the high-firing cells in our data, we only observed a ripple-associated positive modulation in spiking (likely due to limited sampling). Perisomatic-targeting PV⁺ interneurons have been shown to be critical for the initiation of the ripple fast-oscillation through their recurrent connectivity leading to highly organized inhibition which creates opportunity for synchronous pyramidal cell ensemble activity in CA1/CA3 (Ellender et al., 2010; Schlinghoff et al., 2014; Stark et al., 2014; Valero et al., 2015). Pharmacologically blocking perisomatic inhibition on pyramidal cells impairs spontaneous ripple activity and decreases SWR amplitude (Stark et al., 2014; Schlinghoff et al., 2014; Gan et al., 2017); moreover, inhibitory conductance in pyramidal neurons during ripples is more dominant than excitatory conductance, correlates with ripple amplitude, and depends on PV⁺ interneurons (Gan et al., 2017). The effects of inhibitory neurons also trail the SWR event, where inhibitory synaptic input leads to the collective afterhyperpolarization of local principal cells following ripples, visible as a postripple deflection in the LFP (English et al., 2014; Hulse et al., 2016). These results are consistent with our finding that spiking of putative PV⁺ interneurons is associated with both larger amplitude ripples and the postripple "inhibitory" wave. The observed increase in ripple amplitude and PRW amplitude during quiescence could therefore be a result of greater PV interneuronal activation in that state compared to during the task. The increased pyramidal-cell synchrony and larger ensemble activity associated with PV IN ripple activity could form a spatiotemporal "burst" to better propagate efferent signals during sleep, consistent with BOLD responses seen in macaques under anesthesia (Logothetis et al., 2012). Other mechanisms are likely to underlie the differences we observed in waking, for example, during the memory-guided search.

Waking ripples are increasingly implicated in memory-guided decision-making (Jadhav et al., 2012; Papale, Zielinski, Frank, Jadhav, & Redish, 2016; Wu et al., 2017). In rodents, waking ripples contain a higher proportion of co-activated cell pairs during correct memory recall in a spatial alternation task, suggesting a higher level of

coordinated neural activity on remembered trials (Singer et al., 2013). In primates, waking ripples in a visual-search task occur more frequently and closer to the target during remembered trials suggesting a possible role in memory retrieval (Leonard & Hoffman, 2017). Since the amplitude indexes the size of ripple-associated ensembles (Csicsvari et al., 2000; Taxis et al., 2015), it is possible that on average, larger and/or more synchronized ensembles are activated during ripples on remembered trials, though we note that the magnitude of the effects in this study was modest. It is possible that familiar scene stimuli and/or prediction of reward support stronger, more coherent excitatory drive to activate relevant ensembles during the SWR, though determining how such drive modifies ripple magnitude and no other features warrant further study.

ACKNOWLEDGMENTS

This study was supported by the National Science and Engineering Research Council (NSERC) Discovery Grant, NSERC CREATE Vision Science and Applications, Alfred P. Sloan Foundation, Canada Foundation for Innovation, the Krembil Foundation, Brain Canada, and Alzheimer Society of Canada.

CONFLICT OF INTEREST

The authors have no conflicts of interest.

ORCID

Kari L. Hoffman  <https://orcid.org/0000-0003-0560-8157>

REFERENCES

- Anastassiou, C. A., Perin, R., Buzsáki, G., Markram, H., & Koch, C. (2015). Cell-type-and activity-dependent extracellular correlates of intracellular spiking. *Journal of Neurophysiology*, *114*, 608–623.
- Atherton, L. A., Dupret, D., & Mellor, J. R. (2015). Memory trace replay: The shaping of memory consolidation by neuromodulation. *Trends in Neurosciences*, *38*, 560–570.
- Belluscio, M. A., Mizuseki, K., Schmidt, R., Kempter, R., & Buzsáki, G. (2012). Crossfrequency phase-phase coupling between θ and γ oscillations in the hippocampus. *The Journal of Neuroscience*, *32*, 423–435.
- Bragin, A., Engel, J., Wilson, C. L., Fried, I., & Buzsáki, G. (1999). High-Frequency Oscillations in Human Brain. *Hippocampus*, *9*, 137–142.
- Buzsáki, G. (2015). Hippocampal sharp wave-ripple: A cognitive biomarker for episodic memory and planning. *Hippocampus*, *25*, 1073–1188.
- Carr, M. F., Jadhav, S. P., & Frank, L. M. (2011). Hippocampal replay in the awake state: A potential substrate for memory consolidation and retrieval. *Nature Neuroscience*, *14*, 147–153.
- Chau, V. L., Murphy, E. F., Rosenbaum, R. S., Ryan, J. D., & Hoffman, K. L. (2011). A flicker change detection task reveals object-in-scene memory across species. *Frontiers in Behavioral Neuroscience*, *5*, 58.
- Constantinou, M., Gonzalo Cogno, S., Elijah, D. H., Kropff, E., Gigg, J., Samengo, I., & Montemurro, M. A. (2016). Bursting Neurons in the Hippocampal Formation Encode Features of LFP Rhythms. *Frontiers in Computational Neuroscience*, *10*, 1–18.
- Csicsvari, J., Hirase, H., Czurkó, A. S., Mamiya, A., Rgy, G., & Ki, B. (1999). Oscillatory coupling of hippocampal pyramidal cells and interneurons in the behaving rat. *The Journal of Neuroscience*, *19*, 274–287.
- Csicsvari, J., Hirase, H., Mamiya, A., & Buzsáki, G. (2000). Ensemble patterns of hippocampal CA3-CA1 neurons during sharp wave-associated population events. *Neuron*, *28*, 585–594.
- Csicsvari, J., O'Neill, J., Allen, K., & Senior, T. (2007). Place-selective firing contributes to the reverse-order reactivation of CA1 pyramidal cells

- during sharp waves in open-field exploration. *The European Journal of Neuroscience*, 26, 704–716.
- Diba, K., & Buzsáki, G. (2007). Forward and reverse hippocampal place-cell sequences during ripples. *Nature Neuroscience*, 10, 1241–1242.
- Dzhala, V. I., & Staley, K. J. (2004). Mechanisms of fast ripples in the hippocampus. *The Journal of Neuroscience*, 24, 8896–8906.
- Ego-Stengel, V., & Wilson, M. A. (2010). Disruption of ripple-associated hippocampal activity during rest impairs spatial learning in the rat. *Hippocampus*, 20, 1–10.
- Ellender, T. J., & Paulsen, O. (2010). The many tunes of perisomatic targeting interneurons in the hippocampal network. *Frontiers in Cellular Neuroscience*, 4, 1–11.
- English, D. F., Peyrache, A., Stark, E., Roux, L., Vallentin, D., Long, M. A., & Buzsáki, G. (2014). Excitation and inhibition compete to control spiking during hippocampal ripples: Intracellular study in behaving mice. *The Journal of Neuroscience*, 34, 16509–16517.
- Eschenko, O., Ramadan, W., Molle, M., Born, J., & Sara, S. J. (2008). Sustained increase in hippocampal sharp-wave ripple activity during slow-wave sleep after learning. *Learning & Memory*, 15, 222–228.
- Esglhaei, M., Daliri, M. R., & Treue, S. (2017). Local field potentials are induced by visually evoked spiking activity in macaque cortical area MT. *Scientific Reports*, 7, 1–11.
- Foster, D. J., & Wilson, M. A. (2006). Reverse replay of behavioural sequences in hippocampal place cells during the awake state. *Nature*, 440, 680–683.
- Gan, J., Weng, S. M., Pernía-Andrade, A. J., Csicsvari, J., & Jonas, P. (2017). Phase-Locked Inhibition, but Not Excitation, Underlies Hippocampal Ripple Oscillations in Awake Mice In Vivo. *Neuron*, 93, 308–314.
- Girardeau, G., Benchenane, K., Wiener, S. I., Buzsáki, G., & Zugaro, M. B. (2009). Selective suppression of hippocampal ripples impairs spatial memory. *Nature Neuroscience*, 12, 1222–1223.
- Girardeau, G., & Zugaro, M. (2011). Hippocampal ripples and memory consolidation. *Current Opinion in Neurobiology*, 21, 452–459.
- Gomperts, S. N., Kloosterman, F., & Wilson, M. A. (2015). VTA neurons coordinate with the hippocampal reactivation of spatial experience. *Elife*, 4, e05360.
- Hajos, N., Karlocai, M. R., Nemeth, B., Ulbert, I., Monyer, H., Szabo, G., ... Gulyas, A. I. (2013). Input-output features of anatomically identified CA3 neurons during hippocampal sharp wave/ripple oscillation in vitro. *Journal of Neuroscience*, 33, 11677–11691.
- Harris, K. D., Henze, D. A., Csicsvari, J., Hirase, H., & Buzsáki, G. (2000). Accuracy of tetrode spike separation as determined by simultaneous intracellular and extracellular measurements. *Journal of Neurophysiology*, 84, 401–414.
- Hemond, P., Epstein, D., Boley, A., Migliore, M., Ascoli, G. A., & Jaffe, D. B. (2008). Distinct classes of pyramidal cells exhibit mutually exclusive firing patterns in hippocampal area CA3b. *Hippocampus*, 18, 411–424.
- Henze, D. A., Borhegyi, Z., Csicsvari, J., Mamiya, A., Harris, K. D., & Buzsáki, G. (2000). Intracellular features predicted by extracellular recordings in the hippocampus in vivo. *Journal of Neurophysiology*, 84, 390–400.
- Hulse, B. K., Moreaux, L. C., Lubenov, E. V., & Siapas, A. G. (2016). Membrane potential dynamics of CA1 pyramidal neurons during hippocampal ripples in awake mice. *Neuron*, 89, 800–813.
- Jadhav, S. P., Kemere, C., German, P. W., & Frank, L. M. (2012). Awake hippocampal sharp-wave ripples support spatial memory. *Science*, 336, 1454–1458.
- Ji, D., & Wilson, M. A. (2007). Coordinated memory replay in the visual cortex and hippocampus during sleep. *Nature Neuroscience*, 10, 100–107.
- Klausberger, T., Magill, P. J., Szűl, L., Márton, F., David, J., Roberts, B., Cobden, P. M., Buzsáki, G., Somogyi, P. (2003). Brain-state-and cell-type-specific firing of hippocampal interneurons in vivo. *Nature*, 421, 844–848.
- Klausberger, T., Marton, L. F., Baude, A., Roberts, J. D. B., Magill, P. J., & Somogyi, P. (2004). Spike timing of dendrite-targeting bistratified cells during hippocampal network oscillations in vivo. *Nature Neuroscience*, 7, 41–47.
- Klausberger, T., & Somogyi, P. (2008). Neuronal Diversity and of Hippocampal Circuit Operations. *Science*, 321, 53–57.
- Le Van Quyen, M., Bragin, A., Staba, R., Crepon, B., Wilson, C. L., & Engel, J., Jr. (2008). Cell type-specific firing during ripple oscillations in the hippocampal formation of humans. *The Journal of Neuroscience*, 28, 6104–6110.
- Lee, A. K., & Wilson, M. A. (2002). Memory of sequential experience in the hippocampus during slow wave sleep. *Neuron*, 36, 1183–1194.
- Leonard, T. K., & Hoffman, K. L. (2017). Sharp-wave ripples in primates are enhanced near remembered visual objects. *Current Biology*, 27, 257–262.
- Leonard, T. K., Mikkila, J. M., Eskandar, E. N., Gerrard, J. L., Kaping, D., Patel, S. R., ... Hoffman, K. L. (2015). Sharp wave ripples during visual exploration in the primate hippocampus. *The Journal of Neuroscience*, 35, 14771–14782.
- Logothetis, N. K., Eschenko, O., Murayama, Y., Augath, M., Steudel, T., Evrard, H. C., ... Oeltermann, A. (2012). Hippocampal-cortical interaction during periods of subcortical silence. *Nature*, 491, 547–553.
- Masukawa, L. M., Benardo, L. S., & Prince, D. A. (1982). Variations in electrophysiological properties of hippocampal neurons in different subfields. *Brain Research*, 242, 341–344.
- Montefusco-Siegmund, R., Leonard, T. K., & Hoffman, K. L. (2017). Hippocampal gamma-band synchrony and pupillary responses index memory during visual search. *Hippocampus*, 27, 425–434.
- Nadásdy, Z., Hirase, H., Czurko, A., Csicsvari, J., & Buzsáki, G. (1999). Replay and time compression of recurring spike sequences in the hippocampus. *The Journal of Neuroscience*, 19, 9497–9507.
- Nokia, M. S., Mikkonen, J. E., Penttonen, M., & Wikgren, J. (2012). Disrupting neural activity related to awake-state sharp wave-ripple complexes prevents hippocampal learning. *Frontiers in Behavioral Neuroscience*, 6, 84.
- O'Neill, J., Senior, T., & Csicsvari, J. (2006). Place-selective firing of CA1 pyramidal cells during sharp wave/ripple network patterns in exploratory behavior. *Neuron*, 49, 143–155.
- Papale, A. E., Zielinski, M. C., Frank, L. M., Jadhav, S. P., & Redish, A. D. (2016). Interplay between hippocampal sharp-wave-ripple events and vicarious trial and error behaviors in decision making. *Neuron*, 92, 975–982.
- Patel, J., Schomburg, E. W., Berenyi, A., Fujisawa, S., & Buzsáki, G. (2013). Local generation and propagation of ripples along the septotemporal axis of the hippocampus. *The Journal of Neuroscience*, 33, 17029–17041.
- Pennartz, C. M., Lee, E., Verheul, J., Lipa, P., Barnes, C. A., & McNaughton, B. L. (2004). The ventral striatum in off-line processing: Ensemble reactivation during sleep and modulation by hippocampal ripples. *The Journal of Neuroscience*, 24, 6446–6456.
- Peyrache, A., Khamassi, M., Benchenane, K., Wiener, S. I., & Battaglia, F. P. (2009). Replay of rule-learning related neural patterns in the prefrontal cortex during sleep. *Nature Neuroscience*, 12, 919–926.
- Qin, Y. L., McNaughton, B. L., Skaggs, W. E., & Barnes, C. A. (1997). Memory reprocessing in corticocortical and hippocampocortical neuronal ensembles. *Philosophical Transactions of the Royal Society of London. Series B, Biological Sciences*, 352, 1525–1533.
- Ray, S., Crone, N. E., Niebur, E., Franaszczuk, P. J., & Hsiao, S. S. (2008). Neural correlates of high-gamma oscillations (60–200 Hz) in macaque local field potentials and their potential implications in electrocorticography. *The Journal of Neuroscience*, 28, 11526–11536.
- Roumis, D. K., & Frank, L. M. (2015). Hippocampal sharp-wave ripples in waking and sleeping states. *Current Opinion in Neurobiology*, 35, 6–12.
- Sadowski, J. H., Jones, M. W., & Mellor, J. R. (2011). Ripples make waves: Binding structured activity and plasticity in hippocampal networks. *Neural Plasticity*, 2011, 960389.
- Scheffer-Teixeira, R., Belchior, H., Leão, R. N., Ribeiro, S., & Tort, A. B. (2013). On high-frequency field oscillations (>100 Hz) and the spectral leakage of spiking activity. *The Journal of Neuroscience*, 33, 1535–1539.
- Schlingloff, D., Kali, S., Freund, T. F., Hajos, N., & Gulyas, A. I. (2014). Mechanisms of Sharp Wave Initiation and Ripple Generation. *Journal of Neuroscience*, 34, 11385–11398.
- Schomburg, E. W., Anastassiou, C. A., Buzsáki, G., & Koch, C. (2012). The spiking component of oscillatory extracellular potentials in the rat hippocampus. *The Journal of Neuroscience*, 32, 11798–11811.

- Schwartzkroin, P. A. (1975). Characteristics of CA1 neurons recorded intracellularly in the hippocampal in vitro slice preparation. *Brain Research*, 85, 423–436.
- Singer, A. C., Carr, M. F., Karlsson, M. P., & Frank, L. M. (2013). Hippocampal SWR activity predicts correct decisions during the initial learning of an alternation task. *Neuron*, 77, 1163–1173.
- Skaggs, W. E., McNaughton, B. L., Permenter, M., Archibeque, M., Vogt, J., Amaral, D. G., & Barnes, C. A. (2007). EEG sharp waves and sparse ensemble unit activity in the macaque hippocampus. *Journal of Neurophysiology*, 98, 898–910.
- Stark, E., Roux, L., Eichler, R., Senzai, Y., Royer, S., & Buzsáki, G. (2014). Pyramidal cell-interneuron interactions underlie hippocampal ripple oscillations. *Neuron*, 83, 467–480.
- Taxidis, J., Anastassiou, C. A., Diba, K., & Koch, C. (2015). Local field potentials encode place cell ensemble activation during hippocampal sharp wave ripples. *Neuron*, 87, 590–604.
- Valero, M., Cid, E., Averkin, R. G., Aguilar, J., Sanchez-Aguilera, A., Viney, T. J., Gomez-Dominguez, D., Bellistri, E., de la Prida, L. M. (2015). Determinants of different deep and superficial CA1 pyramidal cell dynamics during sharp-wave ripples. *Nature Neuroscience*, 18, 1281–1290.
- Wang, D. V., & Ikemoto, S. (2016). Coordinated interaction between hippocampal sharp-wave ripples and anterior cingulate unit activity. *The Journal of Neuroscience*, 36, 10663–10672.
- Wu, C. T., Haggerty, D., Kemere, C., & Ji, D. (2017). Hippocampal awake replay in fear memory retrieval. *Nature Neuroscience*, 20, 571–580.

How to cite this article: Hussin AT, Leonard TK, Hoffman KL. Sharp-wave ripple features in macaques depend on behavioral state and cell-type specific firing. *Hippocampus*. 2018;1–10. <https://doi.org/10.1002/hipo.23046>

Title: Dissociations in retrosplenial and hippocampal synchrony for remotely learned events

Ahmed T. Hussin, Saman Abbaspour, Kari L. Hoffman

A. T. H.: Department of Biology, Centre for Vision Research, York University, Toronto, ON, Canada; athussin@yorku.ca

S. A.: Department of Psychology, Center for Integrative and Cognitive Neuroscience, Vanderbilt Vision Research Center, Vanderbilt Brain Institute, Vanderbilt University, Nashville, Tennessee.

K. L. H.: Department of Psychology, Centre for Vision Research, Toronto, ON, M3J 1P3; Department of Psychology, Center for Integrative and Cognitive Neuroscience, Vanderbilt Vision Research Center, Vanderbilt Brain Institute, Vanderbilt University, Nashville, Tennessee.

Corresponding author

K. L. H.: Department of Psychology, Vanderbilt University, kari.hoffman@vanderbilt.edu;

Conflict of Interest: None

Introduction

A long-standing question in neuroscience is how neural population activity supports memory and how this support changes with time. Current evidence suggests that memory representations form simultaneously within the hippocampal formation and the neocortex during encoding (Tse et al. 2011, Lesburgueres et al. 2011, Cowansage et al. 2014, Bero et al. 2014, Kitamura 2017; Abate et al. 2018; Matos et al. 2019). The hippocampal representation is thought to serve as an index of the neocortical memory representation, or the activity pattern activated by an experience. Reactivation of this hippocampal index serves to also reactivate the associated neocortical representation bringing about memory recall (Teyler & DiScenna, 1986).

What happens with time as memories get older remains unclear. A sizable cross-species body of literature supports a model where memories are initially dependent on the hippocampus when they are relatively new (or recent) and that as they get older (or remote) they are recalled independently of the hippocampus, relying instead on their neocortical representations (Bontempi et al. 1999; Frankland et al. 2004; Maviel et al. 2004; Teixeira et al. 2006; Quinn et al. 2008; Restivo et al. 2009; Smith & Squire, 2009; Yamashita et al. 2009; Miller et al. 2010; Corcoran et al. 2011; Goshen et al. 2011; Vetere et al. 2011; Tayler et al. 2013; Bero et al. 2014; Cowansage et al. 2014; Einarsson et al. 2015; Kitamura et al. 2017). However, comparably strong evidence also exists suggesting that the hippocampus is required for recall of memories regardless of their age, particularly where the memory is context rich, as in episodic memories (Rosenbaum et al. 2001; Steinvorth et al. 2005; Lehmann et al. 2007; Corkin 2002; Maguire & Frith, 2003; Addis et al. 2004; Gilboa et al. 2004; Rosenbaum et al. 2005; Viard et al. 2007; Winocur et al. 2007; Goshen et al. 2011, Sutherland et al. 2008; Sparks et al. 2011, Bonnici et al.

2012; Broadbent & Clark, 2013; Denny et al. 2014; Ocampo et al. 2017; Sekeres et al. 2017, 2018; Barry & Maguire, 2018).

The retrosplenial cortex (RSC) is one of the neocortical areas that has emerged as an important node in the memory network, particularly in episodic memory in humans (Valenstein, 1987, Maguire, 2001, McDonald et al. 2001, Osawa et al. 2006, Maddock, 1999, Svoboda et al. 2006, Spreng et al. 2009) and nonhuman primates (Buckley & Mitchell, 2016), as well as spatial memory in rodents (Sutherland et al. 1988, Whishaw et al. 2001, Vann & Aggleton, 2002, Vann et al. 2003, Vann & Aggleton, 2004, Harker & Whishaw, 2004, Keene & Bucci, 2008a, 2008b; Lukoyanov & Lukoyanova, 2006, Pothuizer et al. 2008, St-Laurent et al. 2009; Hindley et al. 2014, Czajkowski et al. 2014, Cowansage et al. 2014, Milczarek et al. 2019; de Sousa et al. 2019). In humans, the RSC is involved in spatial navigation (Maguire 2001, Epstein 2008), processing of objects-in-scenes (Barr & Aminoff, 2003; Barr, 2004), landmarks (Auger et al. 2012, Auger & Maguire, 2013, Mullally et al. 2012, Spiers and Maguire, 2006), and especially familiar landmarks (Sulpizo et al. 2013, Sherrill et al. 2013, Shine et al. 2016, Patai et al. 2019). While numerous studies have implicated the RSC as a site of remote memory representation (Anagnostaras et al. 1999, Bontempi et al. 1999, Maviel et al. 2004, Frankland et al. 2004; Frankland & Bontempi, 2005; Haijima & Ichitani, 2008, Corcoran et al. 2011, Tayler et al. 2013, Katche et al. 2013, 2017; Buckley & Mitchell; 2016; Todd et al. 2016; Jiang et al. 2018), few imaging studies have found the opposite, with more RSC activity during recent memory (Gilboa et al. 2004, Woodard et al. 2007, Oddo et al. 2008).

Evidence for the current views on remote memory and its dependence on the hippocampus and RSC have largely come from human damage and imaging studies or rodent lesion, imaging and optogenetic studies. While these approaches have been useful in determining

necessity and sufficiency of brain areas to memory retrieval, they have not contributed to an understanding of the physiology underlying how these areas contribute to the retrieval process. An examination of the electrophysiological responses of the hippocampus and RSC during recall of remote memory is therefore key to ascertain their involvements and contributions. To address this need, we conducted simultaneous recordings of the neural population activity in the HPC and RSC using chronically implanted multi-channel electrode arrays in non-human primates, as they completed an episodic-like memory visual search task using remote and recently learned stimuli.

Materials and Methods

Surgical procedures

Two adult female macaques (*Macaca mulatta*, “LE” and “RI”, 12.4 and 9.7Kg respectively) were implanted with indwelling flexible, polyamide-based intracortical multichannel electrode arrays (‘Microflex’, Blackrock electrodes are the currently available models), targeting the hippocampus, cingulate and retrosplenial cortices of the left hemisphere, as described in Talakoub et al., 2019. We successfully acquired neural signal from all areas in both animals except for the cingulate cortex where we managed to acquire signal for only one animal (RI). All surgical and experimental protocols were conducted with approval from the local ethics and animal care authorities (Animal Care Committee, Canadian Council on Animal Care). Surgery was performed and data were collected at York University, Toronto, Canada.

Task design

Both monkeys completed a memory-guided visual search task 12-18 months prior to the present recordings. During this task, a target object was embedded in a naturalistic scene, and presented alongside other objects-in-scenes, comprising the ‘remote’ stimuli used in this study (stimuli N= 276 for LE and 104 for RI). During the present experiments, the animals performed two task versions within each daily session: ACQUISITION and RECALL trials. During an acquisition trial, the scene is displayed for 2s and the animal is allowed to view the scene freely, followed by presentation of a target unique to the scene that is cued by alternating between original (500ms) and complementary colours (60ms), making the target salient and appearing to “pop out” to the observer. Target cueing began at 2s and continued until the target was selected

(designated as a HIT) or until the end of the 7s trial (designated as a MISS). Selection of the target was accomplished by holding gaze in the target region for a prolonged duration (≥ 800 ms). During a recall trial, the scene is presented without the cue and the animal had 7s to find and select the (un-cued) target for juice reward (HIT or remembered) or the trial ends without reward (MISS or forgotten). All trials ended with a giveaway, where the original and colour-modified scene alternate (100ms each x 5) revealing the target to the animal. An inter-trial interval of 4s of black screen followed each trial (Figure 1A).

Scenes were grouped into sets of 12 (monkey RI) or 16 (monkey LE) scenes. Number of scenes in a set was estimated to account for individual performance differences. Each set had three types of scenes; *recent*, *remote* and *highly familiar*. Recent scenes were novel to the animal during the first set (i.e. acquisition). Remote scenes were scenes used during initial task training 12-18 months prior. Highly familiar scenes were a preselected subset of six remote scenes that were repeated regularly throughout the experiment, and therefore have a high HIT rate. Two of these were included in each set. A set was initially presented in acquisition, followed immediately by a recall and a third presentation as either a second acquisition (monkey RI) or a second recall (monkey LE). Whether the third presentation was an acquisition or recall varied across monkeys in a way that yielded optimal performance. The following day's session began with a recall of sets from the previous day. Two new sets were presented each day. Daily sessions started and ended with a 5-minute rest period where a black screen was presented. Eye movements were recorded at 1250 Hz using video-based eye tracking (iViewX Hi-Speed Primate Remote Infrared Eye Tracker). For the analysis we excluded trials where the animals spent $>20\%$ of trial duration looking off-screen (monkey LE: 238/2755 or 8%, monkey RI: 50/1310 or 4%), to ensure only trials where the animals were attending to the task were included.

Neural recordings

Local-field potentials (LFP) were recorded simultaneously from the hippocampus, anterior cingulate and retrosplenial cortices, digitally sampled at 32 kHz using a Digital Lynx acquisition system (Neuralynx, Inc.) and filtered between 0.5 Hz and 2 kHz. The neural signal was downsampled to 1 kHz, and a notch filter (59.9 to 60.1 Hz) was used to remove 60 Hz noise. All offline behavioral and neural analysis was conducted in MATLAB using custom-written scripts and FieldTrip (Ostenveld et al. 2011; fieldtrip.fcdonders.nl).

Generalized eigendecomposition (GED)

For analyses of power, phase concentration and coherence, we designed linear spatial filters to isolate the independent, reliable sources that form the dynamics of the neural signal (based on methodology described in Cohen, 2018). These filters provide a weighted combination of electrode activity guided by the goal of isolating sources of independent variance in multichannel data. Spatial filters were defined by the generalized eigendecomposition (GED) of channels covariance matrices. In GED, two separate covariance matrices are created based on pre-defined criteria resulting in eigenvectors that maximally differentiate the two matrices. If the signal features to be accentuated and those to be attenuated are designated by S and R respectively, the eigendecomposition problem can be written as $SW = WR\Lambda$. The solution of this problem yields W which is a matrix of eigenvectors and Λ that is a diagonal matrix of eigenvalues. The resultant filters, defined by eigenvectors, are then applied to multichannel electrode time series to obtain a set of component time series. If GED was unable to differentiate between various sources of variance, shrinkage regularization was employed 1 percent.

For power and phase concentration analyses, the S matrix was created from 1 second of signal after scene onset (start of trial) and R matrix from 1 second of baseline activity prior to the scene onset. In this design, we sought to attenuate continuous noise in the signal and accentuate the dynamics that are relevant to the task. For coherence analysis, we created the S matrix from the band-pass filtered electrode time series in 10-20Hz. R matrix was then formed from the broadband electrode time series. In this case, the column in W with the highest corresponding eigenvalue then corresponds to the eigenvector that maximally enhances the 10-20Hz frequency activity. The inputs to the GED were signal from multiple channels and trials from a given probe and the output was a single weighted time-series component per trial per probe. The analyses that follow use the resultant GED components that represent the weighted combination of activity from multiple channels in each probe.

Spectral analysis

Grand power was computed using a Fourier transform and a Hanning multi-taper frequency transformation, averaging over the whole duration of search trials including both acquisition and recall trials (N trials for LE = 1152, RI = 422). Mean power spectral density was examined in 500ms windows with a 1ms sliding window conducted on individual trials then averaged across trials. For mean time-frequency spectra, we implemented a Morlet wavelets multi-taper transformation with a width of five cycles and a frequency step-size of 1 Hz.

Phase concentration

To examine phase alignment with eye movement we inspected the LFP signal in 600ms windows centered around fixation onsets (peri-fixation signal). We examined all recall trial fixations split by remembered and forgotten trials. Mean phase concentration spectrograms were computed on the peri-fixation signal (± 1000 ms around fixations) using a sliding window of 200ms in 1ms steps to identify frequency bands for subsequent analysis. Based on these spectrograms which showed phase-concentration between 4-9 Hz, we bandpass filtered the peri-fixation neural signal between 4-9 Hz, then the phase angles of the Hilbert transform were used to compute the mean resultant vector length (or phase concentration). Circular statistical analyses were performed using the Circular Statistics Toolbox for MATLAB (Berens et al. 2009).

Bout detection

For detection of oscillatory bouts of activity in dominant frequency bands, the signal from all trials was bandpass filtered between 10-15 Hz for RSC, then the envelope of the analytic signal was used to detect oscillatory events crossing a threshold of 2 SDs above the mean, with a minimum duration of 100ms beginning and ending at 1 SD. This time period defined the bout duration and the amplitude was defined as the maximum peak of the envelope. Control bouts were chosen as threshold-crossings in the opposite direction to identify windows of time of weakest bandlimited power (Supp. Fig 1).

Phase synchrony

Phase locking during oscillation bouts was calculated from the cross-spectral density of the bout signal and the corresponding HPC signal using the debiased weighted phase lag index (wPLI). The debiased wPLI measure of phase-synchronization minimizes the influence of volume-conduction, noise and the sample-size bias (Vinck et al. 2011).

Statistical analysis

Proportions of hit rate and bout occurrence across scene types were compared using a two-tailed Chi-square test for comparing proportions. Search times were compared using a two-tailed rank-sum Wilcoxon test. Time-frequency spectra were compared using nonparametric permutation tests using the Monte Carlo sampling method and a cluster-based correction for multiple-comparisons. To test for statistical significance of differences between phase concentration and synchrony (wPLI values) during the recent and remote conditions, we performed a nonparametric permutation test with the difference in phase concentration or coherence between conditions as our test statistic. The test statistic was calculated for each frequency bin, then bins whose statistic value was <2.5th or >97.5th percentiles were selected, and cluster-level statistics were calculated by summing the test statistic within a cluster. This testing method corresponds to a two-tailed test with false-positive rate of 5% corrected for multiple comparisons across frequencies (Nichols & Holmes, 2002, Maris & Oostenveld, 2007, Jutras et al. 2009).

Results

Overall, we recorded 62 sessions (LE = 37, RI = 25), including 926 acquisition (LE = 686, RI = 240) and 1870 recall trials (LE = 1386, RI = 485). Both animals had a >90% hit rate (i.e. target found %) on acquisition trials, and during recall, a higher hit rate on highly familiar scenes compared to recent (LE: $X^2(1, 300) = 268, p < 0.05$, RI: $X^2(1, 395) = 44, p < 0.01$) and remote scenes (LE: $X^2(1, 312) = 138, p < 0.05$; RI: $X^2(1, 448) = 23.0, p < 0.001$). Remote scenes had a higher hit rate compared to recent scenes (LE: $X^2(1, 395) = 35, p < 0.01$; RI: $X^2(1, 395) = 44, p < 0.01$). Correspondingly, recall during highly familiar trials had shorter search times than recent (LE: $z = 2.40, p < 0.05$, RI: $z = 6.45, p < 0.001$) and remote trials (LE: $z = 4.52, p < 0.001$, RI: $z = 2.63, p < 0.01$). Remote scenes were found faster than recent scenes in one animal (RI: $z = 4.55, p < 0.001$), while for the second animal there was no difference in search time for remote and recent scenes (LE: $z = -1.58, p = 0.11$; Figure 1B).

Remote memory is associated with greater beta power in the RSC

We first examined the grand spectral power during search and found a prominent peak between 10-20 Hz in the RSc and HPC of both animals (Figure 1D). We then examined whether spectral power in this range varied by memory age in two main epochs; *scene-onset* consisting of the first 2s of acquisition and recall trials when the scene is first presented, and *remembered target* consisting of the last 1.5s before a trial-ending fixation on remembered recall trials (Figure 2). A nonparametric permutation test revealed greater 10-15 Hz mean power spectral density in the RSC between 0.5-2s after scene-onset (Figure 2B) and 1.25-0.25s before trial-end on remembered trials (Figure 2F). In the time-frequency representation, a non-parametric cluster-

based permutation test showed remote trials to have greater power ($p < 0.05$) in a cluster beginning as early as 1s after scene-onset (Figure 2C) and 1.25s before trial end (Figure 2G). We found no differences in HPC power between remote and recent trials (Figure 2D and 2H).

General linear regression model

We observed that the bandlimited 10-15 Hz RSC oscillation occurs in brief bursts or bouts throughout search trials. We then used an envelope thresholding approach to identify suprathreshold RSC bouts of activity between 10-15 Hz (described in Methods). This was followed by a linear regression model to examine how task variables contribute to the magnitude of these bouts. We detected 4564 bouts across all trials (LE: 3278, RI: 1286), with 1290 bouts during acquisition (LE = 894, RI = 396) and 3274 during recall trials (LE = 2384, RI = 890). Bouts occurred more frequently during recent compared to remote trials during both acquisition (LE; $X^2(1, N = 894) = 6.18, p < 0.05$, RI; $X^2(1, N = 396) = 28.2, p = 1.1 \times 10^{-7}$) and recall (LE; $X^2(1, N = 2384) = 42.3, p = 7.6 \times 10^{-11}$, RI; $X^2(1, N = 890) = 336.4, p < 0.01$). Remote recall trials therefore had fewer, but greater bouts compared to recent trials.

A regression analysis was used to test whether the following task variables on recall trials predicted bout magnitude; scene age (remote or recent), search time, time from bout peak to trial end, the screen quadrant containing the target (to test for visual-field effects given our unilateral recordings), time to fixate on target and animal ID (to test for differences in bout amplitude by animal). The model accounted for 32% of the variance in bout amplitude ($F(6,3090) = 173, p < 8.3 \times 10^{-242}, R^2 = .32$), and showed that scene age ($t = -3.9, p < 0.001$), search time ($t = 4.2, p = 2.0$

$\times 10^{-5}$), bout peak to end ($t = 5.87$, $p = 4.64 \times 10^{-9}$) and animal id ($t = 2.8$, $p < 0.01$) predict bout amplitude.

Phase synchrony between eye movements and neural oscillations

We then examined the degree by which the eye movements during search are temporally coordinated with oscillations in the different brain areas. We measured the phase concentration in a ± 300 ms window around fixation onsets throughout trials and found that phase alignment was concentrated between 4-9 Hz. Phase concentration was greater in the RSC (Figure 3A and 3B) on remote scenes beginning shortly before fixations (RI: -175 ms, LE: -75 ms) and lasting until 125-200 ms post-fixation compared to recent scenes. This larger phase concentration on remote trials was present only on remembered but not forgotten trials (Supp Fig. 1). Although this phase alignment increased in the HPC as well during both remembered and forgotten trials, we found no difference between recent and remote scenes (Figure 3C and 3D). Collapsing trials by scene age, we compared phase concentration between remembered and forgotten trial fixations in the HPC based on recent reports showing greater phase concentration during remembered trials (Kragel et al. 2020) but found no differences ($p > 0.1$).

Interareal phase synchrony

Having identified bouts of band-limited activity in the RSC that occur with greater power during remote scenes, we examined RSC-HPC synchrony during these bouts using the debiased weighted phase lag index (wPLI). First, we examined RSC-HPC bout synchrony during search, ITI and rest periods of the recordings and found synchrony to be most prominent during search.

We then examined synchrony during search by scene type and compared synchrony across remembered and forgotten trials. We found that during remembered, but not forgotten or control trials (periods of low bout magnitude), RSC-HPC synchrony was greater for recent compared to remote scenes in the ~25-40 Hz range (Figure 4). This difference in synchrony was present only during recall trials and not during acquisition trials.

Discussion

In this study, we measured the neural population activity in the hippocampus and RSC simultaneously as macaques completed an episodic-like memory task. Our findings are 1) onset of remotely learned stimuli is associated with greater beta power in the RSC, 2) neural oscillations in the RSC phase-lock with eye movements during successful recall of remote memory, and 3) greater hippocampal - neocortical phase synchrony during recent memory recall.

We observed greater beta in the RSC during recall of remote memory. Our group has previously shown this to be a prominent band in this region of the primate brain during normal waking behaviours (such as walking and grooming) (Talakoub et al. 2019). Consistently, it was also the most prominent band during visual search in the present study (Figure 1E). The power increase in this band during remote memory suggests that the retrosplenial cortex may be more greatly involved in processing remote compared to recent visual spatial memory. In line with this interpretation, we found stronger phase-locking between retrosplenial cortex oscillations and eye movements made during successful recall of remote memory that began shortly before fixations. This temporal coordination observed during remembered but not forgotten trials, suggests a role for the RSC in guiding gaze towards the correct target on this task. Similar phase-locking of RSC

with fixations to predict remembered trials has been reported using MEG in humans during the encoding of visual stimuli that would later be remembered (Staudigl et al. 2017). Although we observed phase-locking of fixations to hippocampal activity, as has previously been shown (Hoffman et al. 2013, Andrillon et al. 2015, Katz et al. bioRxiv), we found no difference between remote and recent memory, suggesting a unique role for the RSC in the recall of remote memory. These findings suggest a unique role for the RSC in processing remotely learned episodic-like memory. Such a role has been observed using rodent tagging (Tayler et al. 2013, de Sousa et al. 2019), immediate early gene (Bontempi et al. 1999, Maviel et al. 2004, Frankland et al. 2004, Katche et al. 2013, Katche et al. 2017), lesion (Haijimi & Ichitani, 2008, Todd et al. 2016, Jiang et al. 2018) and pharmacological studies (Corcoran et al. 2011), macaque lesion studies (Buckley & Mitchell, 2016), as well as human case (reviewed in Maguire, 2001) and imaging studies (Benuzzi et al. 2018, Patai et al. 2019).

We found greater coupling between RSC and HPC during recent memory recall in the gamma band. Strikingly, we observed this coupling only during remembered trials, and not during forgotten trials. This coupling based on the phases of the oscillations in the two brain areas suggests greater communication (Fries, 2015), although the directionality and functional cause of this coupling remains to be understood. While this coupling could underlie consolidation of newly acquired target-scene associations, it could also indicate retrieval of recently acquired memory. That we only observed this coupling during recall and not acquisition suggests that this may be a retrieval mechanism. The RSC and HPC have strong bilateral connections (Kobayashi et al. 2007) and have been proposed to form part of an extended network of areas involved in episodic memory and spatial navigation (Ranganath & Ritchey, 2012). This coupling was not observed during remote memory recall suggesting that hippocampal

neocortical interaction is not needed to support recall of remote episodic-like memory. Although our findings are correlational, they point to a greater role for neocortical areas in processing remote memory and greater hippocampal-neocortical interactions during recent memory. These findings support standard consolidation theory which suggests a greater role for neocortical areas in supporting remote memory and a decreased role for the hippocampus. Similar observations have been reported in rats using inhibitory avoidance learning where memory initially requires both HPC and RSC (Katche et al. 2013a), but after two weeks no longer requires the HPC (Izquierdo and Medina 1997) and remains dependent on RSC (Katche et al. 2013b).

In summary, our findings represent the first electrophysiological evidence of RSC involvement in the processing of remote memory in primates. We found greater RSC involvement in remote memory recall and preferential RSC-HPC synchrony during recent memory suggesting functional reorganization of memory representation with age.

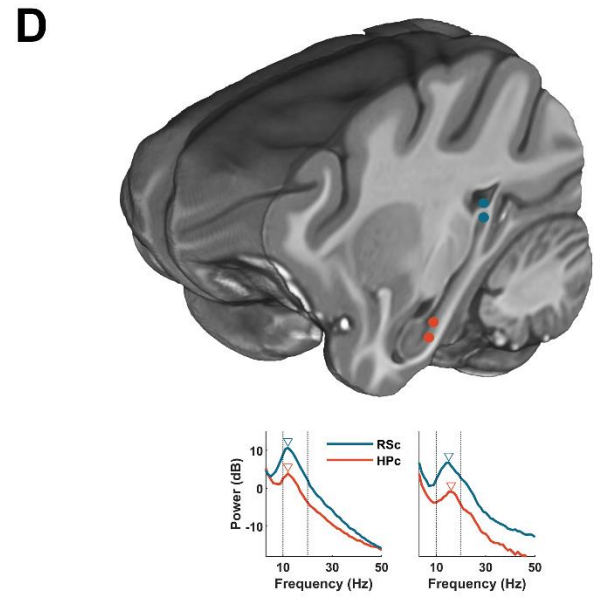
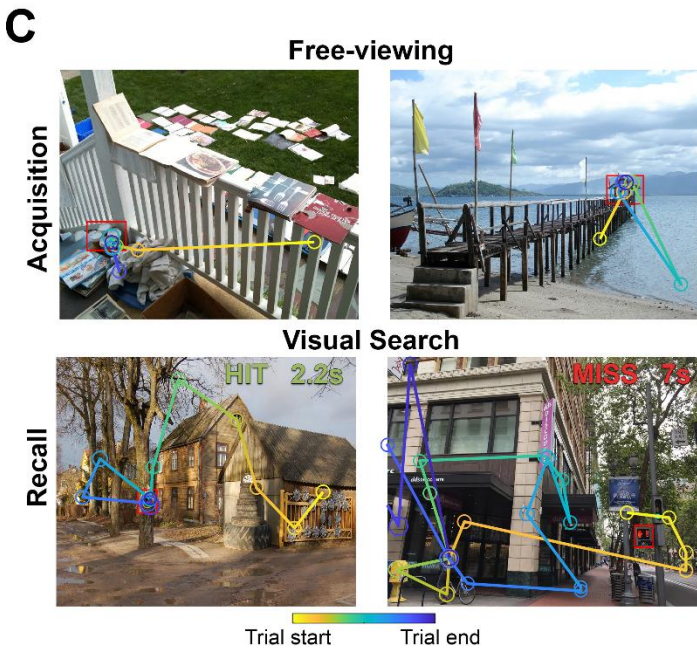
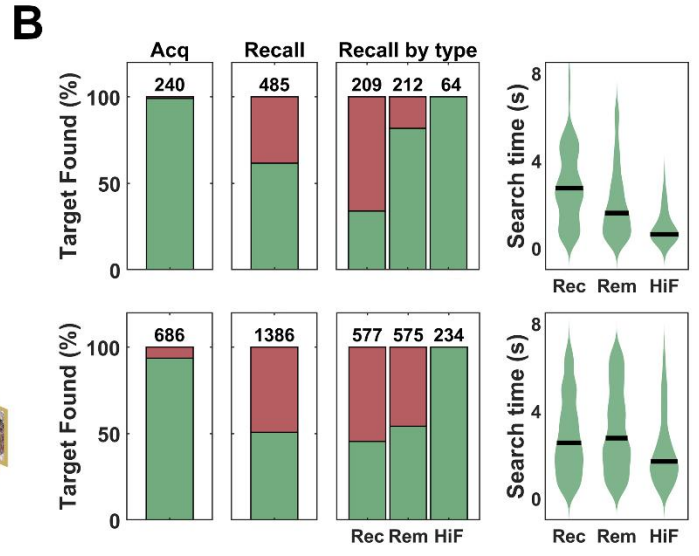
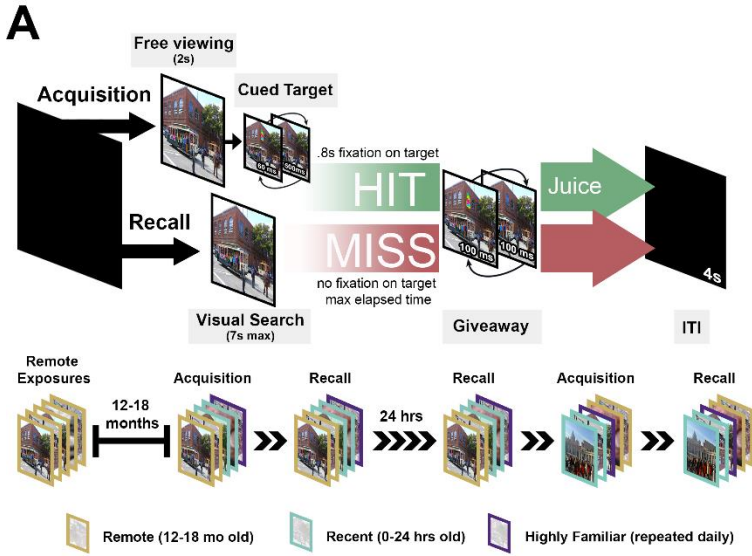


Figure 1. Experimental design, task performance and recording locations. **A)** *Top*; during acquisition, a trial begins with 2s of free-viewing followed by target cueing through quick alternations between a colour-modified version and the original. During recall, the scene is presented without the cue. A trial ends with a 0.8s fixation on target for which a fluid reward is delivered (HIT), or when the maximum trial time is reached (MISS). A *giveaway* presents the cued target for a longer duration (100ms) at the end of a trial followed by the ITI (4s). *Bottom*; scenes were grouped in sets of 12-16 scenes and were of three types: ‘remote’ scenes which were presented 12-18 months prior, ‘recent’ which were novel scenes and ‘highly familiar’ scenes which were six remote scenes with a high HIT rate. In the present recordings, sessions began with a set shown in acquisition followed immediately by recall. Twenty-four hours later, the set is shown in recall before another set is presented in acquisition followed by recall. **B)** *Top*; from left, target found % for acquisition trials, recall trials (both immediate and next day recall), recall trials by scene age and search time during recall per scene age for monkey RI. Black bands in violin plots indicate mean value. *Bottom*; same as top but for monkey LE. Values above bars indicate number of Target Found trials in respective condition. **C)** *Top row*: example scan paths during 2s of free-viewing 2s on acquisition trials of remote scenes. Outlined in red is the target. Note that gaze goes towards the target even before the cue, suggesting preserved memory of the target. *Bottom row*: example scan paths for a HIT (or remembered trial) and a MISS (forgotten trial) during recall trials. Inset in top right of each scene indicates search time in seconds. **D)** Electrode localization. Insets: average power during search for RSC and HPC.

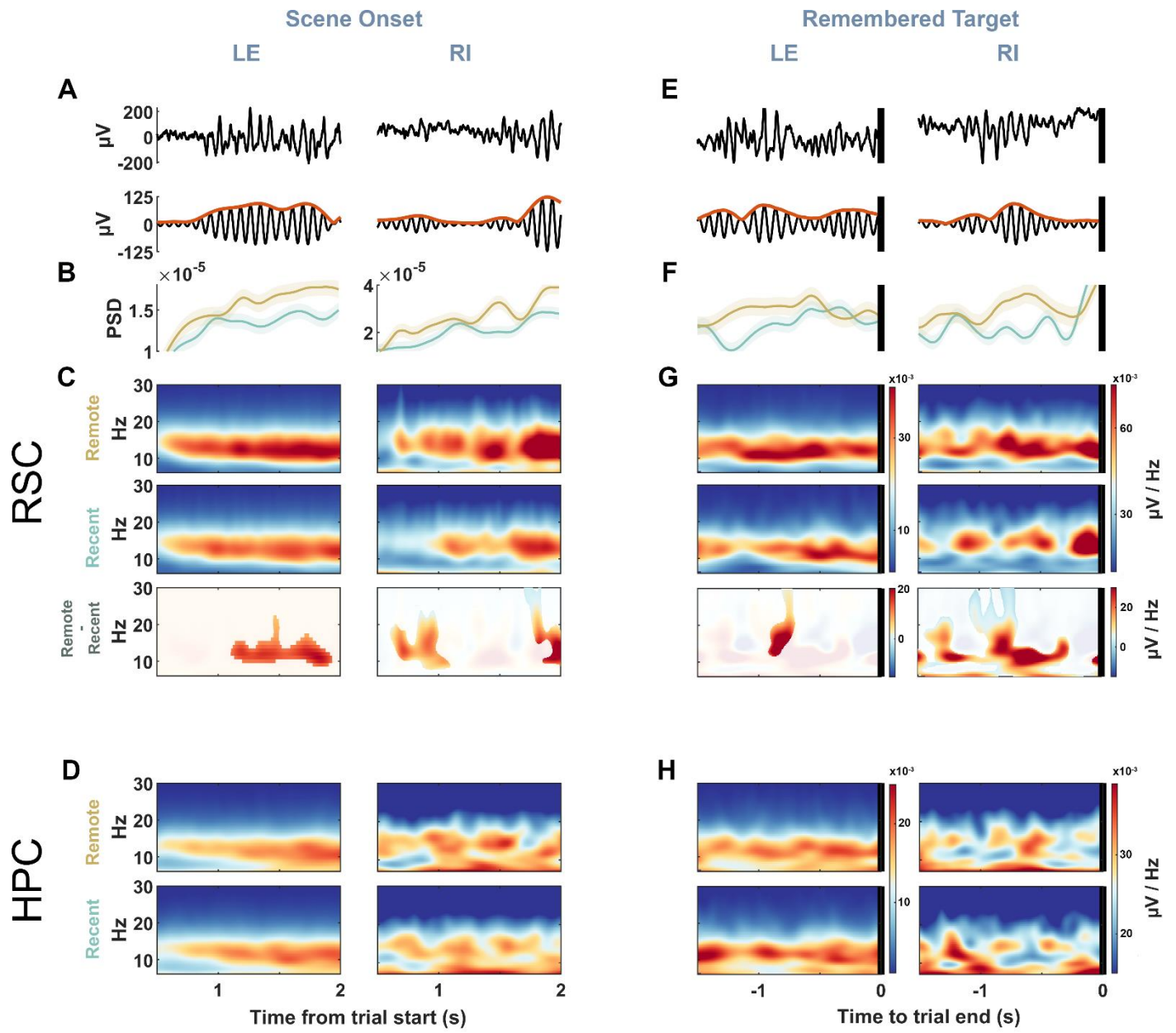


Figure 2. Retrosplenial cortex (RSC) exhibits greater 10-15 Hz power during remote scenes. A) Top; Example broadband signal during first 2s after trial onset when a scene is presented. Bottom; 10-15 Hz filter of signal above. LE indicates data for animal 1, and RI on right indicates data for animal 2. B) mean power spectral density of 10-15 Hz band using 500ms windows in 1ms steps. Shading indicated 95% bootstrap confidence interval. C) Top; mean spectrogram of remote trials (LE n = 594, RI n = 152), middle; recent trials (LE n = 605, RI n = 240), bottom; remote – recent difference spectrogram with the non-greyed region representing clusters with a difference of $p < 0.05$ in a cluster-based permutation test corrected for multiple comparisons. D) Top; mean spectrogram of remote trials in the hippocampus, bottom: recent. E-H same as A-D but for the last 1.5s before the end of remembered trials.

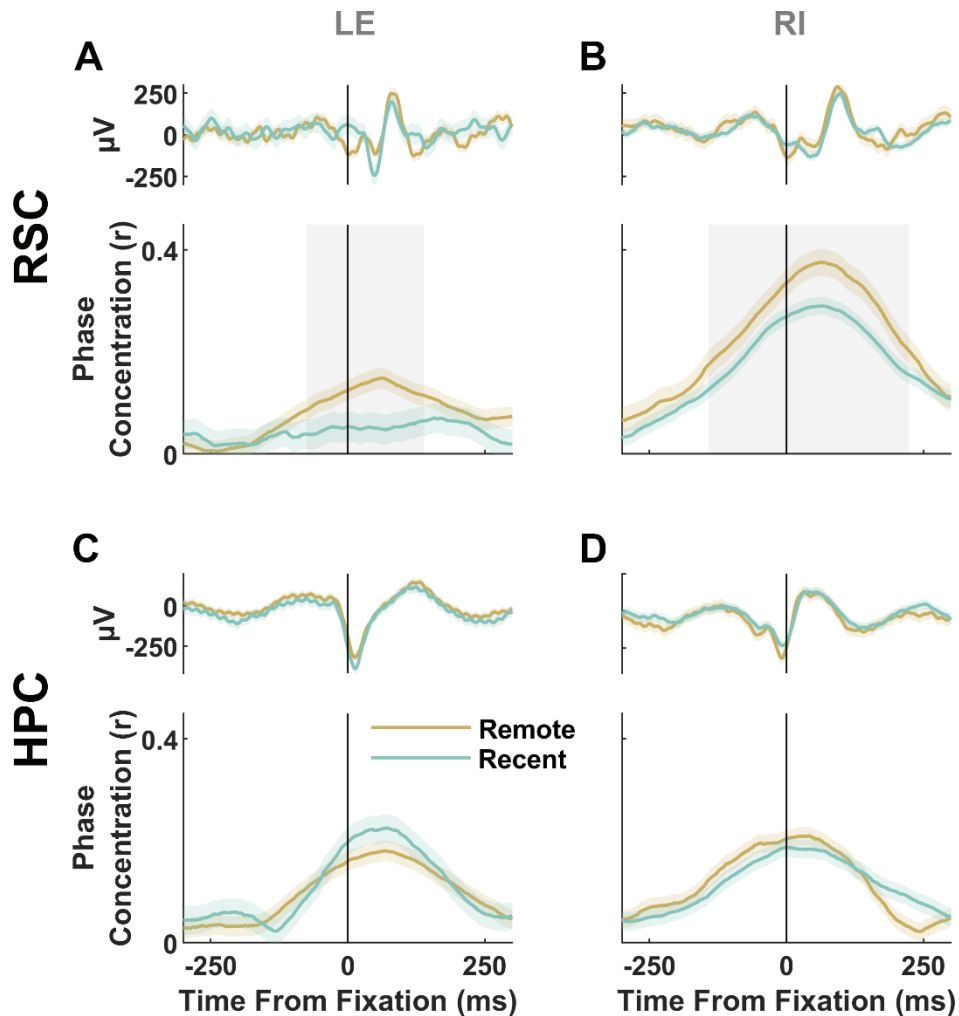


Figure 3. Eye movements on remembered remote trials are phase locked with the phase of retrosplenial cortex (RSC) theta oscillations. A) Top; mean LFP locked to fixations on remembered trials, bottom; mean phase concentration of RSC oscillations around fixations for monkey LE (remote $n = 2134$, recent $n = 1042$). Light shade around mean traces represent 95% bootstrapped confidence intervals. Grey shading represents $p < 0.05$ difference between remote and recent phase concentrations in a two-tailed cluster-based permutation test. B) same as A) but for animal RI (remote $n = 1267$, recent $n = 2921$). C) and D) are similar to A) and B) but for the hippocampus of each animal respectively (LE; remote $n = 2054$, recent $n = 1031$, RI; remote $n = 1297$, recent $n = 2972$).

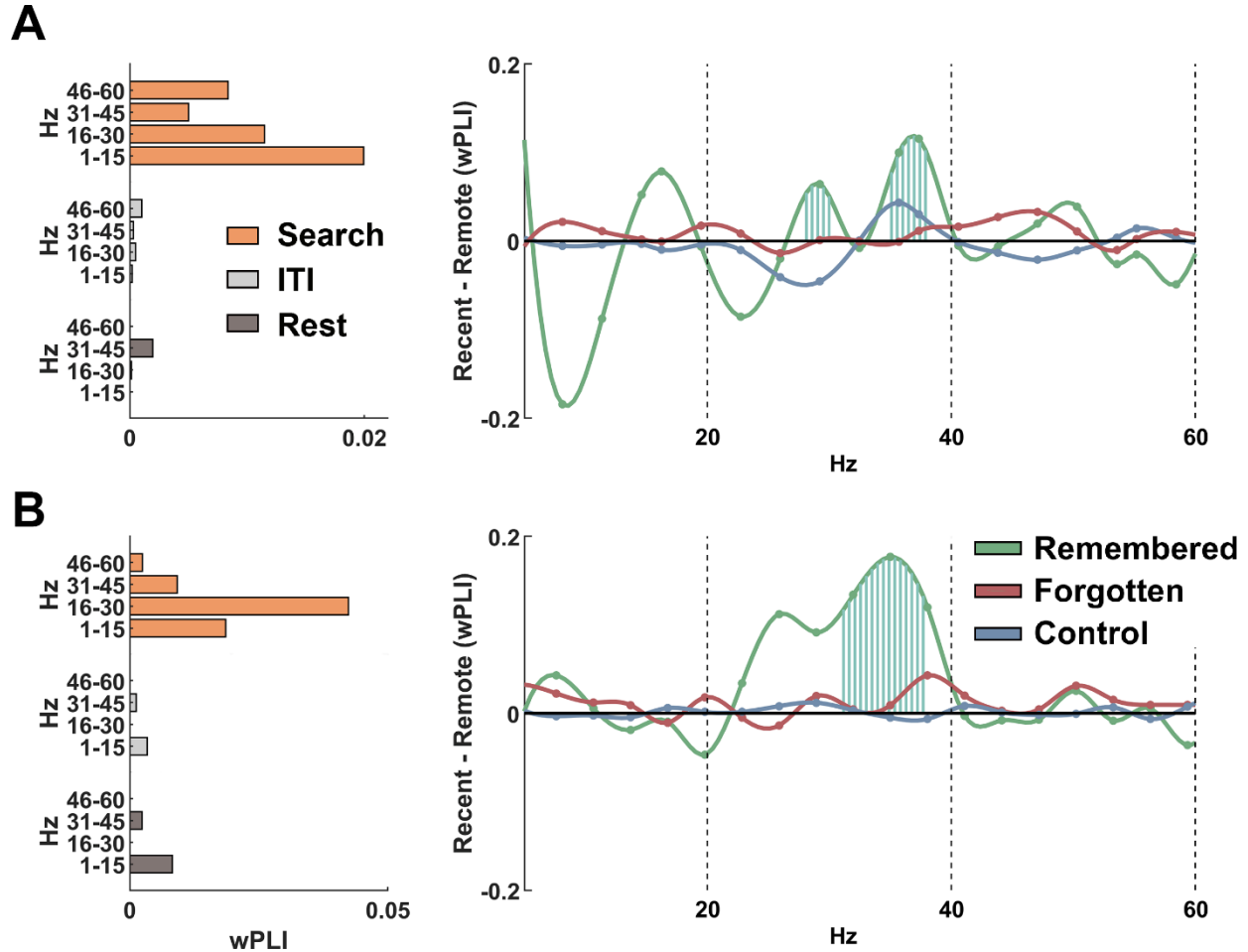
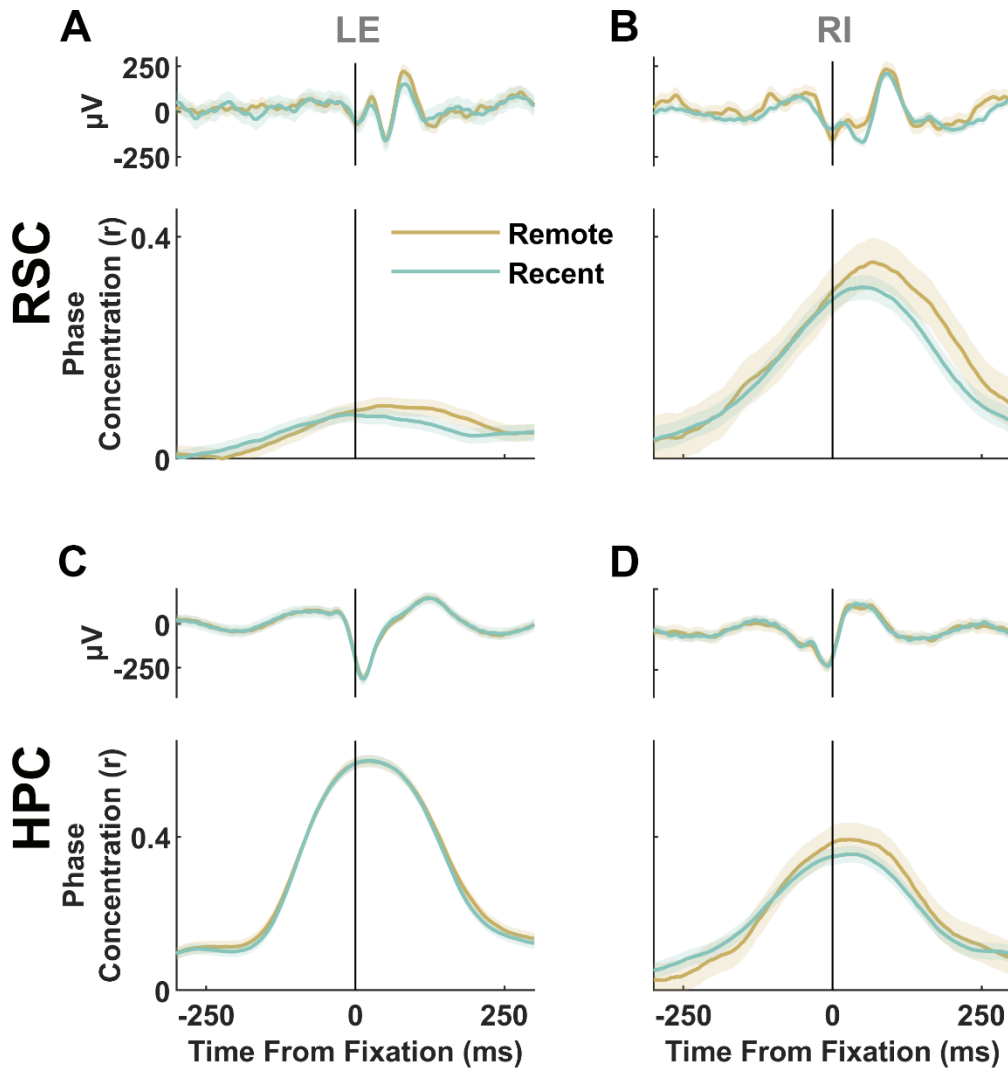


Figure 4. Greater retrosplenial hippocampal phase synchrony during remembered recent scenes. **A** *Left*; phase-locking (wPLI) by frequency during 10-15 Hz RSC bouts across rest ($n = 3346$), ITI ($n = 6423$), search ($n = 2384$) for LE. *Right*; difference in RSC-HPG phase-locking between bouts on recent and remote trials during remembered (recent = 112 bouts, remote = 204 bouts), forgotten (recent = 1159, remote = 909) and control (recent = 2937, remote = 2331) bouts. Vertical blue bars from zero indicate frequencies with a permutation test difference of $p < 0.05$. **B** Same as A but for animal RI, *left*; rest ($n = 2338$), ITI ($n = 1937$) and search ($n = 890$), *right*; remembered (recent = 106, remote = 176), forgotten (recent = 468, remote = 140) and control (recent = 1108, remote = 371).



Supplementary Figure 1. Eye movements are not preferentially locked to the phase of theta oscillations in the RSC during forgotten trials. A) Top; mean LFP locked to fixations on forgotten trials, bottom; mean phase concentration of RSC oscillations around fixations for monkey LE (remote $n = 8139$, recent $n = 9996$). Light shading around mean traces represents 95% bootstrapped confidence intervals. B) same as A) but for animal RI (remote $n = 984$, recent $n = 4114$). C) and D) are similar to A) and B) but for the hippocampus of LE (remote $n = 7777$, recent $n = 9592$) and RI (remote $n = 1013$, recent $n = 4175$) respectively.